博士論文

The regulatory mechanisms of hepatic stem/progenitor cell differentiation

(肝幹・前駆細胞の分化制御機構)

柳田　絢加

Index

1 Abbreviation

AFP, α-fetoprotein;

AGM, aorta-gonad-mesonephros;

APC, allophycocyanin;

bFGF, basic fibroblast growth factor;

BMP, bone morphogenetic protein;

CK, cytokeratin;

CKI, cyclin-dependent kinase inhibitors;

COMT, catechol-O-methyltransferase;

CXCR4, chemokine (C-X-C motif) receptor 4;

CYP, cytochrome P450;

DAPI, 4',6-Diamidino-2-phenylindole dihydrochloride;

Dex, dexamethasone;

Dlk, delta-like 1 homolog;

DMEM, Dulbecco's modified Eagle's medium;

Dox, doxycycline;

E, embryonic day;

EB, embryoid body;

EGF, epidermal growth factor;

EpCAM, Epithelial cell adhesion molecule;

EPHX1, epoxide hydrolase 1, microsomal (xenobiotic);

ES, embryonic stem;

FACS, fluorescence-activated cell sorter;

FBS, fetal bovine serum;

FITC, fluorescein isothiocyanate;

FMO5, flavin containing monooxygenase 5;

Foxa1, forkhead box protein a1;

GAPDH, glyceraldehyde 3-phosphate dehydrogenase;

GFP, green fluorescent protein;

GMEM, Glasgow's modified Eagle's medium;

GSC, goosecoid homeobox;

H-CFU-C, hepatic colony-forming unit in culture;

HGF, hepatocyte growth factor;

Hhex, hematopoietically expressed homeobox;

Hlx, H2.0-like homeobox;

HNF, hepatocyte nuclear factor;

HPC, hepatic progenitor-like cell;

HPRT1, hypoxanthine phosphoribosyltransferase 1;

HSC, hematopoietic stem cells;

ICM, inner cell mass;

IMDM, Iscove’s Modified Dulbecco’s Medium;

iPS cell, induced pluripotent stem cell;

IRES, internal ribosome entry site;

Klf, kruppel-like factor;

KuO, Kusabira Orange;

LIF, leukemia inhibitory factor;

MAO, monoamine oxidase;

Mdk, midkine;

MEF, mouse embryonic fibroblast;

MIXL1, Mix paired-like homeobox;

NOD/SCID, Non-obese Diabetic/Severe Combined Immunodeficiency;

Oct, octamer-binding transcription factor;

ONECUT1, one cut homeobox 1;

OSM, oncostatin M;

PBS, phosphate-buffered saline;

PCLP1, podocalyxin-like protein 1;

PDGFR, platelet-derived growth factor receptor;

PE, phycoerythrin;

PFA, paraformaldehyde;

PKCζ, protein kinase Cζ;

Prox1, prospero homeobox 1;

Ptn, pleiotrophin;

RT-PCR, reverse transcription-polymerase chain reaction;

TAT, tyrosine aminotransferase;

Tbx3, T-box3;

TGFβ, transforming growth factor beta;

TLDA, TaqMan Low Density Array;

Sox, SRY (sex determining region Y)-box containing gene;

STM, septum transversum;

SULT1A, sulfotransferase family, cytosolic, 1A;

2 Abstract

Liver cell transplantation, as an alternative to a whole organ, is considered as a feasible treatment for end-stage liver diseases. However, it is difficult to obtain a large number of mature hepatocytes for cell therapy since they have low proliferative potential *in vitro*. Hepatoblasts, fetal hepatic stem/progenitor cells, possess high proliferative ability and the capacity to differentiate into both hepatocytes and cholangiocytes. It has been proposed that even a small number of hepatic stem/progenitor cells could be enough for cell transplantation following *in vitro* expansion and maturation. This study aims to explore approaches to improving hepatoblast culture systems by two different methods. Using human iPS cells, hepatic progenitor-like cells were successfully generated and purified through CD13 and CD133 expression. It was revealed that these cells could proliferate over long-term culture whilst still retaining their functionality in the presence of ROCK and ALK inhibitor. In a separate approach, it was revealed that the cell cycle inhibitor $p57^{Kip2}$ was specifically expressed in hepatoblasts and mesenchymal cells in fetal livers but not in adult hepatocytes. Retardation of hepatoblast maturation was shown in the prenatal stage livers of $p57^{Kip2}$-/- mice. However, a $p57^{Kip2}$ intrinsic deficiency of hepatoblasts did not suppress maturation of these cells. It has been proposed that hepatoblast maturation was regulated by both intrinsic factors and extrinsic factors. Since $p57^{Kip2}$ intrinsic deficiency of hepatoblasts did not affect hepatoblast maturation, this suggests the possibility that extrinsic expression of $p57^{Kip2}$ could be involved in regulating the hepatoblast maturation process. Elucidating the underlying molecular mechanism of this regulatory system may contribute towards the improvement of hepatoblast culture systems in obtaining large volumes of high quality hepatocytes.

3 General introductions

3-1 Stem cells

Stem cells have the unique characteristics of self-renewal and multipotency. In mammals, broadly speaking, there are two types of stem cells; somatic stem cells and pluripotent stem cells. Somatic stem cells can self-renew and become lineage specific cell types, but have more limited differentiation potential compared with pluripotent stem cells. They are involved in organ formation during the developmental stage as well as organ maintenance and repair in the adult stage. The history of stem cell research began in the 1950s. Hematopoietic stem cells (HSCs), form all the types of blood cells in the body, were the first somatic stem cells to be discovered (*1*). It became a popular model for studying stem cell kinetics and characteristic properties in general. Other somatic stem cells with specific homeostatic functions are found in various tissues or organs.

Embryonic stem (ES) cells are "pluripotent" as they can give rise to tissue derived from the three primary germ layers: ectoderm, mesoderm and endoderm (*2, 3*). However, their clinical application are bound by ethical concerns over the necessity of embryo destruction in their derivation. More recently, mouse induced pluripotent stem (iPS) cells could be generated from dermal fibroblasts by simultaneously introducing four genes (Oct3/4, Klf4, Sox2, and c-Myc) (*4*). iPS cells share the same characteristics of self-renewal and pluripotency as ES cells. Initially iPS cells were generated using either retroviruses or lentiviruses carrying four genes. It is now also possible to generate integration-free iPS cells. The methods include plasmid, sendai virus, adenovirus, proteins, and synthesized RNAs. Additionally, it had been reported that c-Myc is dispensable and mouse iPS cell generated in this way showed reduced a likelihood in

tumor formation (*5-10*). On a practical level, iPS cells are not constrained by the same ethical concerns as with ES cells and their autologous nature allows the issue of immunorejection to be overcome in transplantation therapy. However, there are still difficulties that remain. For example, the efficiency of generation of iPS cells using Yamanaka factors is low. This has now been improved by depleting Mbd3, a core member of the Mbd3/NuRD (nucleosome remodeling and deacetylation) repressor complex, together with Oct3/4, Klf4, Sox2, and c-Myc transduction promoted reprogramming to near 100% efficiency (*11*). Thus the effect of iPS cell clonal variation, gene expression, DNA methylation and pluripotency potential have to be analyzed using these high efficient reprogramming methods. Another difficulty is the molecular mechanism of pluripotent maintenance. iPS cells were generated from not only mouse but also human, porcine and so on (*12-14*). Mouse iPS cells are similar phenotype of inner cell mass (ICM) of pre-implantation stage blastocysts and called naïve state. Non-rodents iPS cells, such as human iPS cells are similar phenotype of mouse epiblasts stem cells generated from post-implantation stage epiblasts and called ground state. A key factor for maintenance of mouse ES cells and iPS cells was leukemia inhibitory factor (LIF) (*15*). Whilst, a key factor for maintenance of human ES cells and iPS cells was basic fibroblast growth factor (bFGF) (*13, 14, 16*). Because molecular mechanisms of maintenance of pluripotency are different between rodent and other species, pluripotency and differentiation stimuli should be different between mouse and human ES and iPS cells. Elucidation of the molecular mechanisms regulating stem cells in each species is important.

3-2 Clinical applications of stem cells

For intractable liver diseases, liver transplantation remains the most effective treatment. However, immune rejection and absolute donor shortages remain barriers to liver transplantation therapy. Artificial organ transplantation, i.e. artificial heart transplant, is available for several tissue diseases. In contrast, an artificial liver that possesses all the innate metabolic functions is currently unavailable. It has been proposed therefore that the transplantation of hepatocytes may act as a viable alternative. More specifically, patient autologous iPS cells could be generated and differentiated into hepatic lineage cells. These may be good sources of transplantation therapy whilst overcoming the issue of immunosuppression. However, there are several issues to use iPS cells for human therapy.

For clinical application, the establishment of efficient differentiation methods from iPS cells into cells of the desired lineage is necessary. Generally speaking, there are two main types of approaches to this, one of which is through an *in vitro* differentiation system. This may be achieved through a number of reported techniques such as gene transfer, cytokines additions, and cell aggregation all of which leads to successful differentiation. However the overall efficiency of this process remains low alongside the possibility of undifferentiated or undesired cell types being present in the differentiation culture. To resolve these problems, generation of more sophisticated differentiation and purification methods are necessary. Improving the existing understanding of organ developmental processes and knowing the genes or stimuli that are critical to these processes may also contribute greatly to the overall efficiency.

The other way is the *in vivo* differentiation of iPS cells into target organs. iPS cells derived pancreas were generated in animal body by microinjecting iPS cells into blastocysts deficient in a gene essential for pancreas (*17*). Theoretically the same

method may be applied to generating both functional and transplantable livers. Although a suitable host animal capable of accommodating a growing human organ remains to be found, this technique is certainly an enterprising approach at addressing the issue of absolute donor shortages.

Another possibility of generating lineage specific cells is through "direct reprogramming" of one somatic cell type into another without transiting through a pluripotency state. The conversion of exocrine cells to endocrine cells has been reported in the mouse pancreases using a combination of three master transcription factors. Not only endocrine cells, but direct reprogramming to neural cell, hepatocytes, and cardiac myocytes were reported soon after (*18-21*). However similar to the challenges encountered with differentiation from pluripotent cells, there remains the challenge of replicating developmental conditions *in vivo*. One possibility may be to attempt in situ direct reprogramming in the future.

3-3 Liver structure and function

The liver is the largest internal organ and plays an important role in metabolism. In the adult stage, the liver performs multiple functions including production of bile acids, metabolism and storage of glycogen, protein, lipids and detoxification of drugs, ammonia, alcohol. During the fetal stage of development, the liver becomes the major fetal hematopoietic organ. Although the liver dramatically changes its function during development, the molecular mechanisms regulating this change remains unclear.

Anatomically the liver is an organ consisting of several lobes. Each lobe is composed of a compact mass of hexagonally shaped functional units (known as hepatic lobes). These units are made up of liver cells arranged in plate-like single cell layers

that radiate from the central vein to the edge of each lobe. The intrahepatic bile duct, portal vein, and hepatic artery runs in parallel with each other within the connective tissue of the hepatic lobe. The sinusoidal space is the area where oxygen-rich blood from the hepatic artery and nutrient-rich blood from the portal vein are exchanged. Most of the liver parenchyma is occupied by hepatocytes. Non-parenchymal cells include cholangiocytes forming the bile duct and the sinusoid cells making up hepatic endothelia. Kupffer cells are the resident macrophages of the liver alongside hepatic stellate cells that store vitamin A. There are also the mesothelial and submesothelial cells that cover liver lobes. These non-parenchyaml cells constitute approximately 40% of the total number of liver cells.

3-4 Liver development

Liver organogenesis begins during early embryonic stages (around embryonic day 9: E9 in mouse). The liver bud is formed from the foregut endoderm. Expression of the Forkhead box proteins a1 (Foxa1) and Foxa2 are required in unison for opening compacted chromatin structures within liver specific target genes and the establishment of competence within the foregut endoderm (*22*). Foregut endodermal cells receive inductive signals such as FGFs from the adjacent cardiac mesoderm and bone morphogenetic protein (BMP) 2 and 4 from the septum transversum mesenchymes (STM) before migrating into it (*23, 24*). Adjacent endothelial cells are also required to form the liver bud. Repression of Wnt and Notch signal in hepatic endoderm by endothelial niche regulates hepatic endoderm expansion and hepatic specification (*25, 26*). The cells in the liver bud obtaining the differentiation ability both hepatocytes and cholangiocytes are hepatic stem/progenitor cells (hepatoblasts). Initially hepatoblasts

have the polarity and are columnars remaining gut morphology (*27*). The thickened liver bud epithelium is primarily a single pseudostratified cell layer. In the process of development, hepatoblasts acquire a pseudostratified morphology before delaminating into the stroma and proliferating to form the liver bud.

It had been reported that the homeodomain transcription factors, hematopoietically expressed homeobox (Hhex) and prospero homeobox 1 (Prox1) have an important role in hepatoblast proliferation and migration into the STM. In E9.0 Hhex-/- embryos, although hepatic endoderm cells transiently express liver genes, epithelium development arrests in a simple columnar state and the hepatoblasts fail to invade the STM (*28*). Prox1-/- mice die around E14.5 and they show a reduction in liver size. Although the differentiation markers Albumin and α-fetoprotein (AFP) are expressed, Prox1-/- hepatoblasts fail to migrate into the adjacent mesoderm because of the continuous basal lamina surrounding the liver bud (*29*). Liver growth is also blocked in H2.0-like homeobox (Hlx) -/- embryo. Since Hlx is normally expressed in visceral mesenchyme lying adjacent to the developing liver but not expressed in hepatoblasts, Hlx regulates a mesenchymal-epithelial type interaction that drives a vital growth phase in visceral organogenesis (*30*).

During the middle liver development stage, hematopoietic stem cells derived from aorta-gonad-mesonephros (AGM) migrate and highly proliferate in the liver. Hepatoblasts also proliferate at a high rate and live size increases dramatically as a result. The factors regulating hepatoblast proliferation and differentiation are secreted from adjacent cells. Oncostatin M (OSM), encoded by one of the interleukin-6 family genes, is secreted from hematopoietic cells that proliferate within the middle stage liver and induces metabolic enzyme gene expression in hepatoblasts (*31*). Pleiotrophin (Ptn)

and midkine (Mdk) secreted from mesothelial cells and submesothelial cells are related to hepatoblast proliferation (*32, 33*). During the late liver developmental stage, hepatoblasts begin to differentiate into hepatocytes and cholangiocytes. At around E14.5, hepatoblasts near the portal vein receive the inductive signals from periportal mesenchymal cells and differentiate into cholangiocytes. Differentiated hepatoblasts form a monolayered ring of biliary cells and a ductal plate is formed around the periportal mesenchyme. Around E15.5, some parts of the ductal plates become bilayered. The portal vein side cells become ductal cells whilst the parenchymal side cells eventually become hepatocytes. The lumen appears between the bilayered cells and forms the duct tube afterwards. Transforming growth factor beta (TGFβ), Wnt, Notch pathway, hepatocyte growth factor (HGF) and epidermal growth factor (EGF) signals are all know to be related to hepatoblast differentiation into cholangiocytes. Jagged1+/- and Notch2+/- (notch ligand genes) double heterozygous mice have defects in bile duct epithelial cell differentiation and morphogenesis (*34*). Human Alagille syndrome patients with autosomal dominant mutations in Jagged1 have defects with the intrahepatic biliary duct (*35-37*).

3-5 Liver research areas

Proliferation and differentiation of hepatoblasts are regulated by both intrinsic factors such as gene expression and extrinsic factors such as a cell-cell interactions with non-parenchymal cells and hematopoietic cells. However, the molecular mechanisms regulating proliferation and differentiation of hepatoblasts remain unknown particularyly in human because *in vivo* analyses of human cells are difficult. To reveal these mechanisms, many *in vivo* analyses using gene deficient animals and *in vitro*

analyses using primary hepatoblasts and hepatic progenitor cell lines were examined. In mice studies, to identify hepatoblasts, mouse fetal livers were collagenased and dissociated cells were used for fluorescence-activated cell sorter (FACS) screening of surface antibodies. Each cell fraction was sorted onto culture dishes and evaluated for their colony forming ability and gene expression of hepatocytic and cholangiocytic markers. From the results large colonies from single cells expressing the hepatocyte marker Albumin and cholangiocyte marker cytokeratin 19 (CK19)-positive were detected in the liver from E9.5 to E14.5. Mouse hepatoblast-specific surface markers, such as delta-like 1 homolog (Dlk), Liv2, CD13, and CD133 were also identified (*38-41*).

Using these specific surface markers and *in vitro* culture of purified hepatoblasts, it was revealed that the interaction with mouse embryonic fibroblast (MEF) cells promoted proliferation of hepatoblasts. In addition, it had been discovered that several transcription factors such as Prox1, T-box3 (Tbx3) and Sall4 regulate proliferation and differentiation of hepatoblasts (*42-44*). However, it remains difficult to maintain the characteristics of hepatoblasts over long-term culture and challenging to differentiate into mature functional hepatocytes *in vitro*. It is clear that much more detailed analyses of hepatoblasts are needed. In humans, because *in vivo* analyses of human cells are difficult, it is necessary to establish *in vitro* culture methods of human hepatoblasts for the analysis of the molecular mechanisms regulating these cells.

Taken together, in order to reveal the molecular mechanisms regulating hepatoblasts proliferation and differentiation from the middle to the late fetal stages, different appraoches were attempted in this study. One is an *in vitro* expansion system to generate human iPS cell-derived hepatic progenitor-like cells that exhibit bipotent

differentiation potential. Here the optimum *in vitro* culture conditions of these hepatic progenitor-like cells for proliferation were optimized that allowed the retaintion of their characteristics. However, it is still difficult to induce differentiaton of these human iPS-derived hepatic progenitor-like cells into mature hepatocytes. Using already established methods *in vitro*, I could not induce hepatic function of these progenitor cells to the same level of *in vivo* hepatocytes. One of the reasons is that the molecular mechanisms governing hepatoblast maturation are still uncertain especially in human. To reveal the molecular mechanisms of hepatoblasts maturation during development, in the other work, I focused on the difference between hepatoblasts and mature hepatocytes. $p57^{Kip2}$ is one of the cell cycle repressor genes. It is highly expressed in hepatoblasts in fetal livers but not in adult hepatocytes. It was reported that $p57^{Kip2}$-/- mice had sever developmental abnormality and died soon after birth. As $p57^{Kip2}$ might be an important gene for development, I had been working on "the identification of $p57^{Kip2}$ function in liver development". In this work, I examined the proliferation and differentiation abilities of $p57^{Kip2}$-/- hepatoblasts using $p57^{Kip2}$-/- mice and chimeric mice. Through this study, I got several results suggesting that $p57^{Kip2}$-/- mesenchymal cells regulate hepatoblasts maturation. It is hoped this dual integrative approach into elucidating regulatory mechanisms of liver development may lead to improve clinical outcomes in the future.

4 An *in vitro* expansion system for generation of human iPS cell-derived hepatic progenitor-like cells exhibiting a bipotent differentiation potential

4-1 Introduction

The differentiation from iPS cells into hepatic lineage cells *in vitro* is thought to be mimicking the same step-wise developmental processes *in vivo*. This makes it possible to obtain hepatic progenitor-like cells (HPCs) from human iPSCs at a similar developmental time point during the differentiation process. It had been previously reported that several endodermal lineage cells such as pancreatic β cells, hepatocytes, and intestinal epithelial cells could be generated from human pluripotent stem cells (*45*). In addition to that, it has recently been shown that hepatic progenitor cells that were differentiated from human ES cells could be prospectively isolated using the cell surface marker N-cadherin (*46*). However, methods for effective purification and cultivation of human iPS-derived HPCs have not been well established. We previously found that CD13 and CD133 are mouse hepatic progenitor-specific cell surface markers expressed during the early and middle (E 9.5–14.5) stages of fetal development (*40, 41*). Mouse $CD13^{+}CD133^{+}$ cells from the middle stage of fetal liver development express hepatic genes and can differentiate into hepatocytic cells and cholangiocytic cells both *in vitro* and *in vivo*. However, it remains unknown whether these mouse hepatic progenitor-specific markers are common to human hepatic progenitor cells. In addition, we previously reported that mouse embryonic fibroblasts (MEFs) have the ability to support *in vitro* proliferation of mouse hepatic progenitors and hepatic gene expression (*41*). As mentioned previously non-parenchymal liver cells are important for the development of hepatic progenitor cells and their further distinction eventually into

becoming either hepatocytes or cholangiocytes. In this study, MEF cells are used to substituted for non-parenchymal cells in the liver and applied in a co-culture system with human iPS cell-derived HPCs in an attempt to replicate the same developmental conditions that are found *in vivo*. Overall the aim is to optimize culture conditions that permits the generation of HPCs from human iPS cells, which can be prospectively isolated by identification of the cell surface markers CD13 and CD133. In order for the clinical application of these cells to become feasible, it will also be necessary to demonstrate the possibility of their maintenance over long-term cultures whilst retaining their bipotent differentiation potential towards either hepatocytes or cholangiocytes.

4-2 Materials and Methods

Human iPS and ES cells and other-types of cells

A human iPS cell line, TkDA3-4, was established from human dermal fibroblasts (Cell Applications, Inc., San Diego, CA) as described previously (*47*). Human ES cells (KhES-3) were obtained from the Institute for Frontier Medical Sciences, Kyoto University (Kyoto, Japan), with approval for human ES cell use granted by the Ministry of Education, Culture, Sports, Science, and Technology of Japan (*48*). The Review Board of the Institute of Medical Science, The University of Tokyo, approved this research. The entire study was conducted in accordance with the Declaration of Helsinki. Human ES cells and human iPS cells were maintained according to previously described standard methods (*47*). Briefly, they were cultured on irradiated mouse embryonic fibroblasts in Dulbecco's modified Eagle's medium/F-12 medium (DMEM/F-12; Sigma, St. Louis, MO) supplemented with 0.1 mM nonessential amino acids (Invitrogen, Carlsbad, CA), 1× penicillin streptomycin glutamine (Sigma), 20% knockout serum replacement (Invitrogen), 0.1 mM 2-mercaptoethanol (Invitrogen), and 5 ng/ml recombinant human basic fibroblast growth factor (basic FGF; Wako Pure Chem., Osaka, Japan). These cells were maintained on mitomycin C (Wako Pure Chem.)-treated MEFs. ES and iPS cells were passaged every 5 days to maintain them in an undifferentiated state.

HepG2 (RCB1886) cells were provided by RIKEN BRC through the National Bio-Resource Project of the MEXT, Japan. Cryopreserved human hepatocytes (Lot HEP187242; BioPredic International, Rennes, France) were used.

Preparation of MEFs

E13.5 ICR or C57BL/6-Tg (CAG-EGFP) mouse embryos (Nihon SLC, Shizuoka, Japan) were dissected, and the head and internal organs were completely removed. The torso was minced and dissociated in 0.05% trypsin-EDTA (Sigma) for 30 min. After washing with phosphate-buffered saline (PBS; Sigma), cells were expanded in DMEM (Sigma) supplemented with 10% fetal bovine serum (FBS; Invitrogen) and 1× penicillin streptomycin glutamine. MEFs were treated with mitomycin C at 37 °C for 2 h and used as feeder cells. Animal experiments were performed with approval of the Institutional Animal Care and Use Committee of the Institute of Medical Science, the University of Tokyo (permit number: PA09-21) and the Institutional Animal Care and Use Committee of Tokai University (permit number: 122047).

Differentiation from human iPS cells toward the hepatic lineage and isolation of HPCs

For hepatic lineage cell differentiation, semi-confluent human iPS cells were cultured in RPMI 1640 (Sigma) containing 2% B27 supplement (Invitrogen). Cells were stimulated with 100 ng/ml recombinant human activin A (PeproTech, Rocky, NJ) at day 0–4, 10 ng/ml basic FGF and 20 ng/ml recombinant human BMP-4 (PeproTech) at day 5–8, and 40 ng/ml recombinant human HGF (PeproTech) at day 9–12. Cells were cultured at 37°C in a 10% O_2 incubator at day 0–4 and in 5% O_2 at day 5–12.

HPCs were isolated from human iPS cells stimulated with cytokines. After 12 days of culture, cells were trypsinized using 0.05% trypsin-EDTA (Sigma). Trypsinized cells were washed with PBS containing 3% FBS, and then incubated with antibodies against cell surface proteins (shown in **Table 1**) for 1 h at 4°C. After washing with PBS containing 3% FBS and staining the dead cells with propidium iodide, the cells were analyzed and sorted using a MoFlo™ fluorescence-activated cell sorter (Dako, Glostrup,

Denmark).

HPC culture and passaging

Mitomycin C-treated MEFs (2×10^5 cells/well) were plated onto 0.1% gelatin (derived from porcine skin; Sigma)-coated 12-well plates the day before sorting. $CD13^{high}CD133^+$ cells were sorted onto MEF feeder layers plated at a low density (280 cells per cm^2). The standard culture medium was a 1:1 mixture of hepatic colony-forming unit (H-CFU-C) medium and DMEM. H-CFU-C medium consisted of DMEM/F-12 supplemented with 10% FBS (Nichirei Biosciences, Tokyo, Japan), 1× Insulin-Transferrin-Selenium X (Invitrogen), 10 mM nicotinamide (Sigma), 10^{-7} M dexamethasone (Sigma), 2.5 mM HEPES buffer solution (Invitrogen), 1× penicillin streptomycin glutamine, and 1× nonessential amino acids. For expansion, the cells were cultured in standard medium supplemented with 0.25 mM A-83-01 (Tocris Bioscience, Bristol, United Kingdom), 10 mM Y-27632 (Wako Pure Chem.), 40 ng/ml HGF, and 20 ng/ml recombinant human epidermal growth factor (EGF; PeproTech). The medium was replaced every 3 days. After 10–12 days of culture, colonies formed by individual human iPS cell-derived $CD13^{high}CD133^+$ cells were trypsinized using 0.05% trypsin-EDTA and replated onto freshly plated MEFs.

Isolation of secondary $CD13^+$ and/or $CD133^+$ cells from human iPS cell-derived HPCs

After differentiation of human iPS cells induced by cytokines, $CD13^{high}CD133^+$ cells were cultured on MEFs derived from C57BL/6-Tg (CAG-EGFP) mice. After 12 days of culture, HPC colonies were trypsinized and stained with PE- and APC-conjugated antibodies against human CD13 and CD133, respectively. $CD13^+$

and/or $CD133^+$ cells in the GFP-negative fraction were sorted using a MoFlo™ fluorescence-activated cell sorter. Sorted cells were seeded onto freshly plated MEFs, and the colony forming activities of these cells were analyzed.

Non-obese Diabetic/Severe Combined Immunodeficiency (NOD/SCID) Xenograft Transplantation

NOD/SCID mice were purchased from Sankyo Laboratory Co. Ltd. (Tsukuba, Japan). 1×10^6 cells or 5×10^5 cells of the human liver cancer cell line (PLC/PRF/5) and the human iPS cell-derived HPCs (from third colony culture) were suspended in 110-120 μl DMEM supplemented with 1.5% knockout serum replacement and 50% Matrigel (BD Biosciences, Bedford, MA) and transplanted to the male NOD/SCID mice (6 weeks old) under anesthesia. PLC/PRF/5 cells and HPCs were injected into the subcutaneous space of the left and right back, respectively. Tumor formation was monitored by observation for 6 weeks.

Immunocytochemistry

Cultured cells were washed with PBS and fixed with 4% paraformaldehyde/PBS. After three washes with PBS, cells were permeabilized with 0.25% Triton X-100 (Sigma)/PBS for 10 min, washed with PBS, and incubated with 5% donkey serum (Millipore, Bedford, MA) in PBS for 1 h at room temperature. The cells were then incubated with diluted primary antibodies either overnight at 4°C. Primary antibodies are listed in **Table 1**. The cells were washed with PBS several times, and then incubated with diluted secondary antibodies for 40 min at room temperature. Then, the cells were washed with PBS and their nuclei were stained with

4',6-diamidino-2-phenylindole dihydrochloride (DAPI; Sigma). Normal goat IgG (Santa Cruz Biotechnology, Santa Cruz, CA), negative control mouse IgG1 (Dako), and normal rabbit IgG (Santa Cruz Biotechnology) were used as negative controls for the appropriate antibodies. Colonies were imaged under a Carl Zeiss Axio Observer Z1 using AxioVision version 4.8 software (Carl Zeiss, Jena, Germany). α-fetoprotein (AFP)- and hepatocyte nuclear factor 4α (HNF4α)-positive colonies were counted using an ArrayScan VTI HCS Reader (Thermo Scientific, Waltham, MA).

Induction of mature hepatocytic functional genes by spheroid formation

Colonies derived from $CD13^{high}CD133^{+}$ cells were trypsinized with 0.05% trypsin-EDTA, washed in DMEM containing 10% FBS, and counted. The culture medium for spheroid formation was DMEM supplemented with 10% FBS, 1× nonessential amino acids, 1× penicillin streptomycin glutamine, and 10^{-7} M dexamethasone, with or without 20 ng/ml recombinant human OSM (R&D Systems, Minneapolis, MN). Individual drops (40 ml) containing 1×10^{4} cells were plated on the inside of lids of 100-mm dishes containing PBS (to avoid desiccation). After 3 days of culture, the spheroids were collected and analyzed.

Real-time RT-PCR analysis

For analysis of hepatic functional gene expressions, total RNA was extracted from human iPS cells, colonies derived from $CD13^{high}CD133^{+}$ cells, and spheroids using TRIzol (Invitrogen). First-strand cDNA synthesized using a High Capacity cDNA Reverse Transcription Kit (Life Technologies, Carlsbad, CA) was used as a template for PCR amplification. For semiquantitative RT-PCR, cDNA samples were normalized by

the number of hypoxanthine phosphoribosyltransferase 1 (HPRT1) mRNA copies. The Universal Library (Roche Diagnostics, Basel, Switzerland) was used for quantitative RT-PCR assays of AFP, catechol-O-methyltransferase (COMT), chemokine (C-X-C motif) receptor 4 (CXCR4), cytochrome P450 (CYP) 3A4, CYP3A7, CYP7A1, epoxide hydrolase 1, microsomal (xenobiotic) (EPHX1), flavin containing monooxygenase 5 (FMO5), goosecoid homeobox (GSC), hematopoietically expressed homeobox (HHEX), hepatocyte nuclear factor (HNF) 3β, HNF4α, HPRT1, monoamine oxidase A (MAOA), MAOB, Mix paired-like homeobox (MIXL1), one cut homeobox 1 (ONECUT1), SRY-box containing gene 17 (Sox17), sulfotransferase family, cytosolic, 1A, phenol-preferring, member 1 (SULT1A1), SULT1A2, and T transcripts. The primer sequences and probe numbers for each gene are shown in **Table 2**.

Induction of cholangiocytic cyst formation by human iPS cell-derived CD13^{high}CD133^{+} cells

Colonies derived from CD13^{high}CD133^{+} cells were trypsinized using 0.05% trypsin-EDTA, washed in DMEM containing 10% FBS, and then counted. The cells were then combined with an extracellular matrix gel consisting of a mixture of 40% collagen type-I (Nitta Gelatin, Osaka, Japan) and 40% Matrigel (BD Biosciences, Bedford, MA), and cultured in 24-well culture plates (1500 cells/50 ml extracellular matrix gel/well). After the 10 min incubation, culture medium was added, followed by incubation for 10–12 days with medium changes every 3 days. The culture medium was a 1:1 mixture of H-CFU-C medium and DMEM/F-12 supplemented with 2% B27 supplement, 0.25 mM A-83-01, 10 mM Y-27632, 20 ng/ml EGF, 40 ng/ml HGF, 40 ng/ml recombinant human Wnt-3a (R&D Systems), and 100 ng/ml recombinant human

R-spondin 1 (PeproTech). Cysts in gels were stained according to previously described methods (*49*), and analyzed under a LSM700 confocal microscope (Carl Zeiss). The antibodies are listed in **Table 1**.

Albumin secretion assay

To detect human albumin secretion, colonies from human iPS cell-derived HPCs (3rd culture) were cultured for a long time (19 days). These cells were differentiated by cell-cell interactions. The differentiated cells and HepG2 cells (standard control) were incubated for 3 days in hepatocyte differentiation medium (DMEM supplemented with 10% FBS, 1× nonessential amino acids, 1× penicillin streptomycin glutamine, 10^{-7} M dexamethasone, 1% dimethyl sulfoxide). Conditioned medium was saved and debris was removed by centrifugation. Human albumin was detected using a Human Albumin ELISA Quantitation Set (Bethyl Laboratories, Montgomery, TX) according to the manufacturer's protocol.

Statistics

Calculations of statistically significant differences between samples using the Student's two-tailed t test as well as the standard deviation (SD) were performed using Microsoft Excel 2007 software.

4-3 Results

Differentiation from human iPS cells toward hepatic lineage cells

Human ES cells and iPS cells have been reported to differentiate into hepatocytes using a stage-wise process that mimics developmental processes (*50, 51*). I speculated that human iPS cell-derived hepatic lineage cell cultures contained HPCs induced by several cytokines such as activin A, basic FGF, BMP-4, and HGF. For hepatic lineage cell differentiation, TkDA3-4 human iPS cells were seeded onto mitomycin C-treated MEFs and stimulated with the cytokines shown in **Figure 1A**. After 12 days of culture, expressions of fetal hepatocytic markers (AFP and HNF4α) were observed in cells stimulated with cytokines (**Figure 1B**). I then tried to isolate HPCs from hepatic lineage cell cultures. As shown previously, several cell surface proteins, such as CD34, CD44, CD49f, CD56, CD117, CD326, and CXCR4, have been used for specific markers of endodermal cells, hepatic progenitor cells, or fetal hepatic cells (*52-57*). We recently found that CD13 and CD133 are specific cell surface markers for mouse hepatoblasts (*40, 41*). To characterize human iPS cell-derived hepatic lineage cells, undifferentiated human iPS cells and cells cultured with or without cytokines were analyzed with antibodies against hepatic progenitor cell-related surface markers by flow cytometry. CD13 was barely expressed in human iPS cells, but was induced during the 12 days of culture without cytokines, indicating that spontaneous differentiation of human iPS cells generated $CD13^{mid}$ cells. Interestingly, $CD13^{high}$ cells were only detected in cultures stimulated with cytokines and expressed CD133, another hepatoblast surface marker (**Figure 1C**). In addition, the expression levels of CD13 and CD133 were increased during hepatic lineage differentiation (**Figure 2**). Moreover, $CD13^{high}CD133^{+}$ cells expressed other hepatic cell surface markers, CD49f and CD326

(**Figure 3A**, and data not shown). In contrast, expression of CD34 and CD56 was barely detected in $CD13^{high}CD133^{+}$ cells (**Figure 3B**). Expression of CD44 and CXCR4 were not significantly changed by the addition of cytokines (**Figure 1C**).

Expressions of differentiation marker genes during differentiation of human iPS cells

When differentiation of human pluripotent stem cells into endodermal cells was induced by addition of activin A, several differentiation marker genes were transiently upregulated (*57*). I analyzed the expressions of mesodermal and endodermal marker genes (GSC, CXCR4, Sox17, MIXL1, T [Brachyury], HNF3β, and hHex) and hepatocytic marker genes (AFP, HNF4α, and ONECUT1) (**Figure 4**). The hepatocytic marker gene expressions were highly increased when iPS cells were stimulated by HGF. I found that most cells derived from human iPS cells differentiated into AFP^{+} and $HNF4\alpha^{+}$ hepatocytic cells during my differentiation steps, although several cell clusters that could not differentiate into the hepatic lineage remained (**Figure 5A**). The pluripotency maker Oct3/4 was not expressed in the AFP^{+} hepatocytic cells at the end of the differentiation steps (**Figure 5B**). Part of AFP^{-} undifferentiated cell clusters expressed T (**Figure 5C**), indicating that expression of T was detected by RT-PCR at the end of the differentiation. In contrast, the expressions of other mesodermal and endodermal marker genes (CXCR4, Sox17, GSC, and MIXL1) were transiently upregulated at the endodermal differentiation stage (by stimulation with activin A) and decreased during hepatocytic differentiation. These results suggested that the iPS cells differentiated into hepatocytic cells through the definitive endodermal pathway.

Purification and *in vitro* culture of human iPS cell-derived CD13^{high}CD133^{+} cells

Next, I analyzed the characteristics of human iPS cell-derived cells expressing hepatic progenitor cell surface markers, CD13 and CD133. During fetal liver development, hepatic progenitor cells interact with non-parenchymal cells such as mesenchymal cells, fibroblasts, mesothelial cells and endothelial cells (*26, 32, 33, 58*). We recently established a co-culture system consisting of mouse early fetal hepatic progenitor cells and mesenchymal feeder cells (*41*). Cell-cell interactions with mesenchymal cells are required for effective expansion of early fetal hepatic progenitor cells *in vitro*. Thus, I sorted CD13^{high}CD133^{+} cells derived from human iPS cell cultures stimulated with cytokines (**Figure 6A**), and cultured the sorted cells on MEFs in H-CFU-C medium supplemented with EGF and HGF. After 12 days of culture, single CD13^{high}CD133^{+} cells produced colonies expressing both AFP and HNF4α (**Figure 6B**). These results suggest that the CD13^{high}CD133^{+} fraction contains HPCs. In this culture system, the addition of an ALK inhibitor, A-83-01, was required for effective expansion of CD13^{high}CD133^{+} cells (**Figure 7A**). The combination of A-83-01 and Y-27632 significantly increased the number of large colonies derived from CD13^{high}CD133^{+} cells. Based on these results, I used standard culture medium supplemented with EGF, HGF, A-83-01 and Y-27632 for expansion of human iPS cell-derived HPCs. To determine which fraction contained HPCs, I sorted the cultured cells into CD13^{-}, CD13^{mid}, CD13^{high}CD133^{-}, and CD13^{high}CD133^{+} fractions, and the cells were plated individually onto MEFs. After these cells were cultured, large single cell-derived colonies containing over 100 cells were obtained and counted. As shown in **Figure 7B**, I found that the CD13^{high}CD133^{+} fraction contained many HPCs and formed large colonies expressing AFP and HNF4α.

Long-term *in vitro* expansion of human iPS cell-derived HPCs

One of the most important characteristics of hepatic stem/progenitor cells is a high proliferative ability. To analyze whether human iPS cell-derived HPCs could proliferate in long-term cultures *in vitro*, colonies derived from $CD13^{high}CD133^{+}$ cells were trypsinized and replated onto new feeder cells. The number of cells was counted at each replating step. The cells continued to proliferate for more than 1 month (**Figure 8A**). After the 4th passage, the $HNF4\alpha^{+}$ human iPS cell-derived HPC colonies expressed the proliferation marker Ki67 (**Figure 8B**). In contrast, these HPC colonies did not express the pluripotency marker Oct3/4, which is expressed in human iPS cells (**Figure 8B** and **C**). Next, I analyzed the expression of hepatocytic and cholangiocytic marker genes in human iPS cell-derived HPCs at each replating step. Colonies were stained with specific antibodies against AFP, HNF3β, HNF4α and cytokeratin 7 (CK7). Expression of the endodermal marker, HNF3β, and hepatocytic markers, AFP and HNF4α, was observed in primary colonies and maintained during *in vitro* expansion (**Figure 9A**). In particular, human iPS cell-derived HPCs were able to proliferate for more than 3 months and still expressed the hepatocytic markers HNF4α and AFP (**Figure 12A** and **B**). Cholangiocytic marker CK7 was not expressed in primary colonies but was induced after several passages. A small number of cells in colonies of the 1st culture expressed albumin, a mature hepatocytic marker gene (**Figure 9B**). $CD13^{high}CD133^{+}$ cells derived from human iPS cells could expand *in vitro* over a long term whilst maintaining hepatocytic and cholangiocytic marker gene expression, indicating that these cells have hepatic progenitor-like potentials. Next, I analyzed *in vivo* tumor formation ability of these iPS-delived cells. PLC/PRF/5 cells, human

hepatocellular carcinoma cell line, could form tumors in NOD/SCID mice after transplantation. In contrast, human iPS cell-derived HPCs (derived from third colony culture) failed to form tumors (**Figure 10**). These results suggested that purified HPCs did not contatin non-differentiated pluripotent cells and some transformed cells.

As shown above, $CD13^{high}CD133^{+}$ cells spontaneously differentiated into CK7-positive cholangiocyte-like cells AFP and HNF4α-negative non-hepatocytic cells during passaging. To determine the cell fraction containing self-renewing cells after serial passaging, human iPS cell-derived HPC colonies at each replating step were analyzed using antibodies against CD13 and CD133 (**Figure 11**). In addition to the $CD13^{+}CD133^{+}$ fraction, $CD13^{-}CD133^{+}$, $CD13^{+}CD133^{-}$ and $CD13^{-}CD133^{-}$ fractions were found in cultures derived from human iPS cell-derived $CD13^{high}CD133^{+}$ cells, indicating that HPCs spontaneously differentiated and lost expression of CD13 and CD133. I analyzed the colony-forming activities of these fractions at replating steps. Cells at each replating step were sorted and cultured on MEFs for 12 days, and then HNF4α-positive colonies derived from each fraction were counted **(Figure 11B-D**). The rate of HNF4α-positive colony formation was high in cultures derived from $CD13^{+}CD133^{+}$ cells at each replating step. Interestingly, $CD13^{+}CD133^{-}$ cells after several passages also formed many HNF4α-positive colonies. These results suggest that CD13 is likely to be a useful surface marker to purify self-renewing HPCs after serial passaging. Next, I analyzed whether the $CD13^{+}$ cells among human iPS cell-derived HPCs had self-renewal potency. When human iPS cell-derived HPCs were passaged twice, the 3rd cultured-cells were stained with suitable antibodies, and $CD13^{+}$ and $CD13^{-}$ cells were sorted. After 11 days of culture, the expanded colonies (4th culture) derived from $CD13^{+}$ and $CD13^{-}$ cells were analyzed by flow cytometry (**Figure 10C**).

Interestingly, the HPC colonies derived from $CD13^+$ cells contained many $CD13^+$ cells. In contrast, the HPC colonies derived from $CD13^-$ cells barely contained $CD13^+$ cells. I obtained similar results using the 5th cultured-cells. In addition, I compared the colony-forming abilities of $CD13^+$ and $CD13^-$ cells in the 5th culture. As shown in **Figure 12D**, $CD13^+$ cells were able to form colonies more efficiently than $CD13^-$ cells. These results suggested that $CD13^+$ cells maintained the self-renewal-like ability to proliferate for a long time. On the other hand, my preliminary data suggested that $CD13^-$ cells had cholangiocytic progrnitor cell-like characteristics.

Differentiation of human iPS cell-derived HPCs toward both mature hepatocytic and cholangiocytic cells

Hepatic progenitor cells in fetal liver development have a bipotent differentiation ability toward hepatocytes and cholangiocytes (*54, 59*). Therefore, I assessed whether human iPS cell-derived HPCs had the potential to differentiate into mature hepatocytic cells. To maintain and induce the functions of mature hepatocytes *in vitro*, three-dimensional (3D) biological structures are known to be important (*60-62*). For this purpose, the hanging drop method is often used to self-assemble hepatic stem/progenitor cells into 3D aggregates (spheroids). For human iPS cell-derived hepatocytic differentiation, human iPS cell-derived HPCs in the 3rd culture were trypsinized and suspended in hepatocyte medium supplemented with dexamethasone, with or without OSM, for spheroid formation (**Figure 13A**). After 3 days of spheroid culture, the expressions of hepatic functional genes in human iPS-derived cells were compared with those in primary human hepatocytes (**Figure 14**). Both phase 1 enzymes (CYP3A4, CYP3A7, CYP7A1, EPHX1, FMO5, and MAOB) and phase 2 enzymes

(COMT and SULT1A2) were expressed in spheroids derived from human iPS cell-derived HPCs from the 3rd culture. Except for MAOA, the expression levels of mature hepatocyte functional marker genes in spheroids without OSM were higher than those in spheroids with OSM. The expressions of several functional genes in human iPS-derived spheroids were significantly lower than those in primary hepatocytes, whereas mature hepatocyte functional marker genes, FMO5, MAOA, MAOB, and SULT1A2, were expressed highly or at similar levels compared with a previous report on human ES and iPS cell-derived hepatocytic cells (*63*). Although, it was reported that OSM promoted hepatoblast maturation (*31*), OSM did not affect HPCs maturation except for the MAOA expression. Several studies described that OSM is used at a final step of differentiation of human ES and iPS cells into mature hepatocytes in plate culture (*64*). In contrast, our 3D culture of hepatoblasts might not require OSM for hepatic maturation. In addition, Standard Deviations of these samples were high, suggesting that the induction of HPC-maturation by spheroid formation was regulated by some unstable mechanism.

Albumin secretion is one of the most important functions of mature hepatocytes. I cultured human iPS cell-derived HPCs at a high density for a long time and induced hepatic maturation by cell-cell interactions (*65*). The HPCs in the high-density culture exhibited significant expression of albumin (**Figure 13B**). Subsequently, the amounts of albumin protein in the conditioned culture media were analyzed by enzyme-linked immunosorbent assays. I compared the albumin secretion levels in these HPCs with those in HepG2 cells. As shown in **Figure 13C**, the albumin secretion levels of HPCs were higher than those of HepG2 cells, and the secreted protein levels were similar to those in a previous report on human iPS cell-derived

hepatocytic cells (*63*). These results suggest that human iPS cell-derived HPCs have the potential to differentiate into mature hepatocytic cells after *in vitro* expansion.

It has been reported that cholangiocytic cells form cysts with an epithelial polarity, demonstrating *in vitro* tubulogenesis in an extracellular matrix gel supplemented with cytokines (*49*). I therefore examined whether human iPS cell-derived HPCs could form a cholangiocytic structure during 3D-gel culture. Human iPS cell-derived HPC colonies were trypsinized and cultured in an extracellular matrix gel supplemented with EGF, HGF, R-spondin 1, Wnt-3a, A-83-01, and Y-27632. After 12 days of culture, many epithelial cysts were formed. I analyzed the expression of F-actin, protein kinase Cζ (PKCζ), integrin α6 (CD49f) and β-catenin as markers for the apical and basolateral domains (*49*). Luminal space surrounded by F-actin bundles and PKCζ was detected, and the expression of integrin α6 and β-catenin was located at the basolateral region (**Figure 15A**). Some of these epithelial cysts expressed CK7 but not expressed hepatocytic marker AFP (**Figure 15B**). CK19, another cholangiocytic marker, was also expressed in these cysts (data not shown). It is suggesting that these cells could form cholangiocyte-like cyst structures with an epithelial polarity. These results indicate that human iPS cell-derived HPCs exhibit a bipotent differentiation ability toward hepatocytes and cholangiocytes.

Purification and expansion of HPCs derived from human ES cells

Differentiated human ES cells (KhES-3) toward hepatic lineage cells also contained $CD13^{high}CD133^{+}$ cells (**Figure 16A**). These human ES cell-derived $CD13^{high}CD133^{+}$ fractions formed large colonies on MEFs in H-CFU-C medium supplemented with EGF, HGF, A-83-01, and Y-27632. To analyze whether human ES

cell-derived $CD13^{high}CD133^{+}$ cells could proliferate in long-term cultures *in vitro*, colonies from human ES cell-derived $CD13^{high}CD133^{+}$ cells were trypsinized and replated onto new feeder cells. Similar to the results for human iPS cells, human ES cell-derived $CD13^{high}CD133^{+}$ cells continued to proliferate for a long time (at least 1 month). $CD13^{high}CD133^{+}$-derived colonies expressed the hepatocytic markers AFP and HNF4α and the endodermal marker HNF3β (**Figure 16B**). A small number of cells in colonies of the 1st culture expressed albumin (**Figure 16C**). The proliferation marker Ki67 and HNF4α were also expressed in human ES cell-derived $CD13^{high}CD133^{+}$-derived colonies after the culture passage (**Figure 17**). These cells did not express Oct3/4. The cells had hepatic progenitor-like potential, similar to HPCs from human iPS cell-derived $CD13^{high}CD133^{+}$ cells. These results indicate that my methods are useful for expansion of HPCs derived from not only human iPS cells, but also human ES cells.

4-4 Discussion

In the present study, I showed that CD13 and CD133 are specific cell surface markers of HPCs derived from human iPS cells. When human iPS cells were stimulated with the necessary cytokines, a population of cells began to express CD13 and CD133 and could be expanded over long-term culture. CD13 and CD133 are specific markers of mouse fetal and adult liver progenitor cells (*40, 41, 66*). CD13 is also expressed in human liver cancer stem cells (*67*). CD133 is known as an important stem cell marker because many types of cancer stem cells and somatic stem/progenitor cells such as neural, intestine and hematopoietic stem cells, express this cell surface marker (*68-71*). These results suggest that somatic and cancer stem/progenitor cells share similar cell surface proteins. A population of human iPS cells cultured without cytokines spontaneously expressed moderate levels of CD13. In contrast, $CD13^{high}CD133^{+}$ cells were only detected in cultures with appropriate cytokine stimulation. Current protocols for induction of the hepatocytic lineage cells from human iPS cells have been established by mimicking the events that occur during developmental stages. Such protocols generally contain 4 steps: (1) induction of endodermal progenitor cells by activin A, (2) hepatocytic specification by basic FGF and BMP-4, (3) differentiation to hepatic stem/progenitor-like cells by HGF, (4) maturation to hepatocytes by OSM. I purified HPCs derived from human iPS cells when these cells were cultured at step (3). Previously it was reported that self-renewing endodermal progenitors could be derived from human ES cells and iPS cells (*45*). These cells expressed both CD117 and CXCR4, endodermal progenitor cell markers and were multipotent in their capacity to differentiate into pancreatic, hepatic, and intestinal cells. In contrast, CXCR4 was not expressed in primary hepatoblasts derived from mouse fetal livers (data not shown). In

this study, $CD13^{high}CD133^{+}$ HPCs also did not express an endoderm progenitor marker CXCR4 but express a hepatoblast marker AFP (**Figure 1C**). These results suggested that our cells resembled hepatoblasts but not endodermal progenitor cells. A previous study reported that N-cadherin was a cell surface marker of hepatic progenitor cells derived from human ES cells stimulated with activin A and basic FGF. However, only a few cells in N-cadherin-positive populations can form large hepatocyte colonies (*46*). In contrast, the present study clearly indicated that the usage of CD13 and CD133 in combination with our culture condition could purify hepatic progenitor-like cells more effeiciently.

A-83-01 and Y-27632 were important for the expansion of human iPS cell-derived HPCs. Human ES and iPS cells are not able to survive as single cells because activation of the Rho-Rock signal induces blebbing and apoptosis of these cells (*72*). Survival and expansion of hepatic progenitor cells derived from early fetal and adult livers are also induced by ROCK inhibition (*41, 66, 73*). Further clarification is necessary regarding the exact cause of the beneficial effects as to whether inhibition of ROCK acts in anti-apoptosis and/or proliferation of human iPS cell-derived HPCs. The TGFβ and ALK signaling pathways are known to be involved in regeneration and epithelial-mesenchymal transition of liver cells (*74*). In this study, I found that inhibition of the ALK signal is required for colony formation by HPCs. The molecular mechanisms of ALK inhibition of human iPS cell-derived HPCs remain unknown. It was reported that phosphorylation of Smad family proteins, Ras/mitogen-activated protein kinase (MAPK) signals, phosphoinositide 3-kinase (PI3K)/Akt signals, p38 signals, c-jun N-terminal kinase (JNK) signals, and Rho-Rock signals lay downstream of TGFβ-ALK signals. However, inhibition of Ras/MAPK signals, PI3K/Akt signals,

p38 signals, and Rho-Rock signals did not have an effect on HPCs colony forming ability (data not shown). Although more detailed analyses are needed, activation of TGFβ-ALK signals, such as phosphorylation of Smad family proteins or JNK signals might cause cell cycle arrest or epithelial-mesenchymal transition of HPCs.

It has been reported that iPS cells generated by retroviral vectors re-express Yamanaka factors in culture during differentiation of several cell types (*47, 75*). In our culture system, HPCs derived from human iPS cells could proliferate over a period of 1 month, whilst retaining bipotent differentiation ability. Interestingly, there was no re-activation of exogenous Yamanaka factors (Oct3/4, Klf4, Sox2, and c-Myc) during expansion of these cells, suggesting that exogenous genes (particularly c-Myc) were not involved in the proliferative ability of our HPCs (data not shown). Cell cycle-dependent kinases and their inhibitors are important regulators for the cell cycle and long-term proliferation of stem/progenitor cells. During *in vitro* expansion of mouse hepatocytic cells, up-regulation of $p19^{ARF}$ ($p14^{ARF}$ in human cells) induces cell cycle arrest and senescence (*76*). In contrast, activation of $p16^{Ink4a}$ and $p14^{ARF}$ was detected during the long-term proliferation of human iPS cell-derived HPCs (data not shown). These results suggest that there may be unknown mechanisms regulating the cell cycle of these cells *in vitro*. Clarification of these mechanisms may be useful *in vivo* hepatic progenitor cell culture conditions.

Analyses of human hepatic progenitor cells are difficult because of the shortage of human fetal tissue samples and culture systems. In this regard, my human HPCs derived from iPS cells might be useful for the analysis of human hepatic cell development. In addition, mature hepatocytes can barely maintain a proliferative ability following cryopreservation, whereas my human iPS cell-derived HPCs have a high

proliferate ability even after cryopreservation. In contrast, as shown by my and other group studies, the hepatic maturation level was significantly low in the hepatic cells derived human iPS cells *in vitro*. Therefore, the involvement of methods to induce maturation of iPS cell-derived HPCs are important. After cell transplantation into the injured livers, hepatic progenitor cells maturated and acquired hepatic functions *in vivo* (Kakinuma and Kamiya, unpublishded data). This suggests that the *in vivo* liver environment is useful for induction of hepatic maturation. To reveal whether huan iPS cell-derived HPCs have the potential to proliferate and differentiate both into mature cells, further analyses are important. However, I think that *in vitro* expansion system presented here may contribute to regenerative therapies of liver diseases using functional human hepatic progenitor cells and hepatocytes.

4-5 Figures

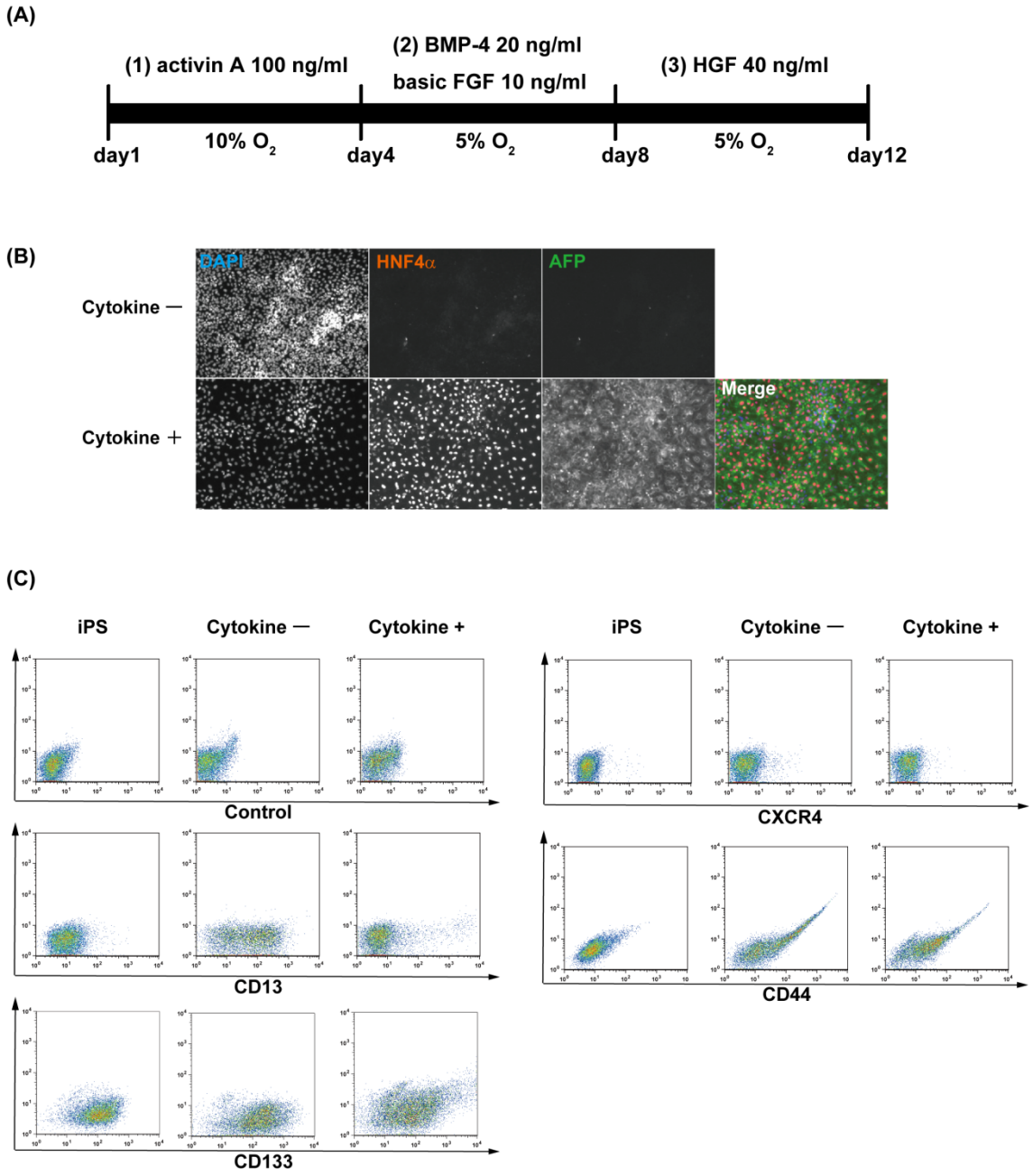

Figure 1. Differentiation from human iPS cells toward hepatic lineage cells.

(A) Schematic of the experimental procedure. Human iPS cells were sequentially stimulated with various cytokines: (1) activin A, (2) basic FGF and BMP-4, and (3) HGF. The cells were cultured in 10% O_2 for days 0–4 and 5% O_2 for days 5–12. (B) After 12 days of culture with or without cytokines, cells were stained with antibodies against AFP and HNF4α. Nuclei were counterstained with DAPI. (C) Expression of cell surface markers in human iPS cell-derived hepatic lineage cells.

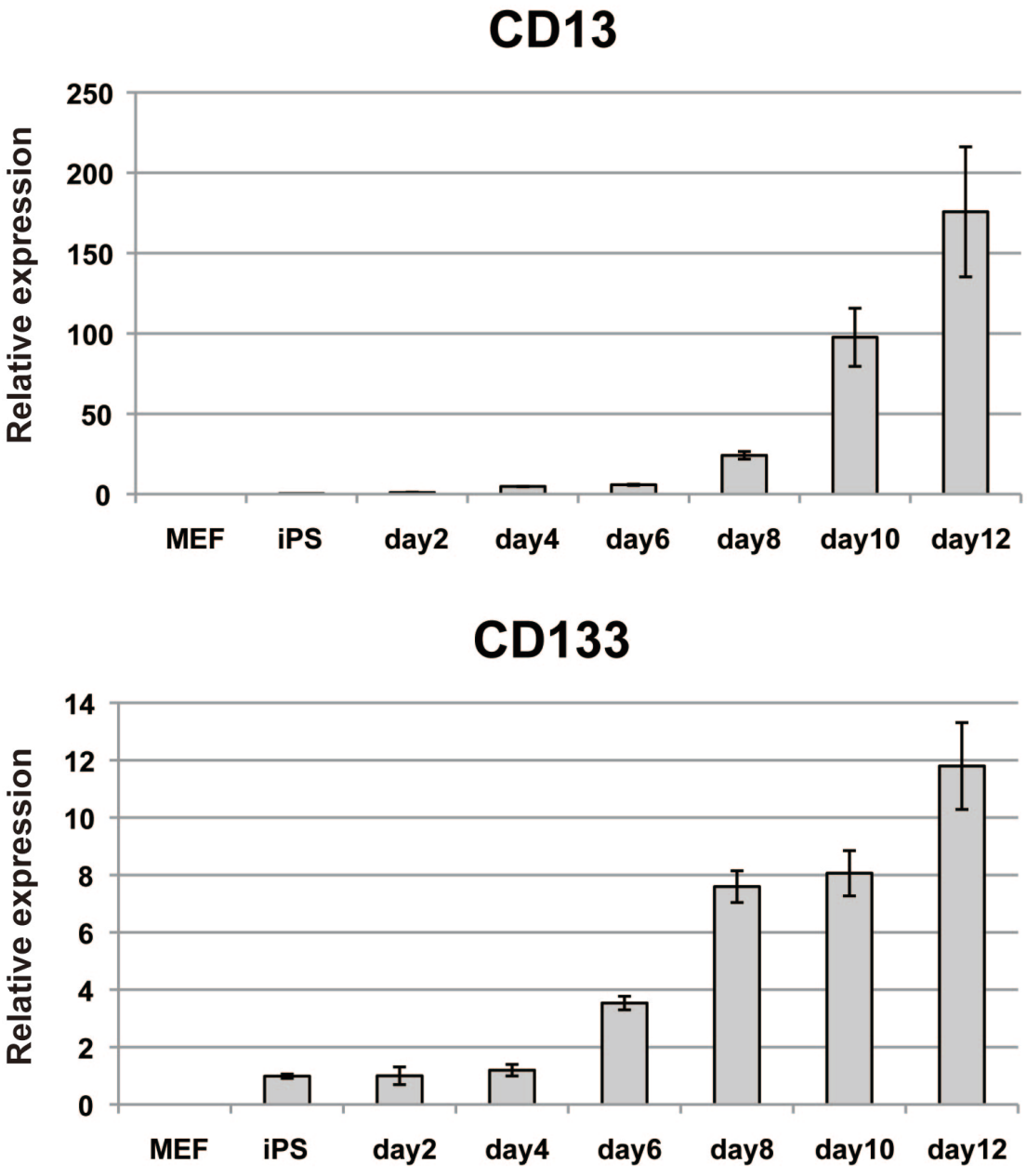

Figure 2. Expression of CD13 and CD133 in human iPS cell-derived cells.

Expressions of CD13 and CD133 were examined in normal human iPS cells (iPS) and differentiated iPS cells. For quantitative PCR analyses, total RNAs were purified from iPS cells in the differentiation culture at each step from day2 to day12 (**Figure 1A**). MEF was used as a negative control. The results are represented as the mean expression ± SD (triplicate samples).

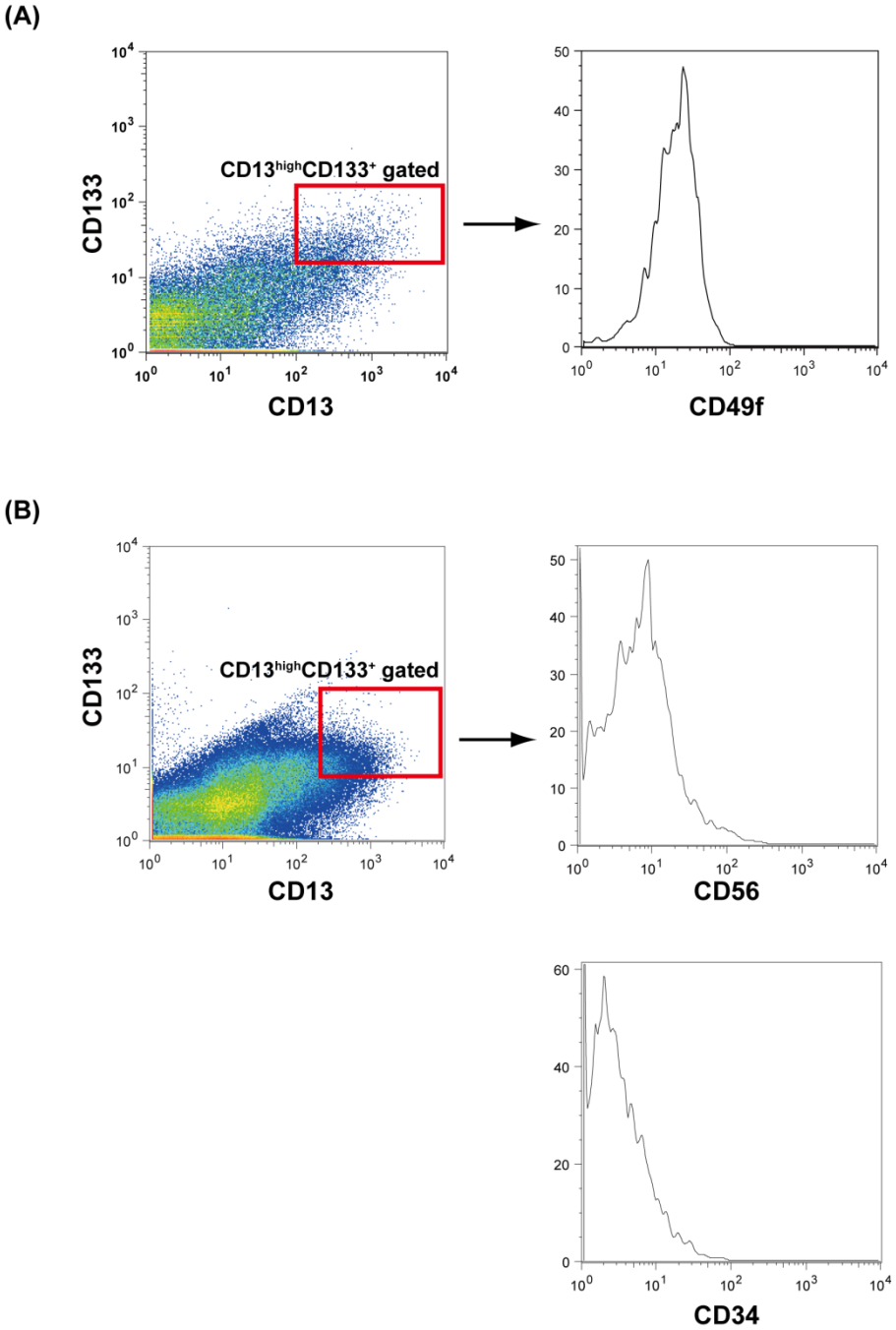

Figure 3. Expression of cell surface markers in human iPS cell-derived hepatic lineage cells.

(A) Expression of hepatic progenitor marker CD49f in $CD13^{high}CD133^{+}$ cells. Human iPS cells were stimulated with cytokines and stained with suitable antibodies. $CD13^{high}CD133^{+}$ cells slightly expressed CD49f. (B) Expression of progenitor cell markers CD56 and CD34 in $CD13^{high}CD133^{+}$ cells.

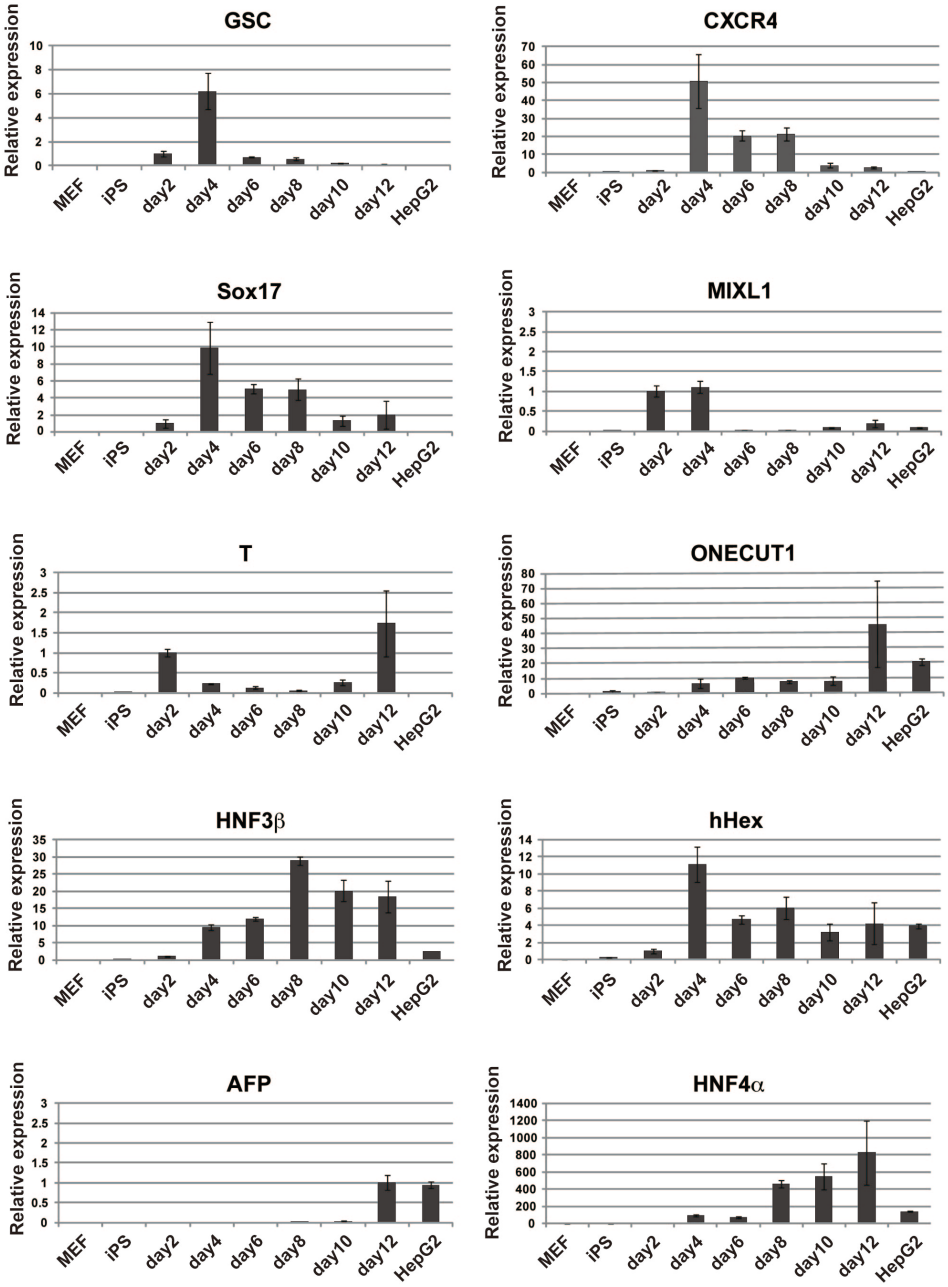

Figure 4. Expressions of undifferentiated and differentiated cell markers in human iPS cell-derived cells.

The expressions of marker genes for mesodermal and endodermal cells (GSC, CXCR4, Sox17, MIXL1, T [Brachyury], HNF3β, and hHex) and hepatic cells (AFP, HNF4α, and ONECUT1) were examined in normal human iPS cells (iPS) and differentiated iPS cells. Total RNAs were purified from iPS cells in the differentiation culture at each step from day2 to day12 (**Figure 1A**). MEF was use d as a negative control. The results are represented as the mean expression ± SD (triplicate samples).

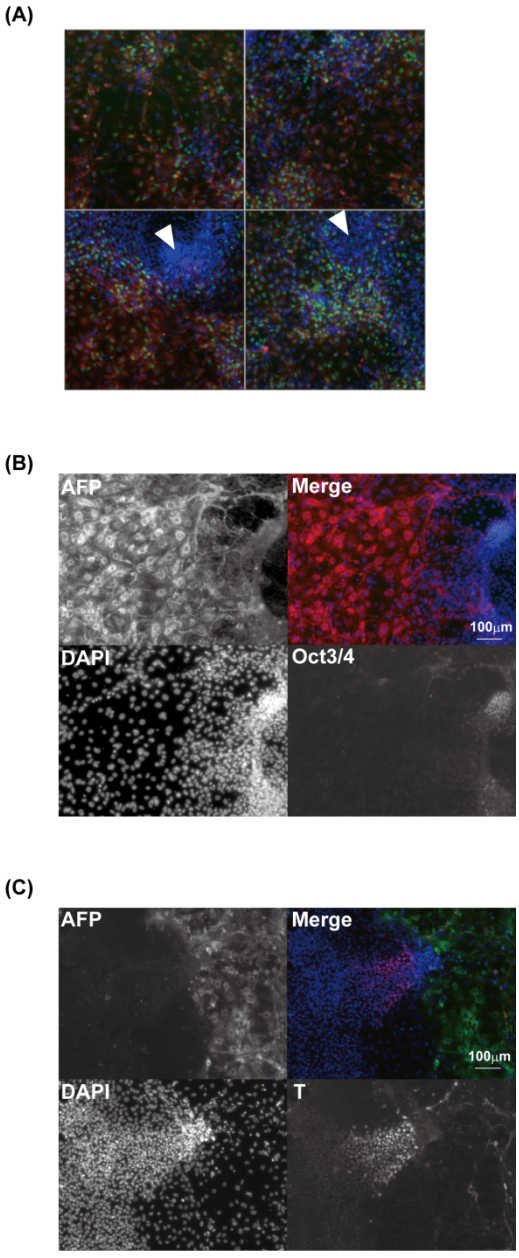

Figure 5. Differentiation of human iPS cells into hepatic lineage cells.

(A) Expressions of AFP (red) and HNF4α (green) in differentiated iPS cells at step (3) in Figure 1. The four fields of view are shown. Many cells have differentiated into AFP- and HNF4α-positive hepatocytic cells, although several cell clusters have not differentiated (arrowheads). (B) Expressions of AFP (red) and Oct3/4 (green) in differentiated iPS cells at step (3). Oct3/4 is not expressed in the AFP-positive cells. (C) Expressions of AFP (green) and T [Brachyury] (red) in differentiated iPS cells at step (3). T is not expressed in the AFP-positive cells. (A-C) Nuclei were stained with DAPI (blue).

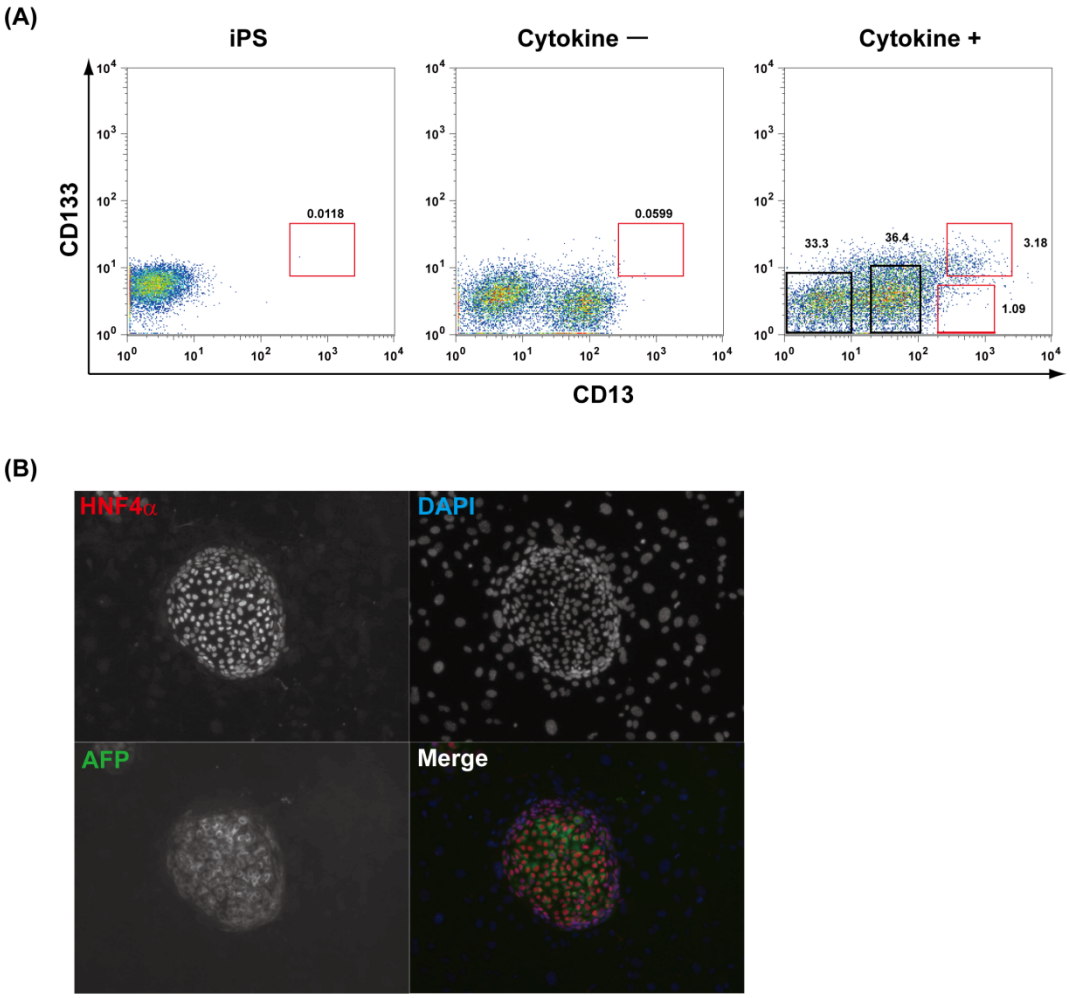

Figure 6. Isolation of HPCs from human iPS cell-derived hepatic lineage cells.

(A) Expression of hepatic progenitor markers in undifferentiated human iPS cells and differentiated cells. After 12 days of culture with or without cytokines, cells were stained with antibodies against CD13 and CD133, and then analyzed by flow cytometry. Ratios of $CD13^{high}CD133^{+}$ cells are shown. (B) Representative images of a colony derived from a single $CD13^{high}CD133^{+}$ cell. Colonies were stained with antibodies against AFP and HNF4α. Nuclei were counterstained with DAPI.

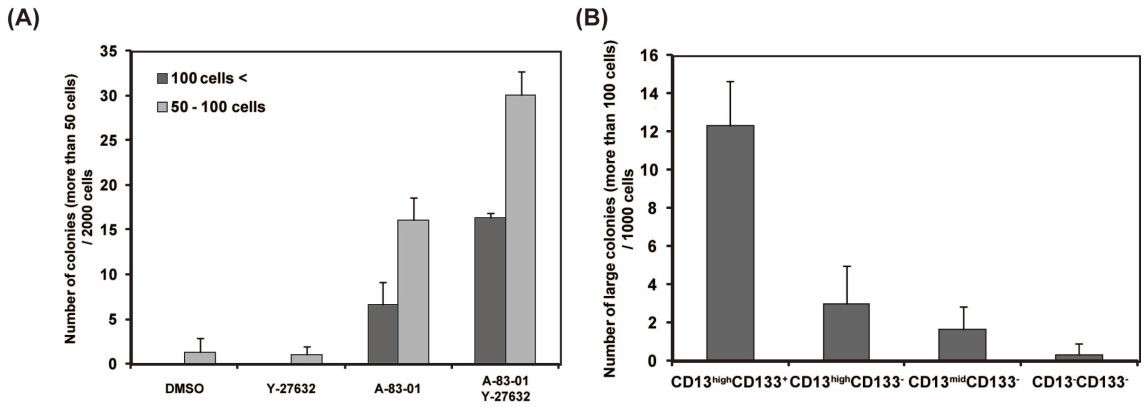

Figure 7. Isolation of HPCs from human iPS cell-derived hepatic lineage cells.

(A) Culture condition of the human iPS cell-derived hepatic progenitor colony assay. $CD13^{high}CD133^{+}$ cells were sorted and cultured on MEFs in the presence or absence of A-83-01 (ALK inhibitor) and Y-27632 (ROCK inhibitor). Results are represented as the mean colony count ± SD (triplicate samples). (B) $CD13^{-}CD133^{-}$, CD13 weakly single positive, $CD13^{mid}$ single positive and $CD13^{high}CD133^{+}$ cells were sorted onto MEFs. The cells were cultured in standard culture media in the presence of A-83-01 and Y-27632. Large colonies (containing more than 100 cells) derived from individual sorted cells were counted. Results are represented as the mean colony count ± SD (triplicate samples).

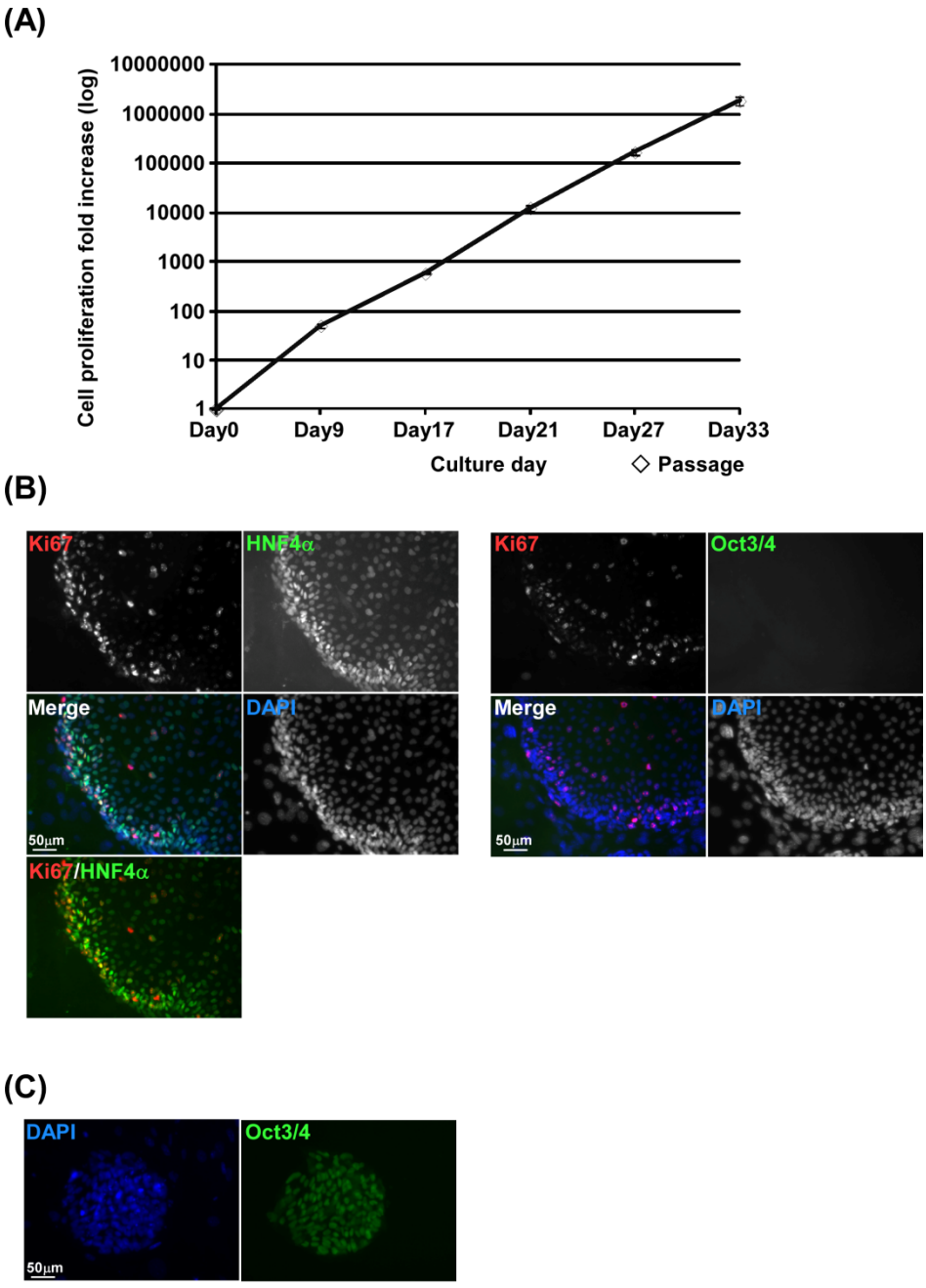

Figure 8. ***In vitro*** **long-term expansion of CD13^{high}CD133^{+} cells.**

(A) Colonies derived from CD13^{high}CD133^{+} cells were trypsinized and replated onto MEFs. The number of cells was counted at each replating step. The cells continued to proliferate for more than 1 month. A representative growth curve is shown. Similar results were obtained in two independent experiments. (B) Expression of the proliferation marker Ki67 in human iPS cell-derived hepatocytic colonies. After the 4th passage, the colonies were stained with antibodies against Ki67, HNF4α, and Oct3/4. (C) Human iPS cells were stained with an antibody against Oct3/4.

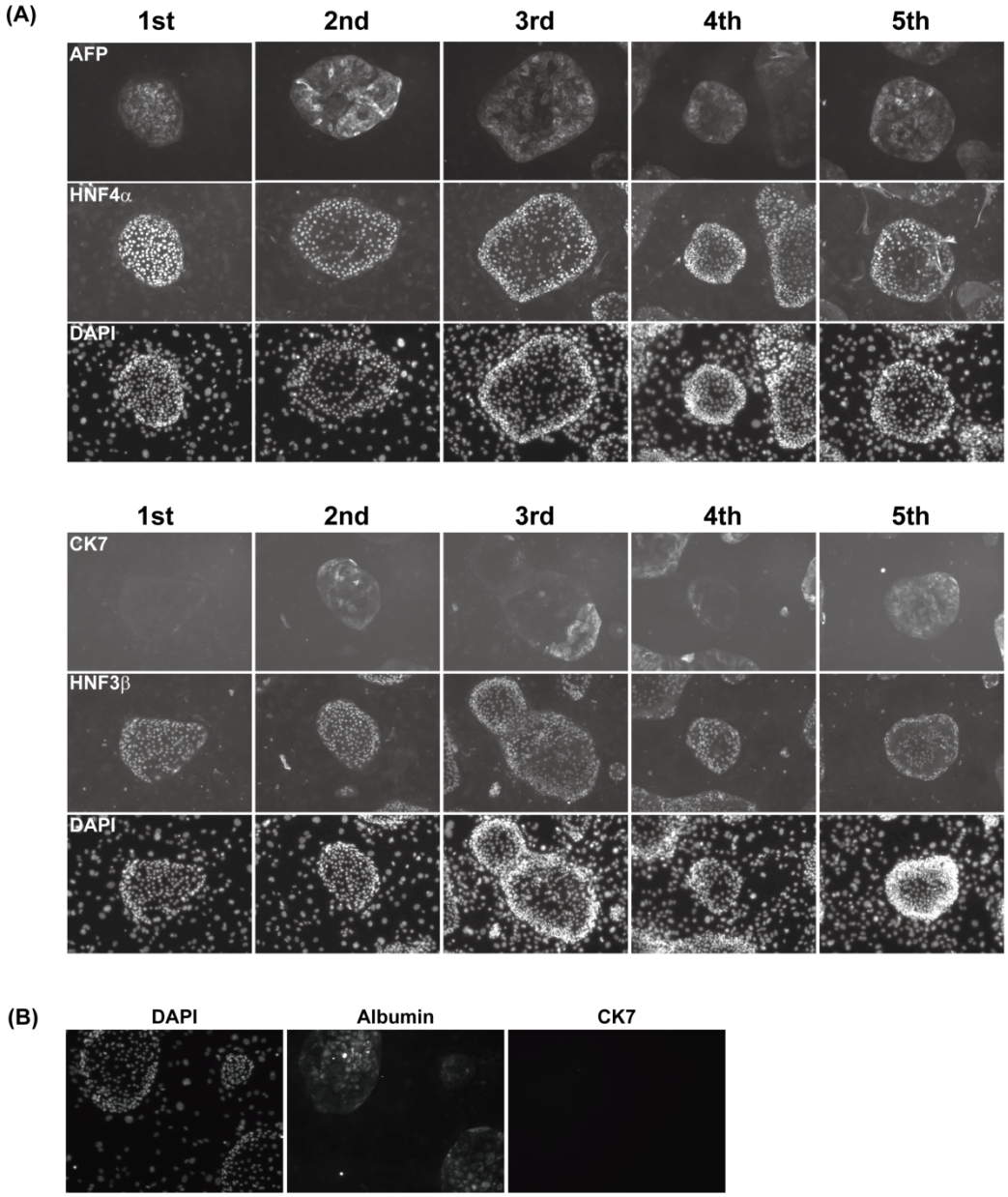

Figure 9. Expression of hepatocytic and cholangiocytic marker genes in human iPS cell-derived hepatic progenitor-like colonies.

(A) Expression of hepatocytic and cholangiocytic markers during *in vitro* expansion. Colonies derived from $CD13^{high}CD133^{+}$ cells were trypsinized and replated onto MEFs. Cells were fixed at each replating step. An endodermal marker (HNF3β), hepatocytic markers (AFP and HNF4α) and a cholangiocytic marker (CK7) were stained with specific antibodies. Nuclei were counterstained with DAPI. (B) Expression of albumin in colonies derived from human iPS cell-derived HPCs. Albumin but not CK7 was detected in several colonies in the 1st culture.

(A)

(B)

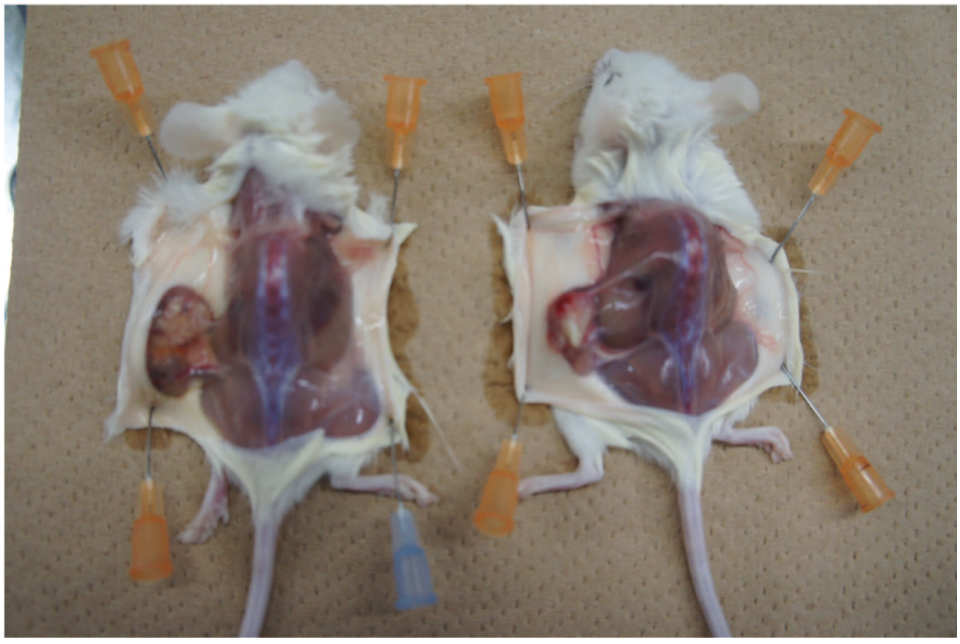

Figure 10. Tumorigenicity in human iPS cell-derived HPCs.

(A) Repressentative subcutaneous tumors (arrows) due to the injection of PLC/PRF/5 cells. Same number of PLC/PRF/5 cells or human iPS cell-derived HPCs were injectd into the subcutaneous space of the left and right back, respectively. (B) 1×10^6 PLC/PRF/5 cells formed tumors at left back. 1×10^6 HPCs faied to form tumors at right back.

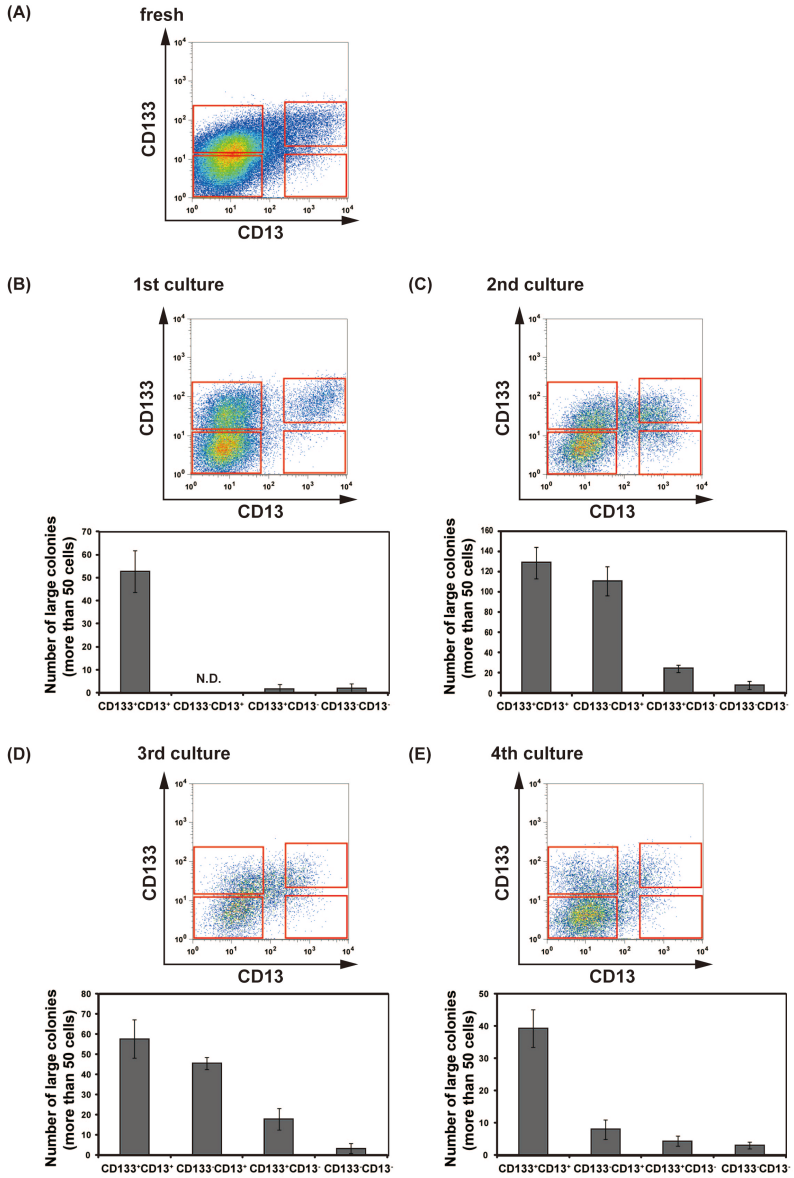

Figure 11. Changes of HPC surface marker expression in human iPS cell-derived hepatic progenitor-like colonies.

(A) After 12 days of culture with cytokines, $CD13^{high}CD133^{+}$ cells were sorted onto GFP-MEFs. After 10–12 days, cells were trypsinized and stained with antibodies against CD13 and CD133. Expression of CD13 and CD133 was analyzed by flow cytometry. (B–E) Colony forming activity of $CD13^{+}CD133^{+}$, $CD13^{+}CD133^{-}$, $CD13^{-}CD133^{+}$, and $CD13^{-}CD133^{-}$ fractions of human iPS cell-derived HPCs. At every replating step, cells stained with antibodies against CD13 and CD133 were sorted onto new GFP-MEFs, and their colony-forming activity was analyzed. Results are represented as the mean colony count ± SD (duplicate samples). N.D. shows "not determined".

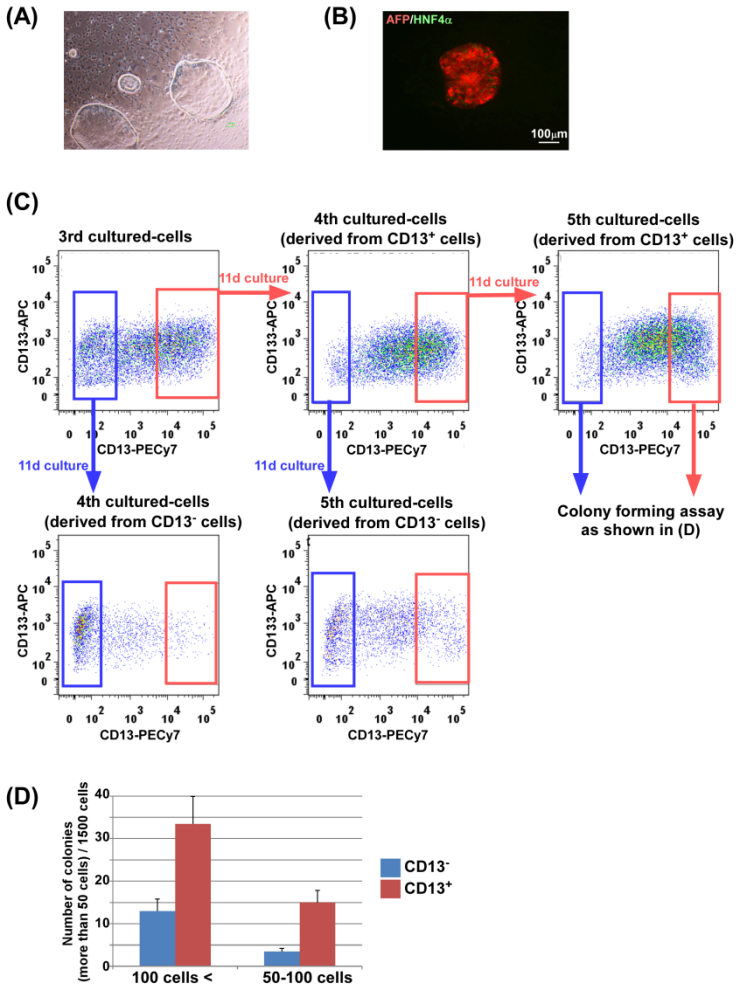

Figure 12. Long-term proliferation of human iPS cell-derived HPCs.

(A) Representative image of colonies of long-term proliferative human iPS cell-derived HPCs. The colonies were passaged six times and cultured for a total of 90 days after the first sorting. (B) Expressions of hepatocytic marker genes in the long-term culture. The colonies were cultured as described for (A) and fixed with 4% PFA. AFP (red) and HNF4α (green) were stained with suitable antibodies. (C) After 12 days of culture with cytokines, $CD13^{high}CD133^{+}$ cells were sorted onto MEFs. After two passages, the 3rd cultured-cells were trypsinized and stained with antibodies against CD13 and CD133. $CD13^{+}$ (red) and $CD13^{-}$ (blue) cells were purified and serially cultured (4th and 5th cultured-cells). 11d culture: 11-day culture. (D) Expansion of $CD13^{+}$ and $CD13^{-}$ cells after long-term culture. As shown in (C), $CD13^{+}$ (red) and $CD13^{-}$ (blue) cells in the 5th-cultured cells were purified and cultured for 9 days on MEFs. The results are represented as the mean colony counts ± SD (duplicate samples).

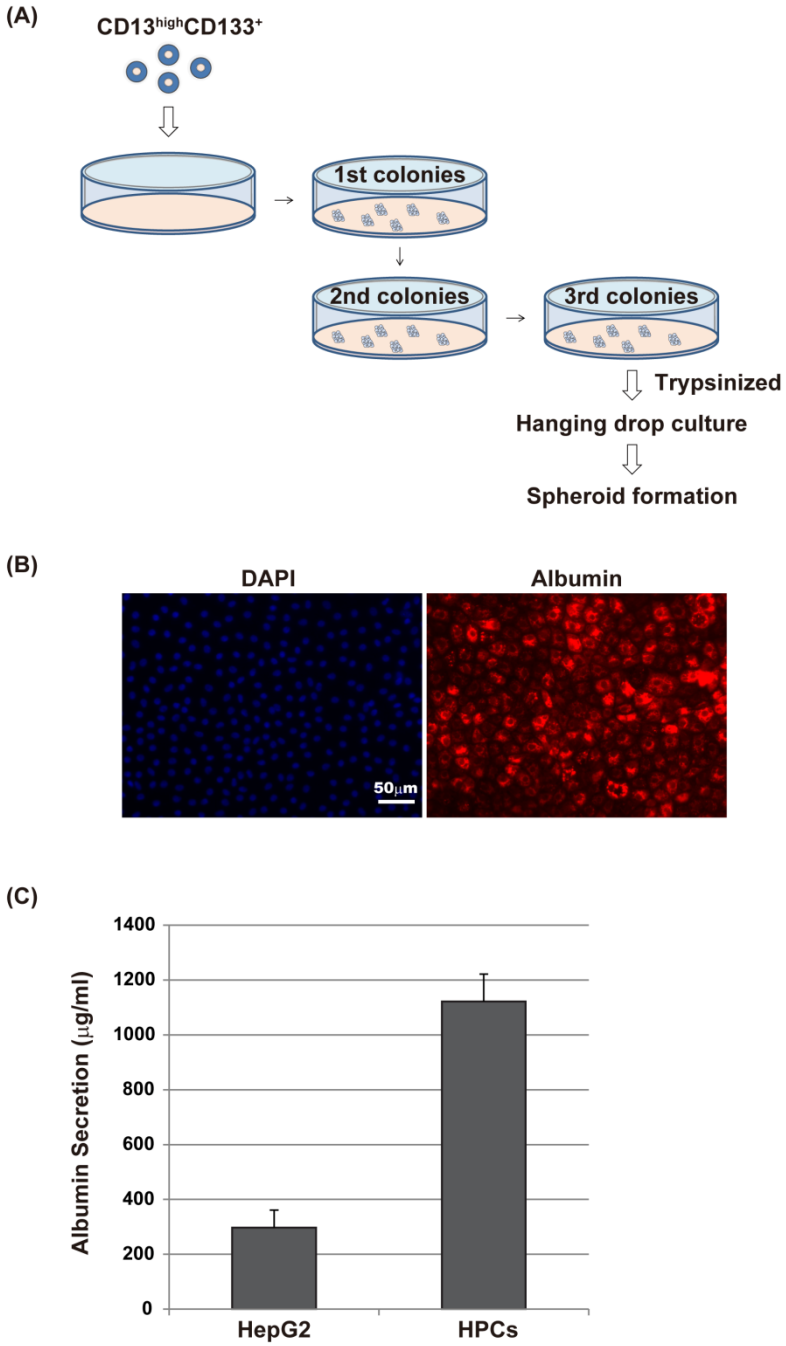

Figure 13. Differentiation of human iPS cell-derived HPCs toward mature hepatocytic cells.

(A) Schematic diagram of the experimental procedure. HPCs in the 3rd culture were dissociated with 0.05% trypsin-EDTA. Spheroids derived from HPCs were formed using hanging drop culture. (B) Expression of albumin in HPCs matured by cell-cell interactions. (C) Albumin secretion by human iPS cell-derived HPCs is identified after 3 days of culture in medium by enzyme-linked immunosorbent assays.

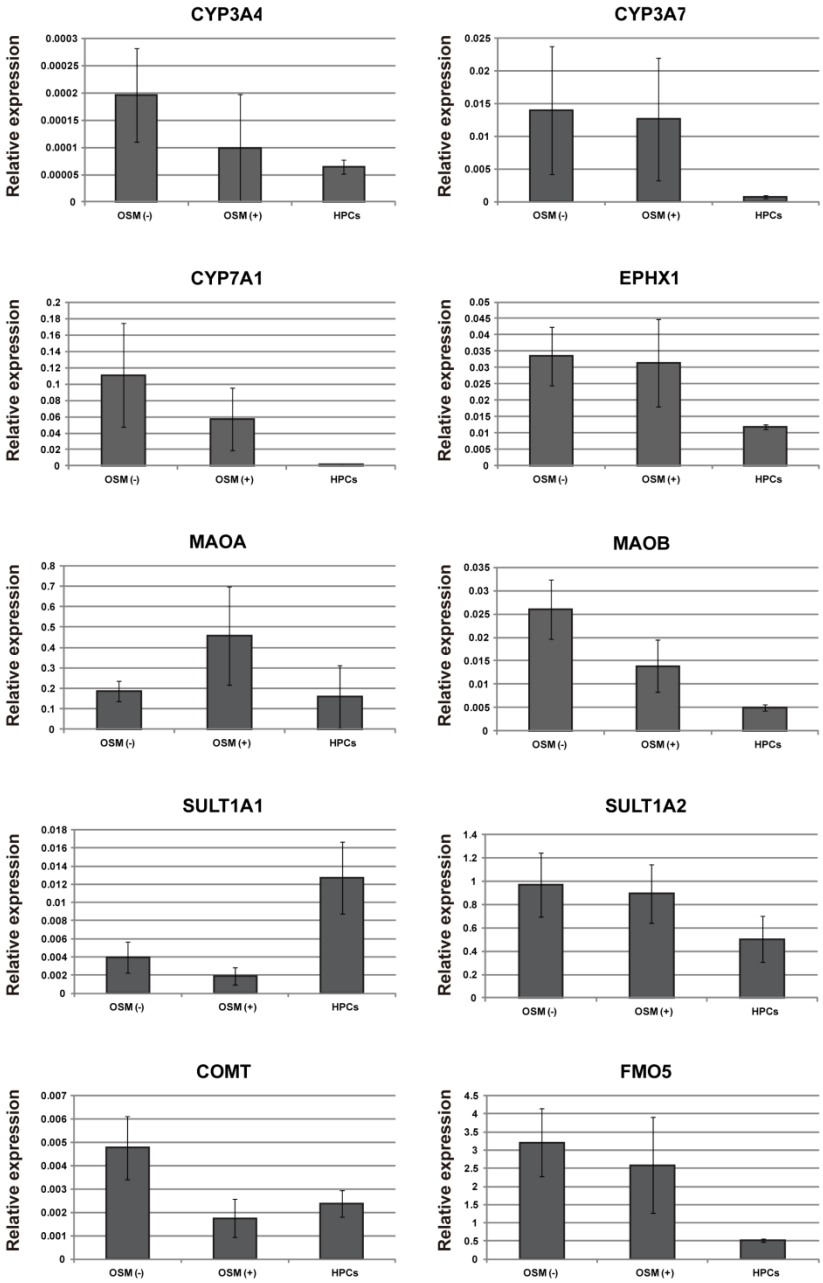

Figure 14. Expressions of hepatic functional genes in differentiated HPCs.

The levels of mRNAs encoding phase 1 and 2 enzymes in human iPS cell-derived HPCs from the 3rd culture, and spheroids derived from human iPS cell-derived HPCs from the 3rd culture are shown as the fold values relative to the levels in uncultured human hepatocytes. Spheroid formation was induced by hanging drop culture in the presence or absence of OSM. The results are represented as the mean expression ± SD (spheroid culture, n=6; HPCs, n=3; uncultured human hepatocytes, n=2).

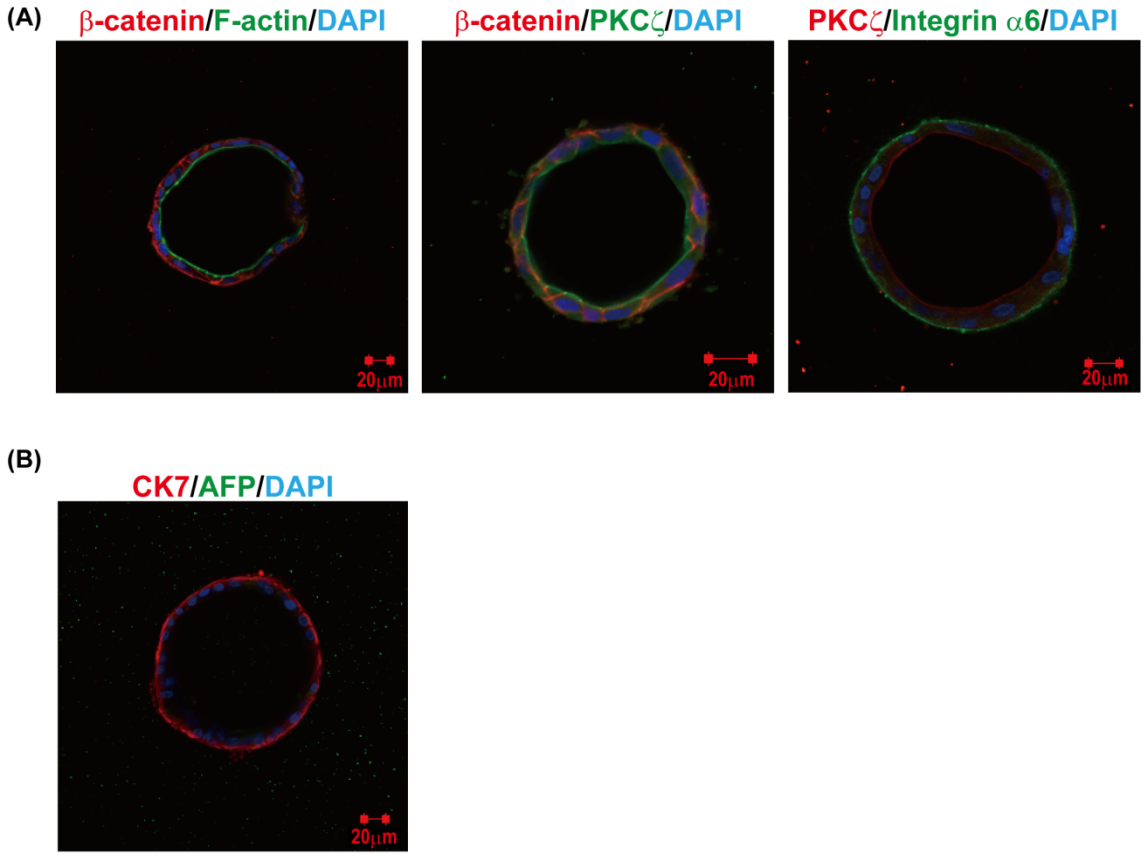

Figure 15. Cholangiocytic cyst formation of human iPS cell-derived HPCs.

(A) Human iPS cell-derived HPC colonies were trypsinized and cultured in an extracellular matrix gel. After 10–12 days of culture, several numbers of epithelial cysts were formed. Expression of β-catenin, F-actin, integrin α6 and PKCζ was detected in cysts. (B) Expression of CK7 in a HPC-derived epithelial cyst. Cells were stained with antibodies against CK7 and AFP. Nuclei were counterstained with DAPI.

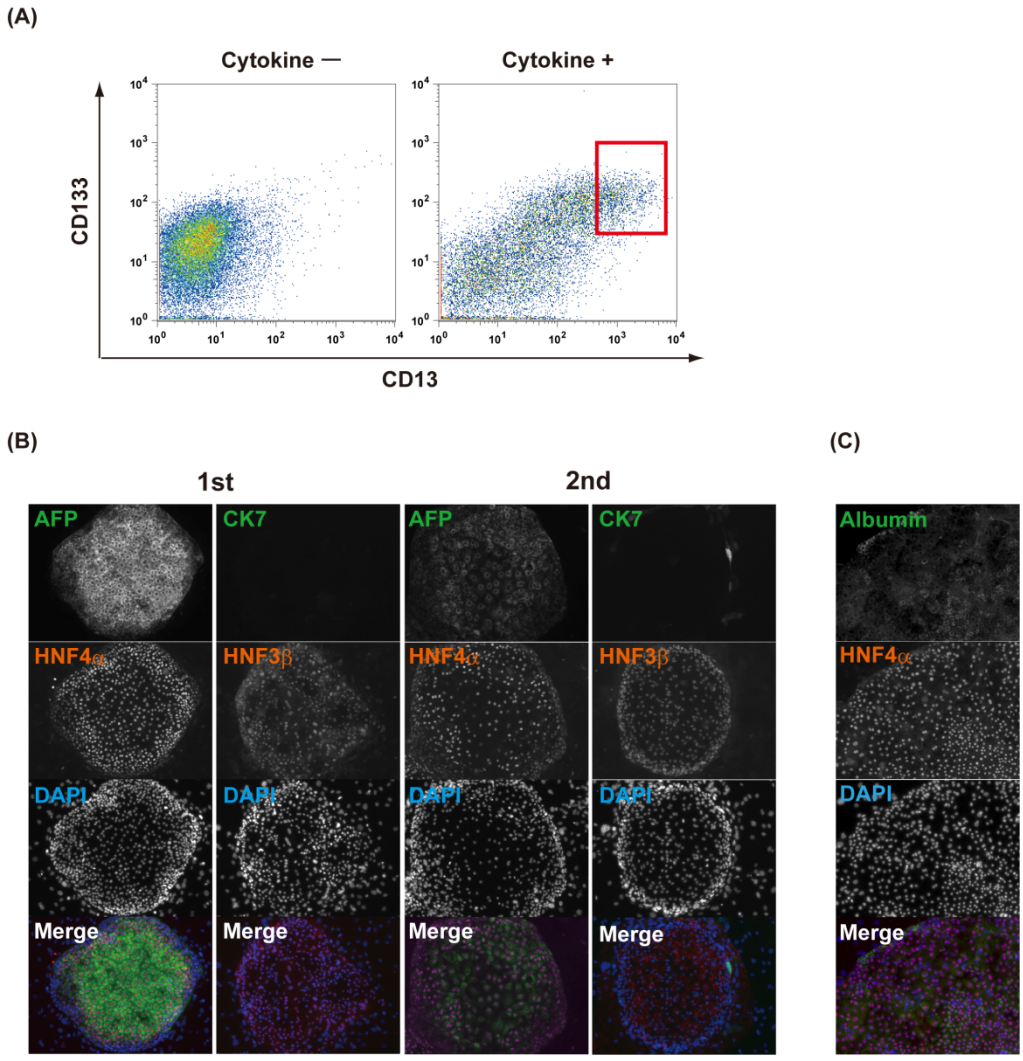

Figure 16. Purification of human ES cell-derived HPCs.

(A) Expressions of CD13 and CD133, cell surface markers of hepatic progenitor cells, in human ES cells cultured with or without cytokines. After 12 days of culture, the cells were stained with antibodies against CD13 and CD133, and then analyzed by flow cytometry. (B) Expressions of hepatocytic and cholangiocytic markers during *in vitro* expansion of human ES cell-derived HPCs. Colonies derived from $CD13^{high}CD133^{+}$ cells were cultured on MEFs. The expressions of several liver markers are detected in the 1st and 2nd cultures. An endodermal marker (HNF3β), hepatocytic markers (AFP and HNF4α), and a cholangiocytic marker (CK7) were stained with specific antibodies. (C) Expression of albumin in colonies derived from human ES cell-derived $CD13^{high}CD133^{+}$ cells. Albumin is detected in several colonies in the 1st culture.

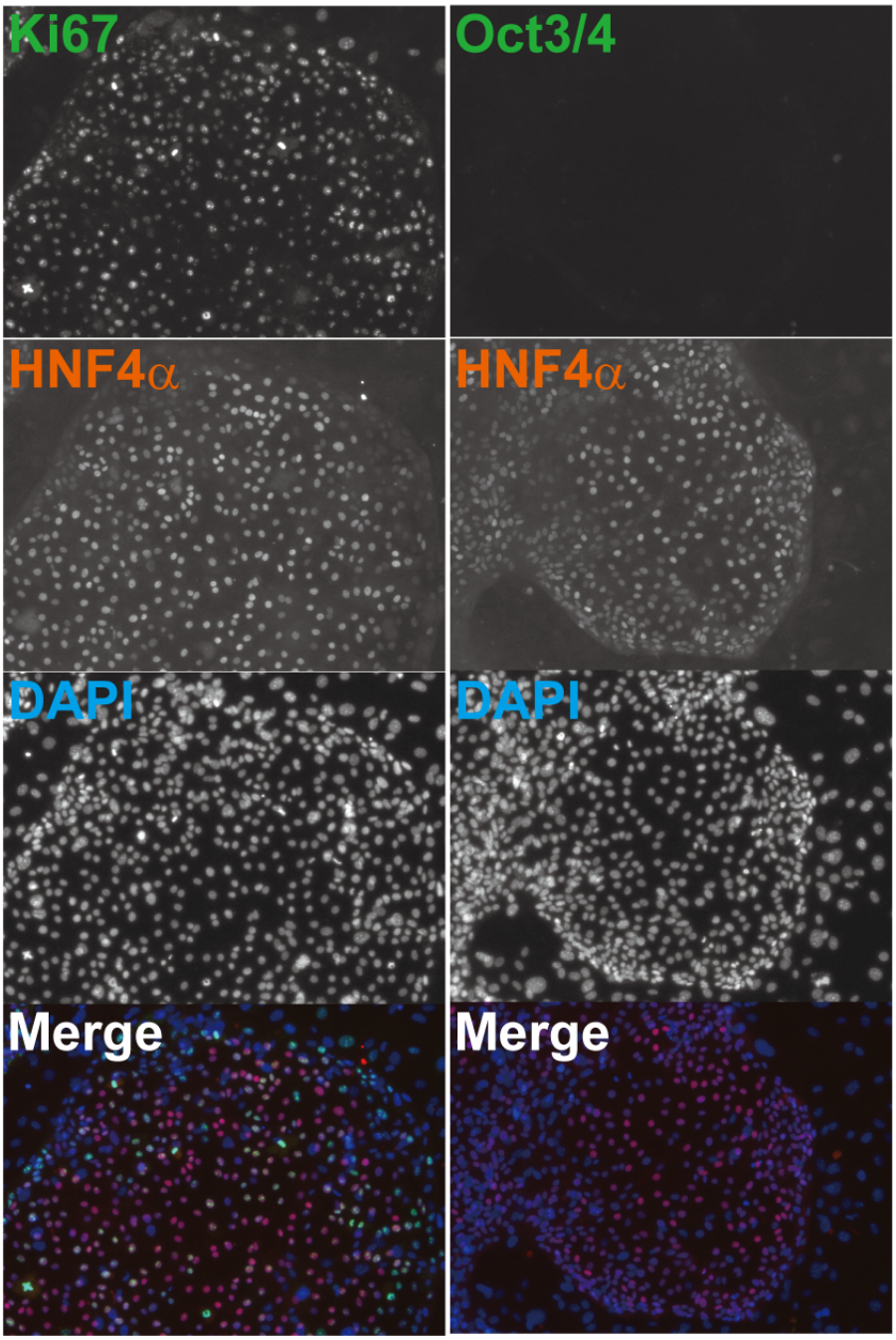

Figure 17. Proliferative ability of human ES cell-derived CD13^{high}CD133^{+} cells. Expressions of a pluripotency marker (Oct3/4) and a proliferation marker (Ki67) are observed in colonies derived from human ES cell-derived CD13^{high}CD133^{+} cells. Ki67-expressing proliferative cells express HNF4α in the 2nd culture. These cells do not express Oct3/4. Nuclei were counterstained with DAPI.

Table 1. List of antibodies used for immunostaining and flow cytometry experiments

Primary antibodies for flow cytometry	Clone	Source	Catalog number
CD13-PE	WM15	BD Pharmingen	555394
CD13-PE-Cy7	WM15	BD Pharmingen	561599
CD34-FITC	581/CD34	BD Pharmingen	555821
CD44-FITC	IM7	eBioscience	11-0441-82
CD49f (Integrin α6)-FITC	GoH3	BD Pharmingen	555735
CD56-PE-Cy7	B159	BD Pharmingen	557747
CD117-APC	YB5.B8	BD Pharmingen	550412
CD133/1-APC	AC133	Miltenyi Biotec	130-090-826
CD184 (CXCR4)-PE	12G5	eBioscience	12-9999-71
CD326-Alexa Fluor 488	9C4	Biolegend	324210

Primary antibodies for immunostaining	Dilution	Source	Catalog number
α-fetoprotein (AFP) (C3)	1/600	Sigma	A8452
α-fetoprotein (AFP) (C3)	1/600	Dako	A0008
Albumin	1/1000	Dako	A000102
β-catenin	1/1000	BD Pharmingen	610154
Brachyury (T) (C-19)	1/250	Santa Cruz	sc-17745
Cytokeratin-7 (CK7) (OV-TL 12/30)	1/1000	Dako	M7018
F-actin (Acti-stain 488 phalloidin)	1/150	Cytoskeleton, Inc.	PHDG1
HNF4α (C-19)	1/600	Santa Cruz	sc-6556
HNF3β (M-20)	1/300	Santa Cruz	sc-6554
Integrin α6 (CD49f) (GoH3)	1/500	BD Pharmingen	555734
Ki67	1/500	Abcam	ab15580
Oct-3/4 (C-10)	1/100	Santa Cruz	sc-5279

Protein kinase ζ (C-20)	1/500	Santa Cruz	sc-216

Secondary antibodies	Dilution	Source	Catalog number
anti-mouse/Alexa Fluor 488	1/1000	Invitrogen	A21202
anti-rabbit/Alexa Fluor 488	1/1000	Invitrogen	A21206
anti-rat/Alexa Fluor 488	1/1000	Invitrogen	A21208
anti-goat/Alexa Fluor 488	1/1000	Invitrogen	A11055
anti-goat/Alexa Fluor 546	1/1000	Invitrogen	A11056
anti-mouse/Alexa Fluor 555	1/1000	Invitrogen	A31570
anti-rabbit/Alexa Fluor 555	1/1000	Invitrogen	A31572
anti-rabbit/Alexa Fluor 568	1/1000	Invitrogen	A10042

Table 2. PCR primers for detection of human gene expression

Human genes	Forward primer (5'–3')	Reverse primer (5'–3')	Probe number
AFP	tgtactgcagagataagtttagctgac	tccttgtaagtggcttcttgaac	61
COMT	tgcacacactaccaatcgttc	gcctgggcccttgtagat	10
CXCR4	ggtggtctatgttggcgtct	actgacgttggcaaagatga	18
CYP3A4	gatggctctcatcccagactt	agtccatgtgaatgggttcc	2
CYP3A7	caaaagactctgagacccacaa	agccagcaaaaataaagataattga	50
CYP7A1	gcaggcacctgtagtcttagc	cggagacgggatctcactaa	64
EPHX1	gatgacccagaagcatgagc	gcgtgtgcaatagctcaaaa	8
FMO5	attagccaaacagccaagca	acacgattcaggatccaagc	73
GSC	cctccgcgaggagaaagt	cgttctccgactcctctgat	29
hHex	cggacggtgaacgactaca	agaaggggctccagagtagag	61
HNF3β	cccaatcttgacacggtga	aaataaagcacgcagaaacca	85
HNF4α	gagatccatggtgttcaagga	gtgccgagggacaatgtagt	68
HPRT1	tgaccttgatttattttgcatacc	cgagcaagacgttcagtcct	73
MAOA	attaagtgcatgatgtattacaaggag	tggagcatcttcatcttcaatg	5
MAOB	ctggcagtcagaaccagagtc	gagggcaaatgtctctccaa	9
MIXL1	ctgaggagccatgactgaca	gcatggaagtcagaaaggaca	14
ONECUT1	cctggagcaaactcaaatcc	ttctttccttttgcatgctg	88
Sox17	acgccgagttgagcaaga	tctgcctcctccacgaag	61
SULT1A1	aagtgtcctacggatcctggt	tctccctttcgggttctc	24
SULT1A2	gacctgggaaagcttcctg	tggtaccaggacccatagga	19
T (Brachyury)	gctgtgacaggtacccaacc	ggagaattgttccgatgagc	23

Afp, α-fetoprotein alpha; COMT, catechol-O-methyltransferase; CXCR4, chemokine (C-X-C motif) receptor 4; CYP, cytochrome P450; EPHX1, epoxide hydrolase 1, microsomal (xenobiotic); FMO5, flavin containing monooxygenase 5; GSC, goosecoid homeobox; hHex, hematopoietically expressed homeobox; HNF, hepatocyte nuclear factor; HPRT1, hypoxanthine phosphoribosyltransferase 1; MAO, monoamine oxidase; MIXL1, Mix paired-like homeobox; ONECUT1, one cut homeobox 1; Sox17, SRY-box containing gene 17; SULT1A1, sulfotransferase family, cytosolic, 1A, phenol-preferring, member1.

5 The function of $p57^{Kip2}$ in liver development

5-1 Introduction

The adult liver plays an important role in metabolism. In contrast, fetal liver has little metabolic functions whilst it supports fetal hematopoiesis. Although the liver dramatically changes its function during development, the molecular mechanisms regulating its change are still unclear. Hepatoblasts, fetal liver stem/progenitor cells, have a high proliferation potential and the ability to differentiate into both hepatocytes and cholangiocytes. Fetal livers are consisted of not only hepatoblasts but also various kinds of cells including hematopoietic cells, mesothelial, and submesothelial cells. Mesothelial and submesothelial cells cover liver lobes and are the origin of stellate cells and mesenchymal cells around vascular. H2.0-like homeobox (Hlx) and LIM homeobox 2 (Lhx2) during development, which are mainly expressed in mesothelial and submesothelial cells of embryonic livers, are important for progression of liver development (*30, 77, 78*). Additionally, midkine (Mdk) and pleiotrophin (Ptn) secreted from mesothelial and submesothelial cells and oncostatin M (OSM) secreted from hematopoietic cells promote hepatoblast maturation and proliferation (*31, 79*). These suggest that both extrinsic factors from various cells in the liver and intrinsic factors by themselves are important for liver development. Even if these stimulation factors are supplied *in vitro* culture, proliferation and differentiation levels of hepatoblasts *in vitro* are less than *in vivo*. There might be unknown mechanisms of regulating hepatoblasts proliferation and differentiation.

The cell cycle is the steps of events that take place in a cell leading to its division and replication. The cell cycle consists of four distinct phases: G_1 phase, S phase (synthesis), G_2 phase (collectively known as interphase) and M phase (mitosis).

The progression of these phases is controlled by the combination of cyclins and cyclin-dependent kinase inhibitors (CKIs). CKIs regulate cell cycle progression by blocking phosphorylation of the retinoblastoma protein (*80, 81*). CKIs have two families, Ink4 family ($p16^{Ink4a}$, $p15^{Ink4b}$, $p18^{Ink4c}$, and $p19^{Ink4d}$) and Cip/Kip family ($p21^{Cip1}$, $p27^{Kip1}$, $p57^{Kip2}$). CKIs play a critical role in regulation of proliferation and differentiation during development. Each Cip/Kip family member is expressed in a dynamic and restricted pattern during development. Although $p21^{Cip1}$-/- and $p27^{Kip1}$-/- mice do not show developmental defects, $p57^{Kip2}$-/- mice reveal severe developmental abnormality and die soon after birth (*82-87*). Because $p57^{Kip2}$ mRNA and protein are expressed in rat livers during only the middle to late fetal stages and the expression levels remarkably decrease after birth (*88, 89*), $p57^{Kip2}$ is considered to contribute to hepatocytes growth arrest that occurs in terms fetuses. However, whether $p57^{Kip2}$ regulates hepatoblasts differentiation remains unknown because $p57^{Kip2}$-/- mice die after birth.

I now show that $p57^{Kip2}$ is specifically expressed in hepatoblasts, mesothelial cells, and submesothelial cells in the mouse embryonic liver. The expression levels of hepatic functional genes in $p57^{Kip2}$-/- late fetal stage livers are lower than these in wild type livers. However, $p57^{Kip2}$-/- and wild type chimeric mice survive after birth and $p57^{Kip2}$-/- derived hepatocytes expressed hepatic functional genes similar levels in wild type cells-derived hepatocytes. These results suggested that expression of $p57^{Kip2}$ in non-parenchymal liver cells but not hepatoblasts is important for hepatocytic maturation.

5-2 Material and methods

Animal strains

p57^{Kip2}-/- mice were obtained by breeding *p57^{Kip2}*+/- females and *p57^{Kip2}*+/- males (kindly provided by Prof. Nakayama, Kyushu University). Fetuses were genotyped by PCR (RED Extract-N-Amp^{TM} Tissue PCR kit, Sigma, St. Louis, MO, primers are listed in **Table 3**) Mice were kept in standard laboratory cages and maintained in a 12 hour light/dark cycle with free access to food and water ad libitum and according to the Animal Care and Use Committee of the University of Tokyo. BDF1 and ICR mice were purchased (Nihon SLC, Shizuoka, Japan).

Cell preparation for flow cytometric analysis and sorting

For isolation of mesenchymal cells, hematopoietic cells, hepatoblasts, and endothelial cells, minced liver tissues from E13.5 mice were dissociated by the collagenase perfusion method. After perfusion, the cell suspension was centrifuged at 900 rpm for 3 min at room temperature. The cells were dissociated with 0.05% collagenase solution. Dissociated cells were washed with phosphate-buffered saline (PBS; Sigma) supplemented with 3% fetal bovine serum (FBS; Invitrogen, Carlsbad, CA) and incubated with antibodies against CD45.2-PECy7, Ter119-PECy7, and CD71-PECy7 or CD45.2-biotin and Ter119-biotin for 15 min at 4^{o}C. After washing with PBS supplemented with 3% FBS, pre-washed anti-Cy7 Micro Beads (Miltenyi Biotec, Bergisch Gladbach, Germany) or Dynabeads MyOne Streptavidin C1 (Invitrogen) were added and incubated for 15 min at 4^{o}C. Hematopoietic cells binding to magnetic beads were removed using magnetic separators. Collected non-hematopoietic cells were incubated with antibodies against cell surface marker for

60 min at 4°C. Antibodies for flow cytometry were shown in **Table 4**. After washing with PBS supplemented with 3% FBS and staining of dead cells with propidium iodide, the cells were analyzed and sorted using a MoFlo™ fluorescence-activated cell sorter (DAKO, Glostrup, Denmark).

Cell preparation from adult livers

For preparation of mature hepatocytes from mouse liver, hepatocytes and non-parenchymal cells were isolated from mouse liver following a 2-step collagenase digestion (*90*). Perfused liver tissues were dissociated with incubation in 0.025% collagenase solution for 15 min at 37°C. Mature hepatocytes were separated from non-parenchymal cells by several episodes of low-speed centrifugation (50 xg, 1 min). Dead-cell debris was removed by centrifugation in 40-50% Percoll solution (GE Healthcare UK, Amersham, England). Non-parenchymal cells were collected by centrifugation (1200 rpm for 5 min) Dead-cell debris was removed by centrifugation in 25% Percoll solution. For $p57^{Kip2}$+/+ or $p57^{Kip2}$-/- chimeric mice analyses, dissociated cells were washed with Dulbecco's modified Eagle's medium (DMEM, Sigma) with 10% FBS and staining of dead cells with propidium iodide. The cells were analyzed and sorted using a MoFlo™ fluorescence-activated cell sorter.

Colony formation assay

$CD45^-Ter119^-CD133^+Dlk^+$ cells in E13.5 fetal livers were plated onto mitomycin C-treated mouse embryonic fibroblasts (MEFs) in 0.1% gelatin (Sigma)-coated 12-well plates (2×10^5 cells per well). my standard culture medium is a 1:1 mixture of H-CFU-C medium (DMEM/Ham's F12 half medium [Sigma] with 10%

FBS, 1× Insulin-Transferrin-Selenium X [Invitrogen], 10 mM nicotinamide [Sigma], 10^{-7} M dexamethasone [Sigma], 2.5 mM HEPES buffer solution [Invitrogen], 1×penicillin streptomycin glutamine [Sigma], and 1×nonessential amino acid solution [Invitrogen]) and fresh DMEM. Cells were cultured for 7 days, in the presence of 40 ng/ml hepatocyte growth factor (HGF; PeproTech, Rocky Hill, NJ), 20 ng/ml epidermal growth factor (EGF; PeproTech), and 0.25 μM PD0325901 (Wako Pure Chem., Osaka, Japan). After 7 days culture, cells were washed with PBS, trypsinized with 0.05% trypsin-EDTA (Sigma), half volume of the cells was seeded into new MEFs plated 12-well plates. Medium was changed every 3 days. For overexpression of *p57^{Kip2}*, retrovirus was infected in the presence of 1 μg/ml protamine sulfate (Sigma) in the co-culture system and the medium was changed next day. After 7 days culture, to count colonies derived from individual single cells, I used an ArrayScan VTI HCS Reader (Thermo Scientific, Waltham, MA) following immunostaining. Albumin-positive colonies were counted.

Retrovirus production

Retroviral vector encoding *p57^{Kip2}* was generated by subcloning E13.5 whole embryo cDNA and into frame pGCDN sam-internal ribosome entry site (IRES)–green fluorescent protein (GFP) retroviral vectors. *p57^{Kip2}* cloning primers were listed in **Table 3**. pGCDN sam p57^{Kip2}-IRES-GFP was transfected with retrovirus packaging vector VSV-G to 293gp cells using the calcium phosphate method. Supernatant of the transfected 293gp cells was collected. To obtain high titer retrovirus, 293gpg cells were transfected with supernatants of 293gp cells containing control- and p57^{Kip2}-IRES-GFP retrovirus. After infection, GFP-positive 293gpg cells were isolated with

fluorescence-activated cell sorter (FACS) and maintained in DMEM medium supplemented with 10% FBS, 1× penicillin streptomycin glutamine, 1 μg/ml tetracycline (Sigma), 2 μg/ml puromycin (Sigma), 0.3 mg/ml G418 (Sigma). For retrovirus production, retrovirus infected 293gpg cells were cultured without tetracycline, puromycin, and G418. Collected supernatant was concentrated by a centrifuge 6000 xg at 4°C for 16 hours and concentrated high titer retrovirus was used for gene overexpression in primary cells.

Immunocytochemistry

Cultured cells were washed with PBS and fixed with 4% paraformaldehyde (PFA) /PBS for 10 min. Embryo and organs were washed with PBS and fixed with 4% PFA or 10% neutral buffered formalin. After fixation, samples were immersed in 10%, 20%, 30% sucrose (Sigma) /PBS to cryoprotect. Then, fixed samples were embedded and frozen in OCT (Tissue TEK, Sakura Finetek, CA). In several experiments, fresh frozen samples with rapid freezing in dry ice-cooled hexane were used. These embedded samples are sectioned with a cryostat (LEICA CM3050S, Wetzlar, Germany). After three washes with PBS, cells were permeabilized with 0.25% Triton X-100 (Sigma) /PBS for 10 min. Non-fixed samples were fixed with 4% PFA or chilled methanol for 10 min before permeabilization. After washing with PBS, and incubated with 5% donkey serum (Millipore, Bedford, MA) in PBS for 1 hour at room temperature. The cells were then incubated with diluted primary antibodies 1 hour at room temperature or overnight at 4°C. Primary antibodies are listed in **Table 4**. The cells were washed with PBS several times, and then incubated with diluted secondary antibodies for 45 min at room temperature. Then, the cells were washed with PBS and

their nuclei were stained with 4', 6-diamidino-2-phenylindole dihydrochloride (DAPI; Sigma). For each analysis, the addition of an appropriate immune serum provided a negative control. Fluorescence images were obtained with a Carl Zeiss Axio Observer Z1 using AxioVision version 4.8 software (Carl Zeiss, Jena, Germany) and KEYENCE HS BZ-9000 (Keyence, Osaka, Japan). Albumin- and cytokeratin 19 (CK19)-positive colonies were counted using an ArrayScan VTI HCS Reader.

In-droplet cell-staining methods

To quantify Ki67 expression in individual cells, in-droplet staining methods were used. 1000 cells of $CD133^{+}Dlk^{+}$ cells derived from fetal livers were sorted by FACS into a drop of PBS supplemented with 3% FBS onto poly-L lysine (Sigma) coated slide glasses (MATUNAMI, Osaka, Japan). The cells are incubated for 30 min at 37°C to settle onto the surface of the slide. After fixation with 2% PFA/PBS and permeabilization with 0.25% Triton X-100/PBS, cells were incubated in 5% donkey serum/PBS for 45 min at room temperature. Then, they were incubated with rabbit anti-Ki67 antibody overnight at 4°C, washed with PBS, and incubated with secondary antibodies (Alexa488-conjugated anti-rabbit IgG antibody) for 40 min at room temperature. The cells were washed with PBS and their nuclei were stained with DAPI. For each analysis, the addition of an appropriate immune serum provided a negative control. Antibody fluorescence intensity was measured using the ArrayScan VTI HCS Reader.

Staining of 5-ethynyl-2'-deoxyuridine (EdU) incorporation

Mice received 100 mg/kg EdU (Invitrogen) in PBS or only PBS via i.p.

injection before 2 hours sampling. EdU-positive cells were detected by immunohistochemistry using Clicl-iT EdU Alexa Fluor 594 Imaging kit (Invitrogen) according to manufacturer's protocol.

Real-time RT-PCR analysis

For gene expression analyses, total RNA was extracted from E17.5 and E19.0 whole livers using TRIzol (Invitrogen). First-strand cDNA synthesized using a High Capacity cDNA Reverse Transcription Kit (Life Technologies, Carlsbad, CA) was used as a template for PCR amplification. For quantitative RT-PCR, cDNA samples were normalized to the number of hypoxanthine phosphoribosyltransferase 1 (HPRT1) mRNA copies or glyceraldehyde 3-phosphate dehydrogenase (GAPDH). GAPDH copy numbers were analyzed by TaqMan Rodent GAPDH Control Reagents VIC^{TM} Probe (Life technology). The Universal probe Library (Roche Diagnosis, Basel, Switzerland) was used for quantitative RT-PCR assays. Primer sequences and the probe numbers for each gene are shown in **Table 3**

For TaqMan Low Density Array (TLDA) quantitative RT-PCR, total RNA was extracted from E13.5 liver-derived $CD13^{+}CD133^{+}$ hepatoblasts and adult hepatocytes using the RNAeasy Micro Kit (QIAGEN). First-strand cDNA synthesized using a High Capacity cDNA Reverse Transcription Kit was used as a template for PCR amplification. For quantitative RT-PCR, cDNA samples were normalized to the number of 18S mRNA copies. Samples derived from E13.5 $p57^{Kip2}$+/+, $p57^{Kip2}$-/- hepatoblasts, and mature hepatocytes were analyzed using custom 386-well TLDA (Life technology). Probe names and gene IDs in custom array were listed in **Table 5**. Results are represented as the mean colony count ± SD. $p57^{Kip2}$+/+ and $p57^{Kip2}$-/-

hepatoblasts are duplicate samples, E13.5 hepatoblasts and mature hepatocytes are triplicate samples.

Preparation of MEFs

For feeder cells, E12.5 ICR mice were used. For the generation of $p57^{Kip2}$+/+ or $p57^{Kip2}$-/- MEFs, E12.5 $p57^{Kip2}$+/+ or $p57^{Kip2}$-/- mice were used. E12.5 mouse embryos were dissected, and the head and internal organs were completely removed. The torso was minced and dissociated in 0.05% trypsin-EDTA for 30 min. After washing with PBS, cells were expanded in DMEM supplemented with 10% fetal FBS and 1× penicillin streptomycin glutamine. MEFs were treated with mitomycin C at 37 °C for 2 hours and used as feeder cells. Animal experiments were performed with the approval of the Institutional Animal Care and Use Committee of the Institute of Medical Science, the University of Tokyo.

Generation of $p57^{Kip2}$+/+ and $p57^{Kip2}$-/- mouse induced pluripotent stem (iPS) cells

To generate $p57^{Kip2}$+/+ and $p57^{Kip2}$-/- iPS cells, $p57^{Kip2}$+/+ and $p57^{Kip2}$-/- MEFs were used. Lentiviral vector carrying three mouse reprogramming factors (Oct3/4, Klf4, Sox2) infected each MEFs. Expression of these factors was controlled by a tetracycline-responsive regulatory elements and with Ubc-promoter-driven reverse tet transcativator (rTA) (*91*). For induction of reprogramming factors, doxycycline (Dox) was added to the culture medium on the day of seeded onto mitomycin-C treated MEFs. The medium was changed to ES medium containing Dox and mouse leukemia inhibitory factor (LIF, ESGRO Millipore, Bedford, MA) on day 3. Morphologically ES-like colonies were picked up and each colony was expanded on

MEFs in ES medium containing LIF. To generate Kusabira Orange (KuO)-iPS cells, KuO-IRES-Zeocin expression plasmid was transfected into $p57^{Kip2}$+/+ and $p57^{Kip2}$-/- iPS cells. Then, zeocin (Invitrogen) resistant and KuO homogeneously positive iPS colonies were picked up. The KuO-$p57^{Kip2}$+/+ and -$p57^{Kip2}$-/- iPS cells ubiquitously expressed KuO under the control of the CAG promoter.

iPS cells culture

iPS cells were maintained on mitomycin-c treated MEFs in DMEM supplemented with 15% FBS (Nichirei Bioscience, Tokyo, Japan), 2% HEPES buffer solution, 0.1 mM nonessential amino acid, 1× penicillin streptomycin glutamine, 0.1 mM 2-mercaptoethanol (Invitrogen) and 1,000 U/ml of LIF. For feeder-free iPS cells culture, iPS cells were maintained on 0.1% gelatin in Glasgow's modified Eagle's medium (GMEM [Sigma] supplemented with 10% FBS, 0.1 mM nonessential amino acid, 1× penicillin streptomycin glutamine, 1 mM sodium pyruvate [Invitrogen], 0.1 mM 2-mercaptoethanol) supplemented with 1,000 U/ml of LIF, 3 mM of GSK3β inhibitor CHIR99021 (Axon Biochemical, Groningen, The Netherlands), and 1 mM of MEK inhibitor PD0325901. iPS cells were trypsinized with 0.25% trypsin-EDTA (Invitrogen) into single cells and plated into new plates with or without MEFs feeder every 3 days.

Alkaline Phosphatase (AP) staining

AP assays were conducted with Vector Red Alkaline Phosphatase Substrate Kit (Vector Laboratories, Burlingame, CA) according to manufacturer’s instructions.

Induction of embryoid body (EB) from iPS cells

For EBs induction, feeder-free cultured iPS cells were trypsinized with 0.25% trypsin-EDTA and counted. 2×10^7 iPS cells were cultured in Iscove's Modified Dulbecco's Medium (IMDM; Life Technologies) supplemented with 15% FBS, transferin (Sigma), 1-thioglycerol (Sigma), ascorbic acid (Sigma) and 1× penicillin streptomycin glutamine on petri culture dishes. After 4 days culture, formed EBs were analyzed using flow cytometery. EB were washed with PBS and trypsinized with 0.25% trypsin-EDTA at 37°C for 10 min. After dissociated cells were washed with DMEM supplemented with 10% FBS and staining of dead cells with propidium iodide, the cells were analyzed and sorted using a MoFlo^{TM} fluorescence-activated cell sorter.

Blastocyst injection and generation of $p57^{Kip2}$+/+ and $p57^{Kip2}$-/- chimeric mice

Chimeric mice were generated by a conventional blastocyst microinjection method. KuO-*$p57^{Kip2}$*+/+ or -*$p57^{Kip2}$*-/- iPS cells were microinjected into day 3.5 blastocysts obtained by an intercross of BDF1 and C57BL/6, followed by transfer into host ICR uteri.

Statistics

Calculations of statistically significant differences between samples using the Student's two-tailed t test as well as the standard deviation (SD) were performed using Microsoft Excel 2007 software.

5-3 Results

p57^{Kip2} is highly expressed in fetal livers among cell cycle repression genes.

Hepatoblasts show high proliferation in fetal livers, whilst mature hepatocytes are in a quiescent G_0 state and seldom proliferate. I speculated that cell cycle control regulated proliferation and differentiation of hepatoblasts. The cell cycle is mainly controlled by the balance of expression of cyclins and CKIs. CKIs have two families, Ink4 family ($p16^{Ink4a}$, $p15^{Ink4b}$, $p18^{Ink4c}$, and $p19^{Ink4d}$) and Cip/Kip family ($p21^{Cip1}$, $p27^{Kip1}$, $p57^{Kip2}$). To identify which cyclins and CKIs regulate hepatoblasts proliferation and differentiation, the expression levels of cell cycle related genes were examined in both purified hepatoblasts ($CD45^{-}Ter119^{-}c\text{-}Kit^{-}Dlk^{+}CD133^{+}$) derived from E13.5 livers and adult hepatocytes using quantitative PCR. Among cell cycle related genes, *p57^{Kip2}* was highly expressed in hepatoblasts but not adult hepatocytes. The expression level of *p57^{Kip2}* dramatically decreased *in vitro* cultured hepatoblasts (**Figure 18**).

$p57^{Kip2}$ is expressed in hepatoblasts, mesothelial cells, and submesothelial cells in fetal livers.

To reveal the localization of $p57^{Kip2}$ expressing cells in the livers during development, serial sections derived from E13.5 and adult livers were stained with antibodies against $p57^{Kip2}$, hepatoblasts and hepatocytes marker hepatocyte nuclear factor (HNF) 4α, cholangiocytes and mesothelial cells marker CK19, mesenchymal cells marker PDGFRα. In E13.5 livers, $p57^{Kip2}$ was expressed in HNF4α-positive hepatoblasts. In addition, $p57^{Kip2}$ was expressed in and CK19-positive mesothelial cells covered liver lobes. In contrast, $p57^{Kip2}$ was not expressed in HNF4α-positive

hepatocytes and CK19-positive cholangiocytes in adult livers (**Figure 19A**). Next, the expression of *p57^{Kip2}* was analyzed in purified cell fractions derived from fetal livers using flow cytometry. Each cell fraction, hepatoblasts, mesenchymal cells, mesothelial cells, endothelial cells, and hematopoietic cells, in E13.5 liver is isolated using specific antibodies. Hematopoietic cells were enriched in CD45$^+$ or Ter119$^+$ or CD71$^+$ fraction, mesenchymal cells were in CD45$^-$CD71$^-$Ter119$^-$PDGFRα$^+$ fraction, mesothelial cells were in CD45$^-$CD71$^-$Ter119$^-$PCLP1$^+$ fraction, hepatoblasts were in CD45$^-$CD71$^-$Ter119$^-$Dlk$^+$ fraction, and endothelial cells were in CD45$^-$CD71$^-$Ter119$^-$Flk1$^+$ fraction. Quantitative PCR data also indicated that *p57^{Kip2}* was expressed in Dlk$^+$ hepatoblasts. In addition, *p57^{Kip2}* was highly expressed in PDGFRα$^+$ mesenchymal cells and PCLP1$^+$ methothelial cells (**Figure 19B**).

Regulation of hepatoblasts proliferation by p57^{Kip2}

Hepatoblasts greatly proliferate in the middle fetal stages from E9.5 to E14.5 and differentiate into both hepatocytes and cholangiocytes. We previously reported that hepatoblasts proliferated and formed large colonies expressing both hepatocyte marker Albumin and cholangiocyte marker CK19 from single cells under the *in vitro* co-culture with MEFs (*41*). These hepatoblasts can expand *in vitro* for 7 days (short-time culture), whilst proliferation of these cells is suppressed by the increase of CKI p16^{Ink4a}/p19^{ARF}. My group recently established the new *in vitro* expansion system of hepatoblasts using feeder cells and found that the addition of MEK inhibitor PD0325901 was able to inhibit the increase of p16^{Ink4a}/p19^{ARF} and induce long-term proliferation of hepatoblasts ((*41*) and Kamiya et al., submitted). To clarify p57^{Kip2} functions in hepatoblasts proliferation and differentiation, I analyzed wild type

($p57^{Kip2}$+/+) and $p57^{Kip2}$-/- hepatoblasts functions using this *in vitro* colony formation assay (**Figure 20**). There is no significant difference between $p57^{Kip2}$+/+ and $p57^{Kip2}$-/- hepatoblasts in the number of large colonies from single cells in the 1 primary colony culture. Both large colonies derived from $p57^{Kip2}$+/+ and $p57^{Kip2}$-/- hepatoblasts contained both Albumin-positive and CK19-positive cells (data not shown). However, when these cells were passaged onto new feeder cells and cultured, the number of large colonies derived from $p57^{Kip2}$-/- hepatoblasts is higher than $p57^{Kip2}$+/+ hepatoblasts in secondary colony culture (**Figure 21A**).

As described above, the expression level of $p57^{Kip2}$ was high in primary hepatoblasts but this expression was down-regulated during *in vitro* culture (**Figure 18**). Thus, I analyzed the function of $p57^{Kip2}$ in hepatoblasts proliferation and differentiation using overexpression with retroviral vectors.. Hepatoblasts were purified and infected mock and $p57^{Kip2}$-overexpressing retroviruses. Then, these cells were analyzed using *in vitro* colony formation assay. The number of large colonies derived from $p57^{Kip2}$-overexpressing hepatoblasts in primary colony culture (7 days culture) is slightly lower than that derived from control cells. When these cells were passaged onto new feeder cells (secondary colony culture), the number of colonies derived from $p57^{Kip2}$-overexpessed hepatoblasts is significantly lower than that derived from mock hepatoblasts (**Figure 21B**). These results suggested that $p57^{Kip2}$ regulated the proliferation ability of hepatoblasts *in vitro*.

To examine whether $p57^{Kip2}$ regulates hepatoblasts proliferation *in vivo*, the expression levels of cell cycle related genes in E13.5 $p57^{Kip2}$+/+ and $p57^{Kip2}$-/- hepatoblasts were analyzed using quantitative PCR. There was no significant difference in the expression levels of CKIs, $p16^{Ink4a}$/$p19^{ARF}$, $p15^{Ink4b}$, $p18^{Ink4c}$, $p19^{Ink4d}$,

p21^{Cip1}, and *p27*^{Kip1}. It was reported that the expression levels of p27^{Kip1} increased in the *p57*^{Kip2}-/- MEF cells. However, the expression levels of *p21*^{Cip1} and *p27*^{Kip1} did not significantly increase in *p57*^{Kip2}-/- hepatoblasts compared to in *p57*^{Kip2}+/+ hepatoblasts (**Figure 22A**). CKIs bind to various cyclin-CDK complexes and inhibit their kinase activities. Among cyclin families, the expression level of only *Cyclin D2* in *p57*^{Kip2}-/- hepatoblasts was lower than in *p57*^{Kip2}+/+ hepatoblasts (**Figure 22A**). These decreases of *Cyclin D2* expression were also detected in E17.5 *p57*^{Kip2}-/- whole livers (**Figure 23**).

Next, the ratio of proliferation marker, Ki67-positive cells were compared between E13.5 *p57*^{Kip2}+/+ and *p57*^{Kip2}-/- hepatoblasts using in-droplet cell staining methods (*92*). The number of Ki67-positive cells of *p57*^{Kip2}-/- hepatoblasts was higher than *p57*^{Kip2}+/+ cells (**Figure 22B**). We also analyzed *in vivo* proliferation rate of hepatoblasts in knockout mice using EdU incorporation. EdU is actively transported into cells whilst dividing and is incorporated into the newly synthesized DNA structure. EdU (100 mg/kg) was received pregnant day 13.5 mice via i.p injection. After 2 hours, hepatoblasts were purified and analyzed using in-droplet cell staining methods. The number of EdU-positive cells of *p57*^{Kip2}-/- hepatoblasts was higher than *p57*^{Kip2}+/+ hepatoblalsts (**Figure 23**). However, the liver mass and the number of hepatoblasts in *p57*^{Kip2}+/+ and *p57*^{Kip2}-/- mouse livers were not significantly different (data not shown). These results suggested that p57^{Kip2} suppressed proliferation of hepatoblasts both *in vitro* and *in vivo*. However, some p57 ^{Kip2}-independent molecular mechanism might control *in vivo* expansion of hepatoblasts.

Regulation of hepatoblast differentiation into cholangiocytes and hepatocytes by

p57^{Kip2}

Expression of several liver-enriched transcription factors and hepatocytic marker genes, such as Albumin and α-fetoprotein (Afp), was analyzed using *p57^{Kip2}*+/+ and *p57^{Kip2}*-/- liver-derived hepatoblasts. However, there were no significant changes, suggesting that no obvious defect was revealed in *p57^{Kip2}*-/- hepatoblasts (**Figure 25A**).

Hepatoblasts begin to differentiate into mature hepatocytes through the acquisition of expression of hepatic functional genes during fetal liver development. To analyze functional maturation of hepatoblasts in p57^{Kip2}-/- mouse livers, the expression levels of hepatic functional genes in E19.0 whole livers were examined. The *p57^{Kip2}* gene is an imprinted gene with the maternal allele being preferentially expressed (*93*). Therefore, I used *p57^{Kip2}* heterozygotes with maternal inheritance of the p57^{Kip2}-null allele (*p57^{Kip2}+/-m*) and *p57^{Kip2}*-/- as functional nulls and also used p57^{Kip2} heterozygotes with paternal inheritance of the p57^{Kip2}-null allele (*p57^{Kip2}+/-p*) and *p57^{Kip2}*+/+ as functional wild types. *p57^{Kip2}* expression in these embryos was confirmed using quantitative RT-PCR assays (data not shown). Expression of hepatic functional genes, *tyrosine aminotransferase* (*TAT*), *Cytochrome P450* (*Cyp*) *1A2*, *Cyp3A11*, and *Cyp7A1* in p57^{Kip2}-null livers were lower than that in p57^{Kip2}-wild type livers (**Figure 25B**). These results suggested that p57^{Kip2}-null liver might retain some of immature liver phenotype.

***p57^{Kip2}*-/- hepatoblasts differentiate into mature functional hepatocytes in chimeric livers**

Hepatic functions were regulated by both intrinsic factors (i.e. expression of

transcription factors) and extrinsic factors (i.e. cell-cell interaction). It is reported that the cell-cell interaction with various cells composed of livers such as hematopoietic cells and mesenchymal cells regulate hepatoblast differentiation of hepatoblasts into mature hepatocytes (*94*). $p57^{Kip2}$ is expressed in mesothelial and mesenchymal cells in addition to hepatoblasts during liver development (**Figure 19**). Therefore, we analyzed the importance of intrinsic and extrinsic factors for the retardation of $p57^{Kip2}$-null liver maturation using chimeric mice technologies. To generate wild type- $p57^{Kip2}$-/- and wild type- $p57^{Kip2}$+/+ chimeric mice, $p57^{Kip2}$+/+ and $p57^{Kip2}$-/- iPS cells were generated from $p57^{Kip2}$+/+ or $p57^{Kip2}$-/- MEFs using three mouse reprogramming factors (Oct3/4, Klf4, Sox2). After confirmation of pluripotent marker expression, iPS cells were ubiquitous labeled with KuO by electroporation of CAG KuO plasmid (**Figure 26**). These KuO-labeled iPS cells derived from $p57^{Kip2}$+/+ and -$p57^{Kip2}$-/- mice were injected into wild-type mouse blastocysts obtained by an intercross of BDF1 and C57BL/6. Although $p57^{Kip2}$-null mice are lethal around the perinatal stage, wild type- $p57^{Kip2}$-/- chimeric mice were normal after birth (**Figure 27A**). To examine $p57^{Kip2}$-/- hepatocytes function in adult livers, each KuO-$p57^{Kip2}$+/+, KuO-$p57^{Kip2}$-/-, and recipient wild-type hepatocytes were isolated from wild type- $p57^{Kip2}$+/+ or wild type- $p57^{Kip2}$-/- chimeric livers at 6 weeks using FACS. Then, expression of hepatic functional genes among KuO-$p57^{Kip2}$+/+, KuO-$p57^{Kip2}$-/-, and recipient hepatocytes was analyzed. There were no significant difference in the expression levels of hepatic functional genes, such as *Albumin*, *Afp*, *Cyp7A1*, *Cyp3A11*, and *Tat* among KuO-$p57^{Kip2}$+/+, KuO-$p57^{Kip2}$-/-, and recipient wild type hepatocytes (**Figure 27B**). To examine whether $p57^{Kip2}$-/- hepatoblasts have the differentiation potential to cholangiocytes and hepatocytes, expression of hepatocytic marker HNF4α and

cholangiocytic marker CK19 were analyzed in wild type-KuO-*p57*^{Kip2}-/- chimeric livers using immunohistochemical staining (**Figure 27C**). Some KuO cells (derived from *p57*^{Kip2}-/- iPS cells) expressed HNF4α, suggesting that these cells differentiated into hepatocytes. In contrast, CK19-positive cholangiocytic cells with KuO expression were not found in our (data not shown). To determine *p57*^{Kip2}-/- iPS cells derived hepatoblasts are able to differentiate into cholangiocytes, wild type-KuO-*p57*^{Kip2}-/- chimeric livers were analyzed with FACS. Epithelial cell adhesion molecule (EpCAM) were reported to the marker of ductal cells (*95, 96*). EpCAM^{+}KuO^{+} cells were existed in the wild type-KuO-*p57*^{Kip2}-/- chimeric livers (**Figure 28**). These results suggested that *p57*^{Kip2}-/- hepatoblasts could differentiate into both hepatocytes and cholangiocytes in wild type- *p57*^{Kip2}-/- chimeric livers. These results suggested that *p57*^{Kip2}-/- hepatoblasts could differentiate into mature hepatocytes in wild type-*p57*^{Kip2}-/- chimeric livers.

5-4 Discussion

Proliferation and differentiation are thought as two distinct and exclusive processes during several organ development. Hepatoblasts highly proliferate during liver development in the middle fetal stage, but their metabolic functions are immature. In contrast, adult hepatocytes have many metabolic functions but these proliferative abilities are low. The CDK inhibitor protein *p57^{Kip2}* was highly expressed in hepatoblasts and that its expression decreased during liver development. Therefore, cell cycle regulation during liver development might be important for differentiation of hepatocytic cells. In this study, we found that *p57^{Kip2}*-/- cells could differentiate into both hepatocytic and cholangiocytic cells *in vivo* (**Figure 27 and 28**). However, the effect of p57^{Kip2} or other CDK inhibitors on fate decision of hepatoblasts still remains unknown. p57^{Kip2} is one of the Cip/Kip family (p21^{Cip1}, p27^{Kip1}, p57^{Kip2}), therefore p21^{Cip1} and p27^{Kip1} might compensate p57^{Kip2} loss. The increase of *p21^{Cip1}* and *p27^{Kip1}* mRNA expression was not observed in *p57^{Kip2}*-/- hepatoblasts. Most abnormalities of p57^{Kip2}-/- mice were found to be corrected in p57^{Kip2}-/-^{p27Kip1KI} mice, which the p57^{Kip2} gene has been replaced with the p27^{Kip1} gene. However, some abnormalities such as placenta dysplasia and dysplasia of the renal papilla still remain in *p57^{Kip2}*-/-^{p27Kip1KI} mice (*97*). Thus, p27^{Kip1} might not compensate for loss of p57^{Kip2} in *p57^{Kip2}*-/- hepatoblasts. To reveal whether p21^{Cip1}, p27^{Kip1}, and other cell cycle-related genes can compensate for loss of p57^{Kip2} in the late stage of hepatoblasts or not, further analyses are needed.

p57^{Kip2}-/- mice exhibited retardation of hepatoblast maturation in the late fetal stage. However, p57^{Kip2}-/- hepatoblasts functioned similarly to wild-type hepatocytes in wild type-*p57^{Kip2}*-/- chimeric liver. Therefore, intrinsic expression of p57^{Kip2} in

hepatoblasts did not specifically regulate differentiation from hepatoblasts into mature hepatocytes. As it was reported that *p57^{Kip2}*-/- adult HSC was found a severe defect in the self-renewal capacity (*98*), intrinsic expression of p57^{Kip2} in stem/progenitor cells might be important to maintain their characters. However *p57^{Kip2}*-/- fetal HSC did not show apparent defect (*99*). In my study, intrinsic deficiency of p57^{Kip2} in hepatoblasts could not be found dramatically defect with differentiation. The intrinsic function of p57^{Kip2} in stem/progenitor cells might be different between fetal and adult stages. I hypothesized that the defect of p57^{Kip2} in non-parenchymal cells caused the suppression of liver functional maturation. Hematopoietic cells expanding in the fetal liver are involved in the regulation of hepatoblasts differentiation (*31*). Although the expression level of *p57^{Kip2}* was significantly lower in CD45^{+}CD71^{+}Ter119^{+} hematopoietic cells, p57^{Kip2} was expressed in fetal hematopoietic stem cells (*99*). In addition, most of the hematopoietic cells populating in the fetal liver are erythrocyte-lineage cells and p57^{Kip2} might regulate erythropoiesis *in vivo* fetal liver development (*100*). However, significant difference could not be found in the population of CD71/Ter119 (differentiation-stage specific markers of erythropoesis) positive cells in E13.5 *p57^{Kip2}*-/- and *p57^{Kip2}*+/+ livers (data not shown). To reveal whether differentiated hematopoietic cells regulate hepatoblasts differentiation in the p57^{Kip2}-/- mice, further analysis are needed.

In this study, p57^{Kip2} was also found to be expressed in mesothelial cells and submesothelial cells in fetal liver. Mesothelial cells and submsothelial cells are the origin of mesenchymal cells of the parenchyma of the liver (*101*). The secretion factors from these cells or cell-cell interaction between hepatoblasts and mesenchymal cells are reported to promote hepatoblasts proliferation and differentiation (*94*). Whether

$p57^{Kip2}$ deficiency affects the differentiation of mesothelial and submesothelial cells into parencymal mesenchymal cells are not clear because cell cycle regulation during the developmental process of these cells is still unknown. In addition, whether $p57^{Kip2}$ deficiency affects secretion of these cell-derived soluble factors, which maintains hepatoblasts stemness or promotes hepatocytic differentiation, remain to be seen. High *p57^{Kip2}*-/- chimeric mice soon died after birth like *p57^{Kip2}*-/- mice. However, in order to support our hypothesis that extrinsic $p57^{Kip2}$ deficiency regulates hepatoblast differentiation, it is necessary to ascertain whether wild type hepatoblasts in high *p57^{Kip2}*-/- chimeric mice reveal maturation retardation or not. As shown in chapter 4, I established an *in vitro* expansion system for generation of human iPS cell-derived HPCs exhibiting bipotent differentiation potential. Although this method yields the possibility of new cell transplantation therapy using patient autologous iPS cells, there still remains challenges in their differentiate into fully mature functional hepatocytes *in vitro*. More detailed analyses of *p57^{Kip2}*-/- mesenchymal cells offer the potential to find new hepatoblasts maturation and proliferation regulating factors.

Mutations in the imprinted *p57^{Kip2}* gene are associated with the childhood developmental disorder Beckwith-Wiedemann syndrome (BWS) (*102*). Although there are some differences in strain background, *p57^{Kip2}*-/- mice display some of they phenotype of BWS such as cleft palate and abdominal wall defects (*103, 104*). Children with BWS have an increased risk of developing childhood tumors including Wilms tumor, hepatoblastoma and so on. Hepatoblastoma originate from immature liver progenitor cells but the mechanisms of hepatoblastoma occurrence in BWS children remain to be seen. Analysis of *p57^{Kip2}*-/- livers may reveal the mechanisms underlying the maturation defects.

5-6 Figures

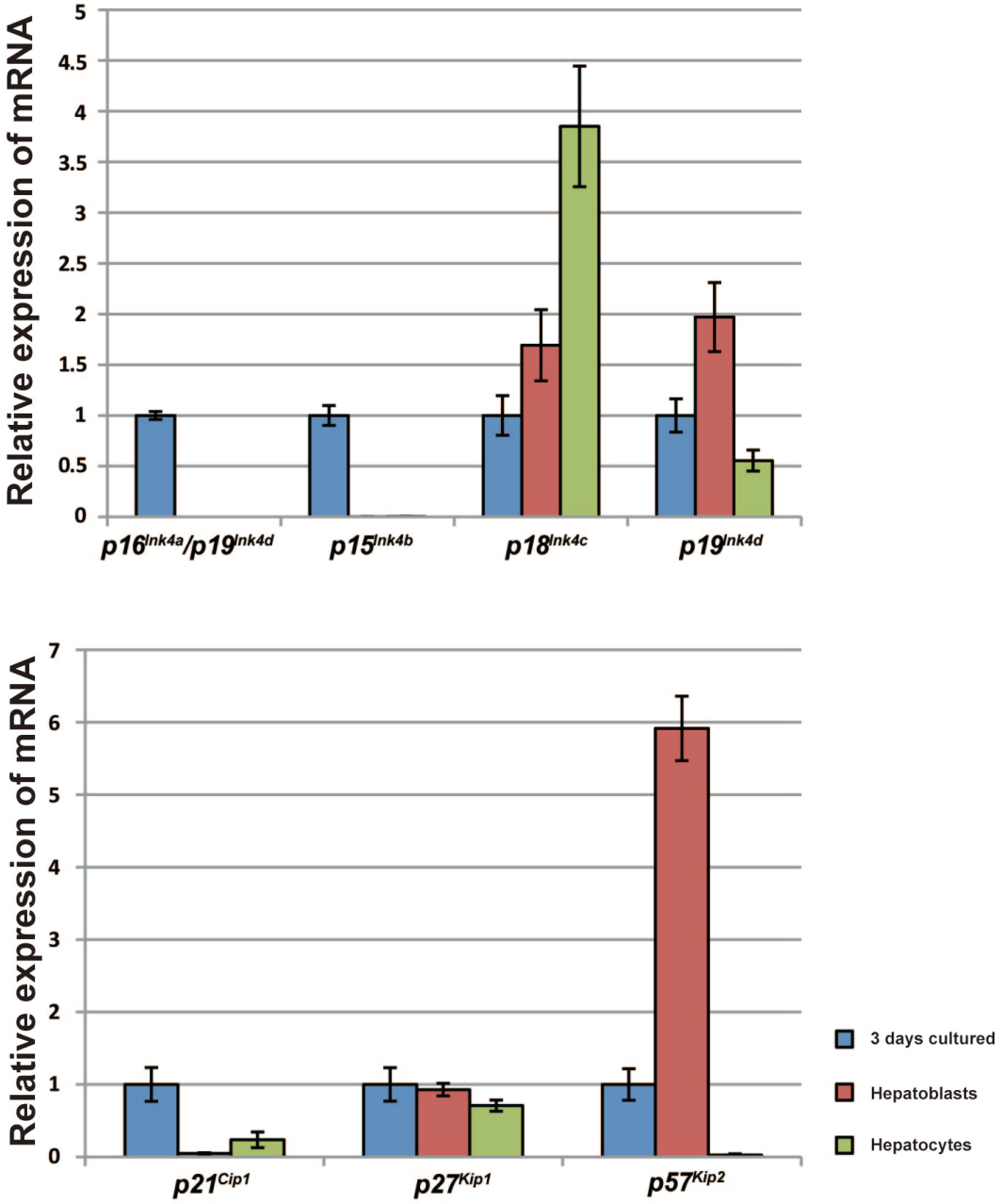

Figure 18. Expression of cell-cycle related genes during liver development.
The expression levels of cell cycle genes mRNA in hepatoblasts and adult hepatocytes. *p57*^{Kip2} highly expressed in hepatoblasts. The expression level in 3 days-cultured hepatoblasts is set to 1.0. Results are represented as the mean colony count ± SD (triplicate samples).

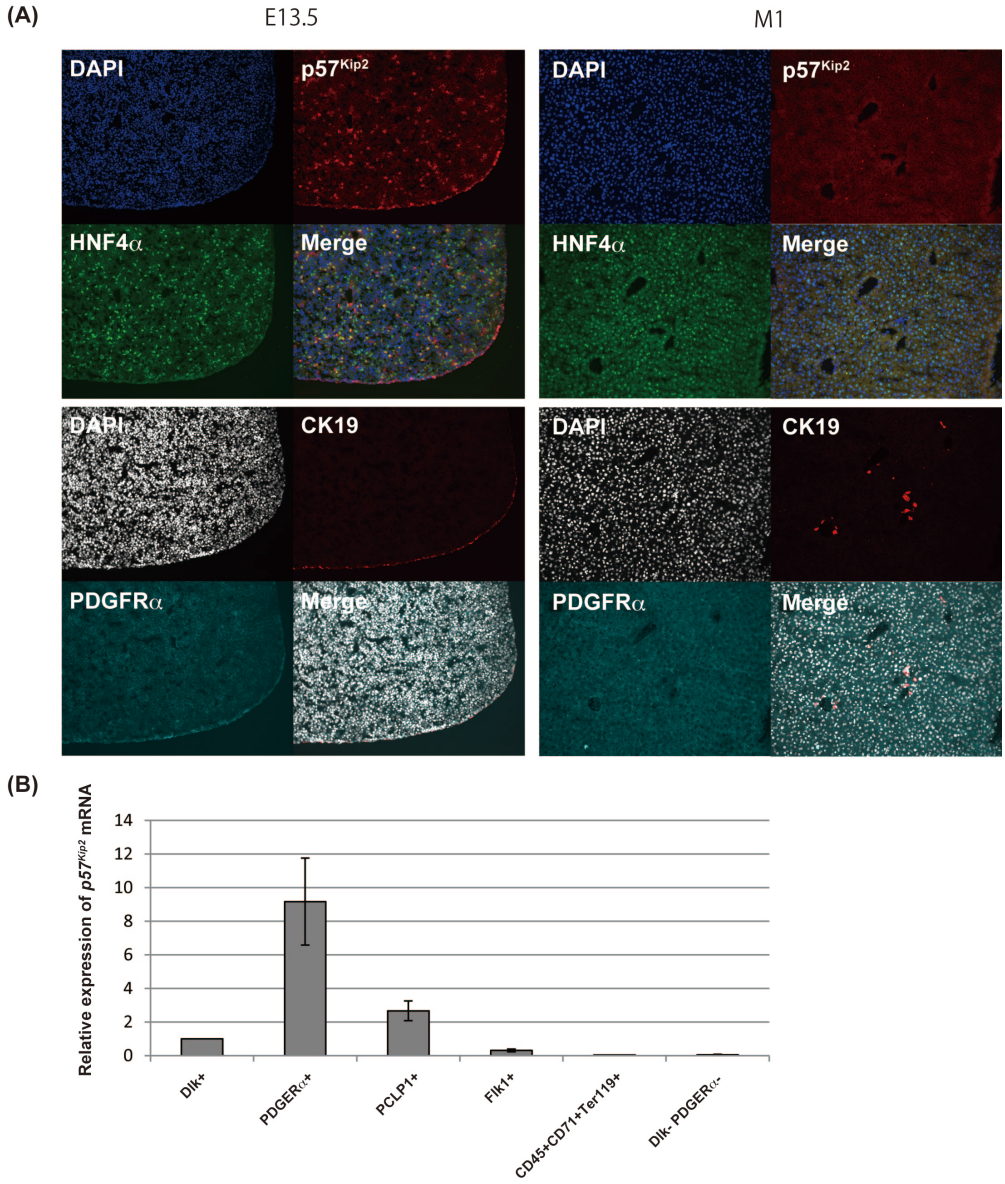

Figure 19. Expression of p57^{Kip2} in embryonic livers.

(A) The expression of p57^{Kip2} proteins in liver in E13.5 and adult (1 month; 1M). Serial sections were stained with p57^{Kip2}, HNF4 α, CK19, and PDGFRα antibodies. Nuclei were counterstained with DAPI. p57^{Kip2} was expressed in HNF4α-positive hapatoblasts and CK19-positive mesotehlial cells at E13.5, but not expressed in HNF4α-hepatocytes and CK19-positive cholangiocyets in adult livers. (B) The Expression level of *p57^{Kip2}* mRNA in hepatoblasts (Dlk^{+}), mesothelial cells (PCLP1^{+}), submesothelial cells (PDGFRα^{+}), endothelial cells (Flk1^{+}), hematopoietic cells (CD45^{+}CD71^{+}Ter119^{+}), and other cells (Dlk^{-}PDGFRα^{-}). Results are represented as the mean colony count ± SD (triplicate samples).

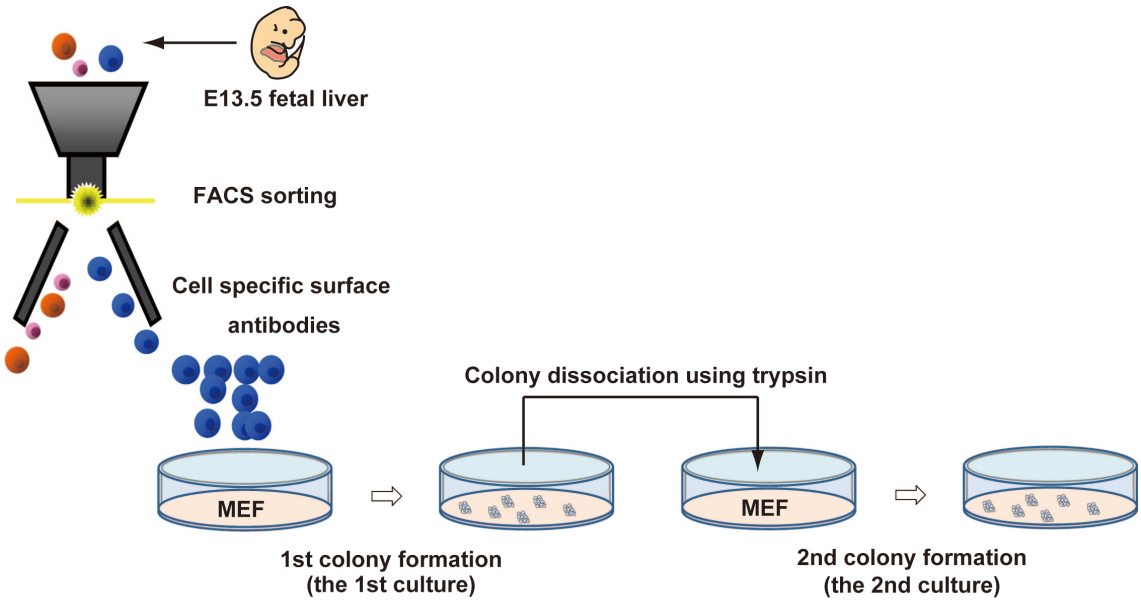

Figure 20. Schematic of the experimental procedure.

Fetal hepatoblasts were purified using FACS and sequentially passaged with trypsin treatment. Colonies in the 1st cultured (short-term culture) and the 2nd cultured (long-term culture) of fetal hepatoblasts were counted.

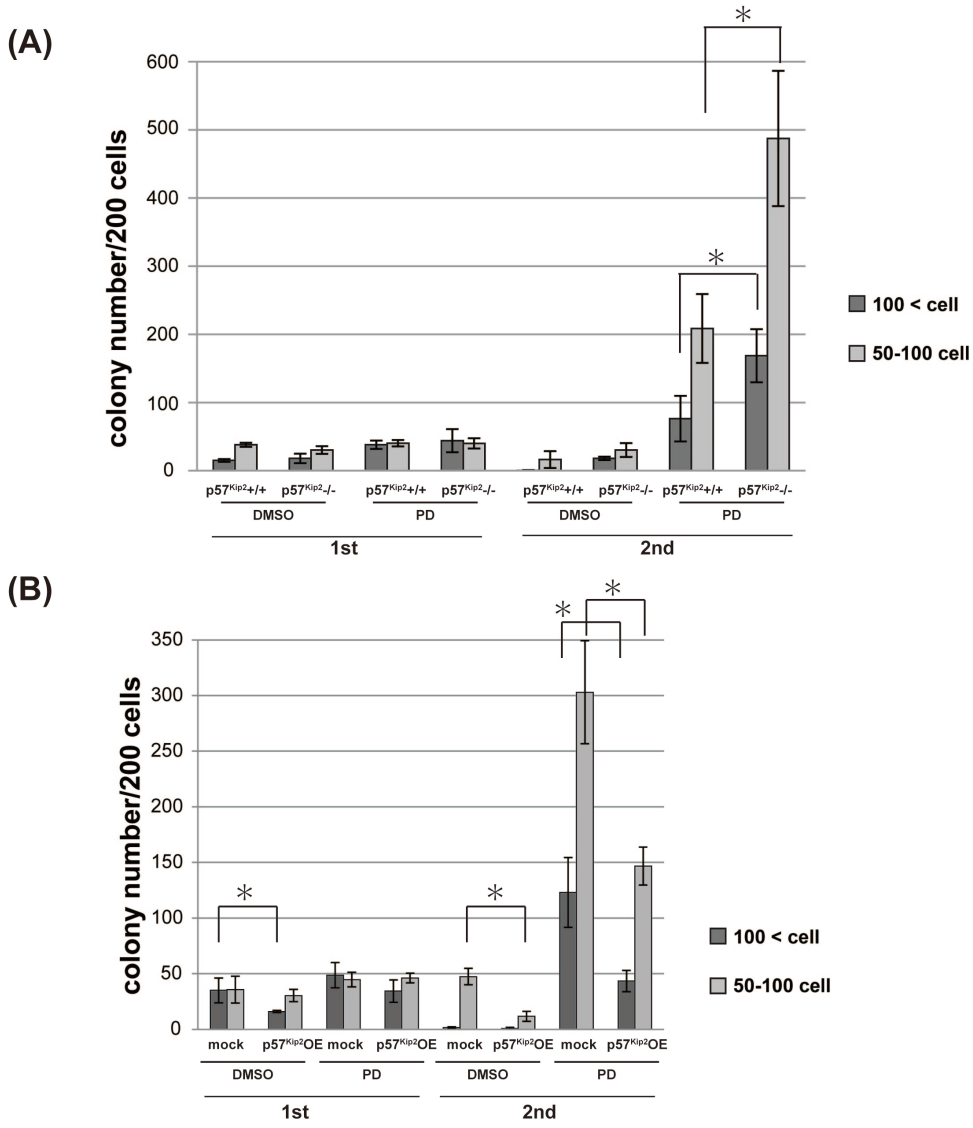

Figure 21. *In vitro* proliferation and differentiation abilities of p57^{Kip2}-/-, *p57^{Kip2}*+/+, and p57^{Kip2}-overexpressed hepatoblasts.

(A) Colony forming ability of *p57^{Kip2}*-/- and *p57^{Kip2}*+/+ hepatoblasts. Numbers of the 1st culture and the 2nd cultures colonies (contained more than 100 cells and 50 cells) were shown. Results are represented as the mean colony ± SD (triplicate samples). (B) Colony forming ability of p57^{Kip2}-overexpressed hepatoblasts (OE). Numbers of the 1st culture and the 2nd culture colonies (contained more than 100 cells and 50 cells) were shown. Results are represented as the mean colony ± SD (triplicate samples). Nuclei were counterstained with DAPI and Albumin-positive colonies were counted. MEK inhibitor PD0325901 (PD) was dissolved in dimethyl sulfoxide (DMSO). ∗ $P<0.05$.

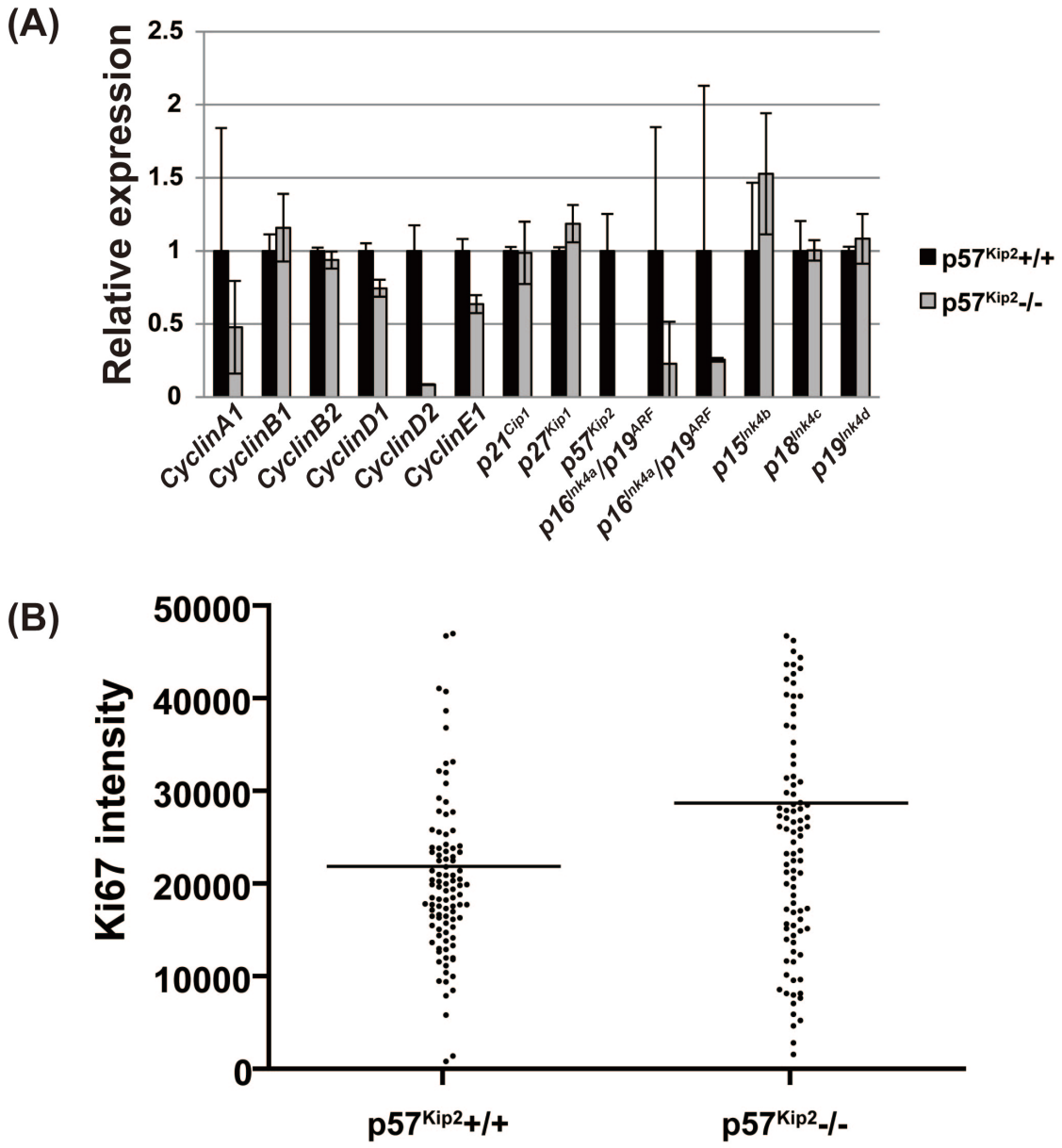

Figure 22. The proliferation ability of *p57^{Kip2}*-/- hepatoblasts in E13.5.

(A) Expression of cell cycle-related genes in hepatoblasts of *p57^{Kip2}*+/+ and *p57^{Kip2}*-/- mice. Hepatoblasts derived from E13.5 *p57^{Kip2}*+/+ and *p57^{Kip2}*-/- livers were purified and expression of cyclins and CDK inhibitors was analyzed using quantitative RT-PCR. Results are represented as the mean colony count ± SD (duplicate samples). (B) In droplet staining of the proliferation marker Ki67 in *p57^{Kip2}+/+* and *p57^{Kip2}*-/- E13.5 hepatoblasts.

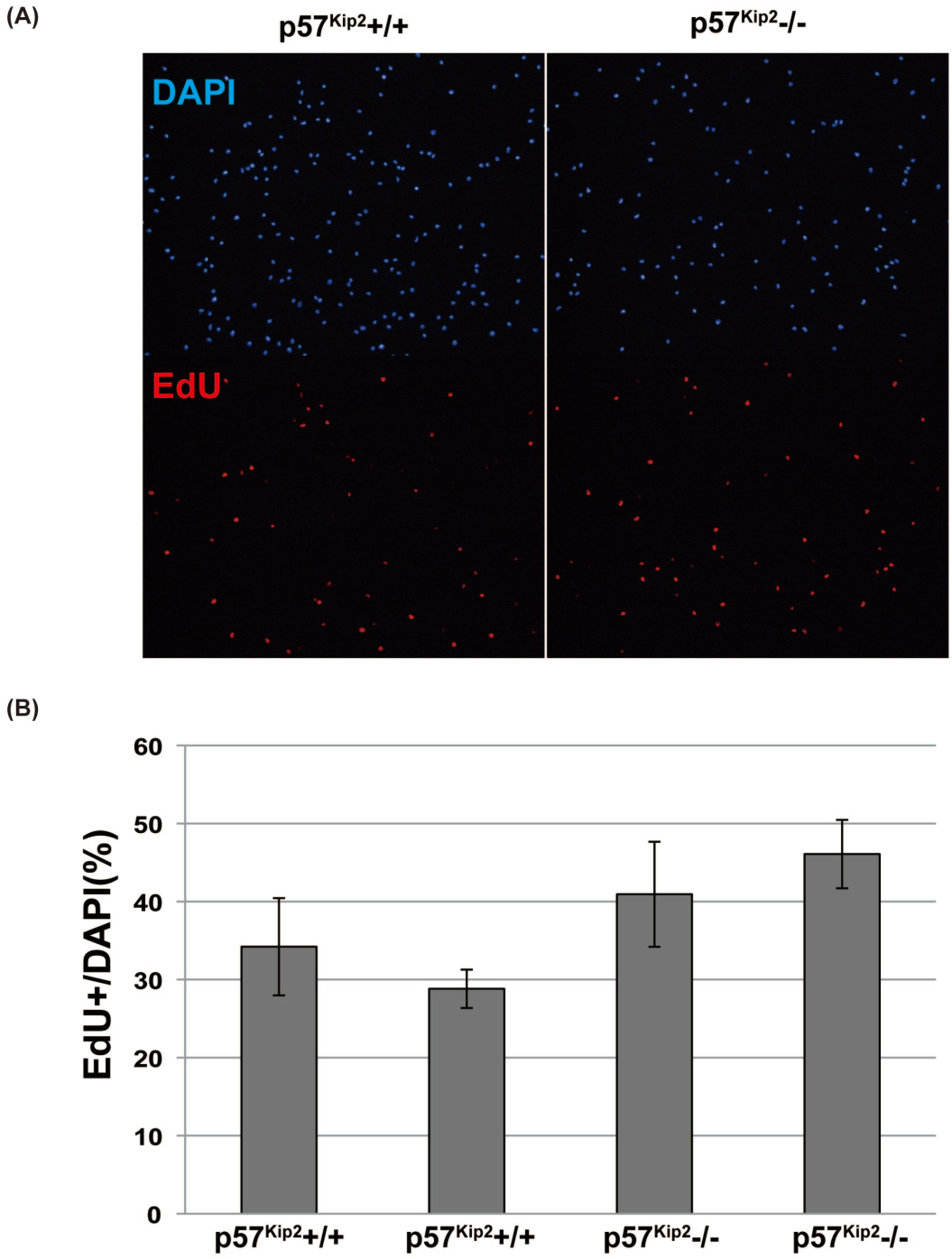

Figure 23. The proliferation ability of *p57^{Kip2}-/-* hepatoblasts in E13.5.

In-droplet staining of EdU in E13.5 *p57^{Kip2}+/+* and *p57^{Kip2}-/-* hepatoblasts. The number of EdU-positive hepatoblasts was counted. Pregnant mice received 100 mg/kg EdU in PBS via i.p. injection before 2 hours sampling. Results are represented as the mean colony count ± SD (duplicate samples).

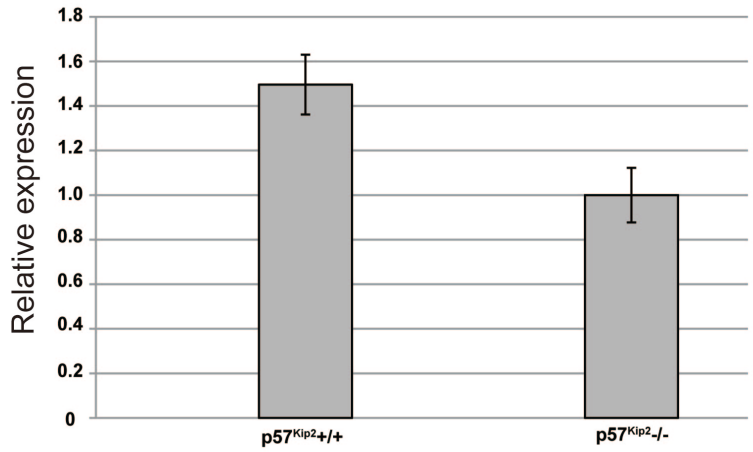

Figure 24. The expression levels of *CyclinD2* in late-fetal livers.

The expression levels of *CyclinD2* mRNA in $p57^{Kip2}$+/+ and $p57^{Kip2}$-/- whole livers at E17.5. mRNAs were purified from E17.5 $p57^{Kip2}$+/+ and $p57^{Kip2}$-/- livers and expression of *CyclinD2* was analyzed by quantitative RT-PCR. Results are represented as the mean colony count ± SD (triplicate samples).

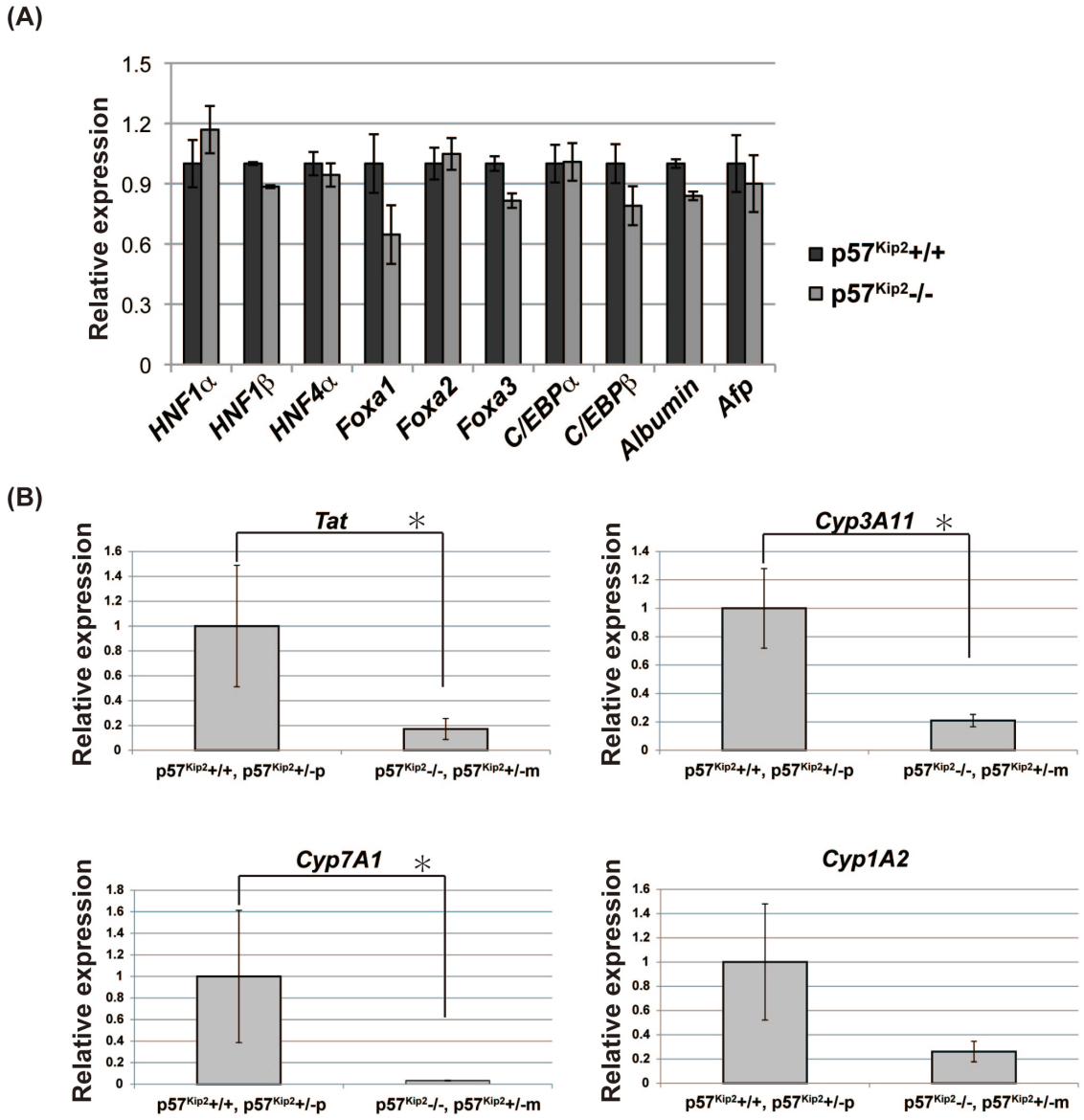

Figure 25. The differentiation ability of p57^{Kip2}-deficient hepatoblasts derived from fetal livers.

(A) Expression of liver-enriched transcription factors and hepatocytic marker genes in E13.5 hepatoblast derived from *p57^{Kip2}+/+* and *p57^{Kip2}-/-* mice. Results are represented as the mean colony count ± SD (duplicate samples). (B) The expression levels of mature hepatocytic functional genes, Tat, Cyp3A11, Cyp7A1, and Cyp1A2 in E19.0 whole fetal liver of *p57^{Kip2}+/+*, *p57^{Kip2}+/-p*, *p57^{Kip2}-/-*, and *p57^{Kip2}+/-m*. Results are represented as the mean colony count ± SD. Results of fetus from four pregnant mice are shown. *p57^{Kip2}+/-p* is p57^{Kip2} heterozygotes with paternal inheritance of the p57^{Kip2}-null allele. *p57^{Kip2}+/-m* is p57^{Kip2} heterozygotes with maternal inheritance of the p57^{Kip2}-null allele.

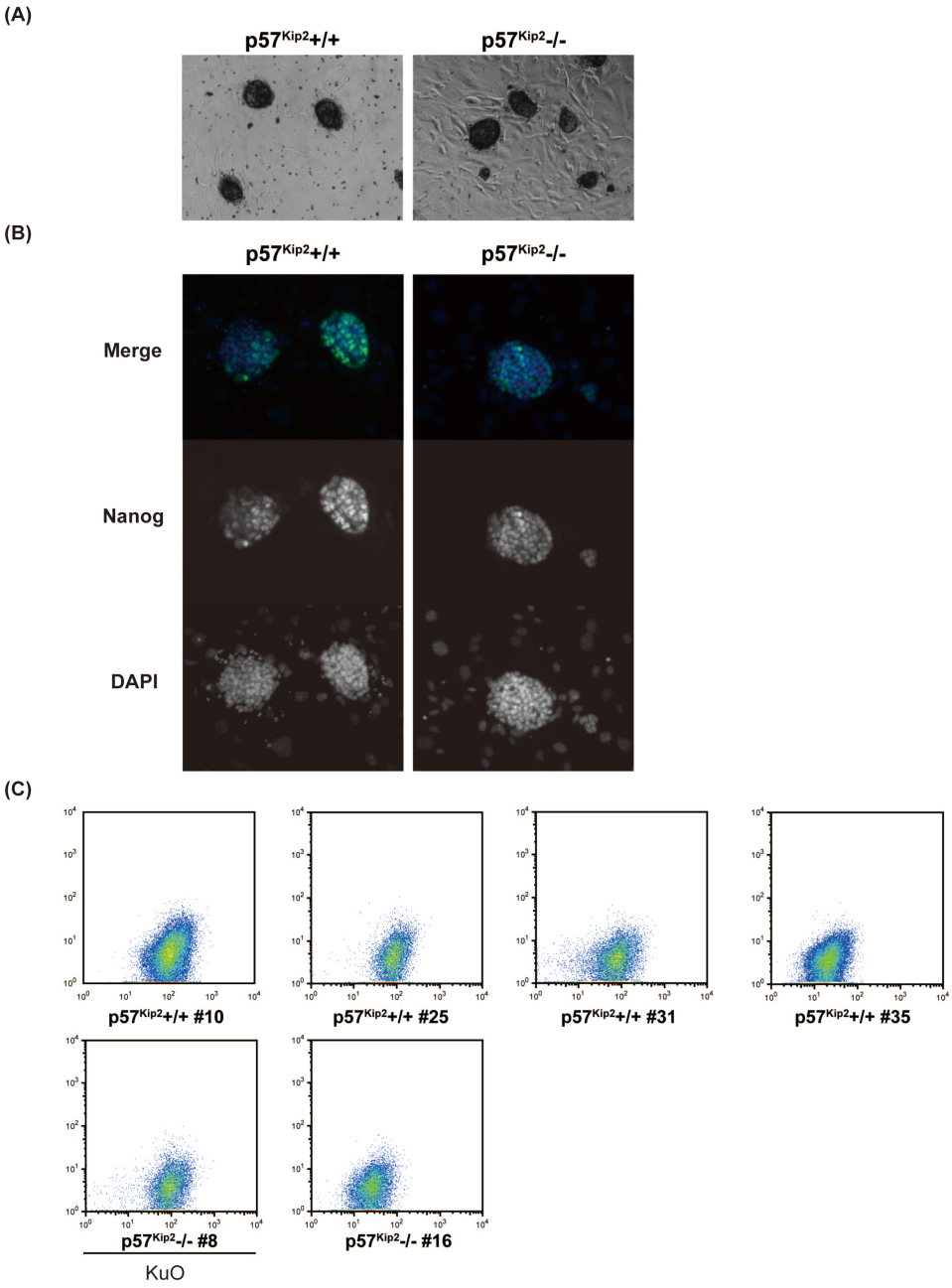

Figure 26. Generation of *p57^{Kip2}*+/+ and *p57^{Kip2}*-/- iPS cells.

(A) Alkaline phosphatase (AP) staining of *p57^{Kip2}*+/+ and *p57^{Kip2}*-/- iPS colonies (10-fold magnification). (B) Immunofluorescsnce staining for *Nanog* in *p57^{Kip2}*+/+ and *p57^{Kip2}*-/- iPS colonies (20-fold magnification). (C) The expression of KuO in embryoid body (EB) formation from KuO transfected *p57^{Kip2}*+/+ and *p57^{Kip2}*-/- iPS cells. # is a clone number.

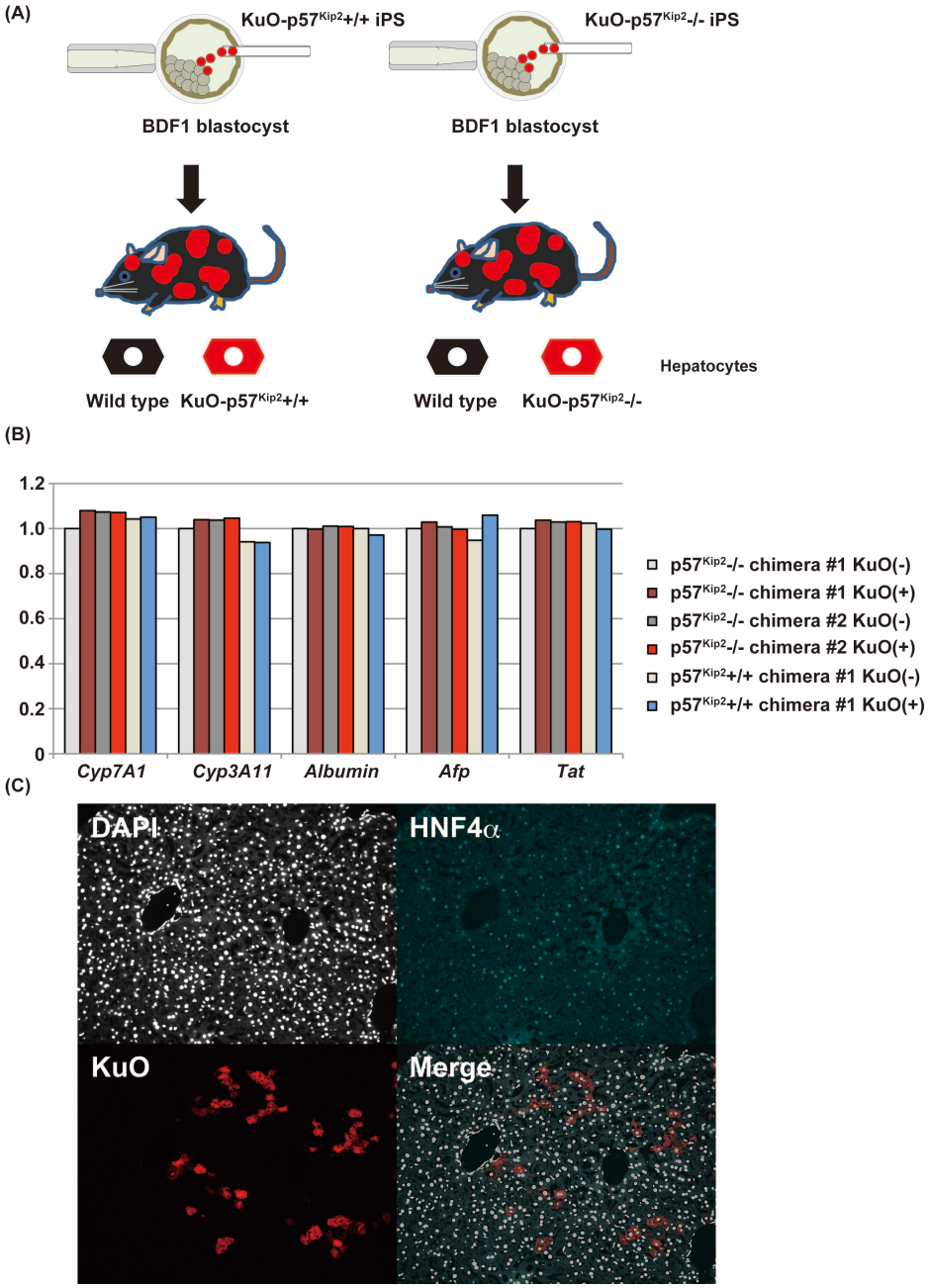

Figure 27. The function of *p57^{Kip2}*-/- hepatocytes in chimeric mice.

(A) The scheme of generation of *p57^{Kip2}*+/+ and *p57^{Kip2}*-/- chimeric mice. (B) The expression of hepatic functional genes, *Cyp3A11*, *Cyp7A1*, *Tat*, and *Albumin*, and immature hepatic marker *Afp* in *p57^{Kip2}*-/- and *p57^{Kip2}*+/+ hepatocytes in adult chimeric mice (6 weeks old). (C) Immunohistochemistry of livers derived from wild type-*p57^{Kip2}*-/- chimeric mice (6 weeks old). *p57^{Kip2}*-/- iPS cells derived cells labeled with KuO were merged with hepatocyte marker HNF4α. Nuclei were counterstained with DAPI.

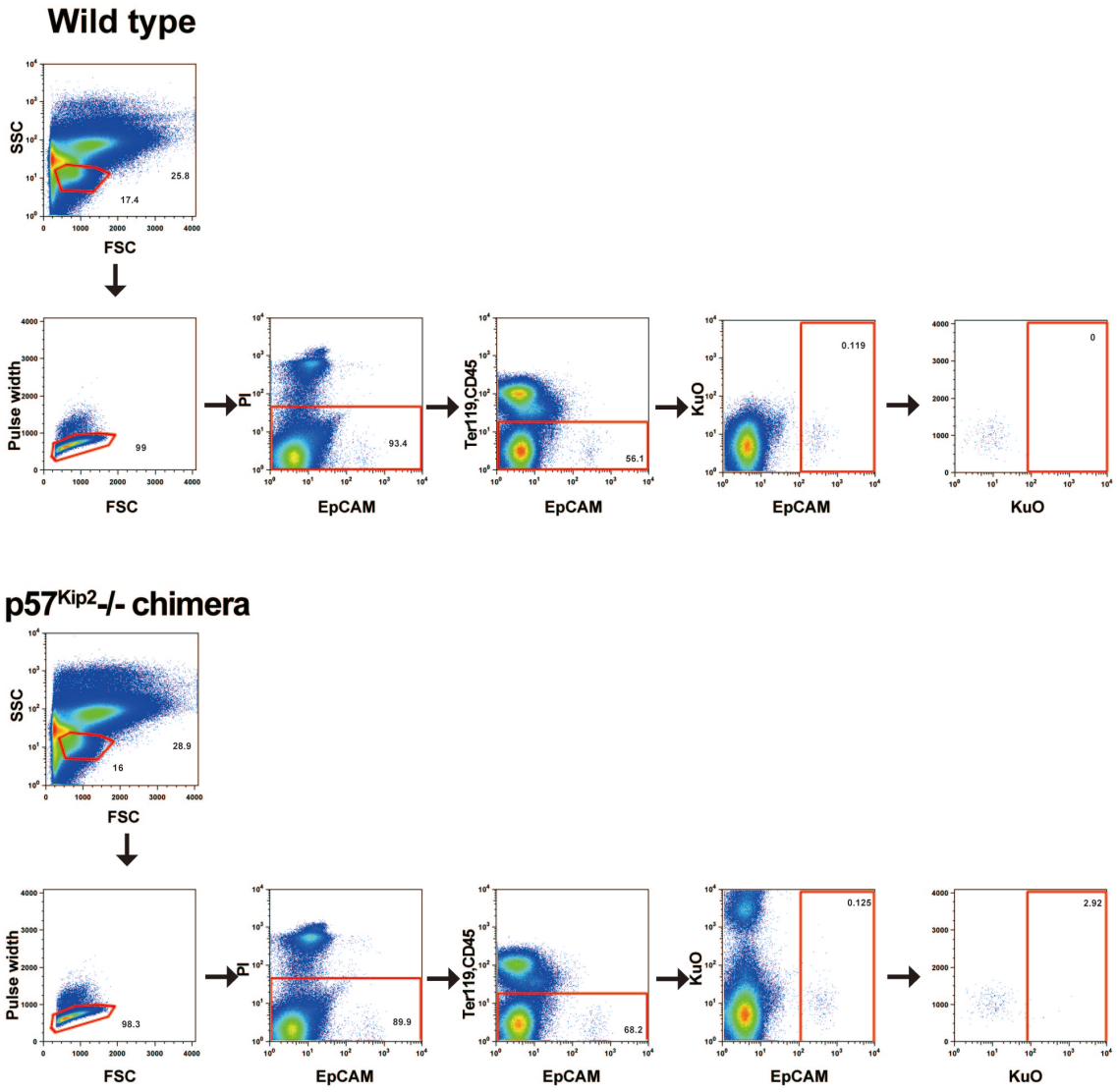

Figure 28. Expression of EpCAM in chimeric mice.

Non-parenchymal cells of wild type or *p57*^{Kip2}-/- chimeric adult liver in the PI^{-} were stained with antibodies against CD45, Ter119 (hematopoietic cell markers) and EpCAM (cholangiocytic marker). Doublet cells and dead cells were eliminated and CD45^{-}Ter119^{-} non-hematopoietic cell fraction was analyzed using antibody against EpCAM. A fraction of EpCAM^{+} cells was merged with KuO^{+} *p57*^{Kip2}-/- iPS cells derived cells.

Table 3. PCR primers for detection of human gene expression

Primer name	Sequence (5'–3')
p57^{Kip2} genotyping1	TGCACTGAGAGCGAGTAGAGATT
p57^{Kip2} genotyping2	AGCGGACCGATGGAAGAACTCTG
p57^{Kip2} genotyping3	GCGAAGGAACAAAGCTGCTATTG
p57^{Kip2}Fw cloning	AATGCGGCCGCTCTACCATGGGCATGGGCATGTCC GACGTGTACCTCCGC
p57^{Kip2}Rev cloning	ATTCTCGAGTCATCTCAGACGTTTGCGCGGGGTCTG

Genes	Forward primer (5'–3')	Reverse primer (5'–3')	Probe number
Albumin	AGTGTTGTGCAGAGGCTGAC	TTCTCCTTCACACCATCAAGC	27
Afp	CATGCTGCAAAGCTGACAA	CTTTGCAATGGATGCTCTCTT	63
p57^{Kip2}	CAGGACGAGAATCAAGAGCA	GCTTGGCGAAGAAGTCGT	17
Tat	GGAGGAGGTCGCTTCCTATT	GCCACTCGTCAGAATGACATC	82
HPRT	CCTGGTTCATCATCGCTAATC	TCCTCCTCAGACCGCTTTT	95
Cyp3A11	CCATGTCGAATTTCCATAAACC	GGGACTCGTAAACATGAACTTTT	53
Cyp7A1	GGCTGCTTTCATTGCTTCA	TCTCAAGCAAACACCATTCCT	50
Cyp1A2	CCTGGACTGACTCCCACACC	CGCAATCTGTACCACTGAAG	19
cyclinD2	CTGTGCATTTACACCGACAAC	CACTACCAGTTCCCACTCCAG	45

Afp, α-fetoprotein; CYP, cytochrome P450; HPRT, hypoxanthine phosphoribosyltransferase 1; Tat, tyrosine aminotransferase.

Table 4. List of antibodies used for immunostaining and FACS experiments

Primary antibodies for FACS	Clone	Source	Catalog number
CD133-APC	13A4	eBioscience	17-1331-81
CD133-PE	13A4	eBioscience	12-1331-82
CD45-PECy7	30-F11	eBioscience	23-0451-82
CD45.2-PECy7	104	Biologend	109830
c-Kit-PECy7	2B8	Biolegend	105814
CD71-PECy7	RI7217	Biolegend	113811
Ter119-PECy7	TER-119	Biolegend	116222
Dlk-PE	24-11	MBL	D187-4
Dlk-FITC	24-11	MBL	D187-5
Biotin-anti-mouse CD45.2	104	Biolegend	109804
Biotin-anti mouseTER-119	TER-119	eBioscience	13-5921-85
EpCAM-APC	G8.8	eBioscience	17-5791-80
Flk1-PE	Avas12a1	eBioscience	12-5821-83
PCLP1-PE	10B9	MBL	D072-5
PDGFRα-PE	APA5	eBioscience	12-1401-81
PDGFRα-APC	APA5	eBioscience	135908

Primary antibodies for immunostaining	Dilution	Source	Catalog number
Nanog (rabbit)	1:500	ReproCELL	RCAB0001P
Rabbit IgG		Santa Cruz	sc-2027
Goat IgG		Santa Cruz	sc-2028
CK19 (rabbit)	1:3000	Kindly gifted by Miyajima lab	
Albumin (goat)	1:750	Beyhyl	A90-134A
HNF4α (C-19) (goat)	1/600	Santa Cruz	sc-6556
$p57^{Kip2}$ (rabbit)	1:500	Abcam	ab4058
Ki67 (rabbit)	1:500	Abcam	ab15580

Secondary antibodies	Dilution	Source	Catalog number

anti-goat/Alexa Fluor 546	1/1000	Invitrogen	A11056
anti-rat/Alexa Fluor 647	1/1000	Invitrogen	A21472
anti-goat/Alexa Fluor 488	1/1000	Invitrogen	A11055
anti-goat/Alexa Fluor 647	1/1000	Invitrogen	A21447
anti-rabbit/Alexa Fluor 488	1/1000	Invitrogen	A21206

Table 5. List of genes for Taqman PCR

Taqman primer probe	Gene Assay ID
18S	Hs99999901_s1
Afp	Mm00431715_m1
Alb	Mm00802090_m1
Ccna1	Mm01292554_m1
Ccnb1	Mm00838401_g1
Ccnb2	Mm01171453_m1
Ccnd1	Mm00432359_m1
Ccnd2	Mm00438071_m1
Ccne1	Mm00432367_m1
Cdh1	Mm01247357_m1
Cdkn1a	Mm00432448_m1
Cdkn1b	Mm00438168_m1
Cdkn1c	Mm00438170_m1
Cdkn2a	Mm00494449_m1
Cdkn2b	Mm00483241_m1
Cdkn2c	Mm00483243_m1
Cdkn2d	Mm00486943_m1
Cebpa	Mm00514283_s1
Cebpb	Mm00843434_s1
Cer1	Mm00515474_m1
Cldn6	Mm00490040_s1
Cxcr4	Mm01292123_m1
Cyp1a1	Mm00487218_m1
Cyp1a2	Mm00487224_m1
Cyp2b10	Mm00456591_m1
Cyp2b9	Mm00657910_m1
Cyp3a11	Mm00731567_m1
Cyp3a13	Mm00484110_m1
Cyp7a1	Mm00484152_m1

Foxa1	Mm00484713_m1
Foxa2	Mm00839704_mH
Foxa3	Mm00484714_m1
G6pc	Mm00839363_m1
Gapdh	Mm99999915_g1
Gsc	Mm00650681_g1
Hhex	Mm00433954_m1
Hnf1a	Mm00493434_m1
Hnf1b	Mm00447459_m1
Hnf4a	Mm00433964_m1
Itgb4	Mm01266840_m1
Krt19	Mm00492980_m1
Nanog;Nanogpd	Mm02384862_g1
Onecut1	Mm00839394_m1
Pou5f1	Mm00658129_gH
Sox17	Mm00488363_m1
Tat	Mm01244282_m1
Tdo2	Mm00451266_m1

6 References

1. J. Till, E. McCulloch, A direct measurement of the radiation sensitivity of normal mouse bone marrow cells. *Radiation research* **14**, 213-222 (1961).

2. M. Evans, M. Kaufman, Establishment in culture of pluripotential cells from mouse embryos. *Nature* **292**, 154-156 (1981).

3. G. Martin, Isolation of a pluripotent cell line from early mouse embryos cultured in medium conditioned by teratocarcinoma stem cells. *Proceedings of the National Academy of Sciences of the United States of America* **78**, 7634-7638 (1981).

4. K. Takahashi, S. Yamanaka, Induction of pluripotent stem cells from mouse embryonic and adult fibroblast cultures by defined factors. *Cell* **126**, 663-676 (2006).

5. K. Okita, Y. Matsumura, Y. Sato, A. Okada, A. Morizane, S. Okamoto, H. Hong, M. Nakagawa, K. Tanabe, K.-i. Tezuka, T. Shibata, T. Kunisada, M. Takahashi, J. Takahashi, H. Saji, S. Yamanaka, A more efficient method to generate integration-free human iPS cells. *Nature methods* **8**, 409-412 (2011).

6. K. Okita, N. Nagata, S. Yamanaka, Immunogenicity of induced pluripotent

stem cells. *Circulation research* **109**, 720-721 (2011).

7. N. Fusaki, H. Ban, A. Nishiyama, K. Saeki, M. Hasegawa, Efficient induction of transgene-free human pluripotent stem cells using a vector based on Sendai virus, an RNA virus that does not integrate into the host genome. *Proceedings of the Japan Academy. Series B, Physical and biological sciences* **85**, 348-362 (2009).

8. M. Stadtfeld, M. Nagaya, J. Utikal, G. Weir, K. Hochedlinger, Induced pluripotent stem cells generated without viral integration. *Science* **322**, 945-949 (2008).

9. L. Warren, P. Manos, T. Ahfeldt, Y.-H. Loh, H. Li, F. Lau, W. Ebina, P. Mandal, Z. Smith, A. Meissner, G. Daley, A. Brack, J. Collins, C. Cowan, T. Schlaeger, D. Rossi, Highly efficient reprogramming to pluripotency and directed differentiation of human cells with synthetic modified mRNA. *Cell stem cell* **7**, 618-630 (2010).

10. D. Kim, C.-H. Kim, J.-I. Moon, Y.-G. Chung, M.-Y. Chang, B.-S. Han, S. Ko, E. Yang, K. Cha, R. Lanza, K.-S. Kim, Generation of human induced pluripotent stem cells by direct delivery of reprogramming proteins. *Cell stem*

cell **4**, 472-476 (2009).

11. Y. Rais, A. Zviran, S. Geula, O. Gafni, E. Chomsky, S. Viukov, A. A. Mansour, I. Caspi, V. Krupalnik, M. Zerbib, I. Maza, N. Mor, D. Baran, L. Weinberger, D. A. Jaitin, D. Lara-Astiaso, R. Blecher-Gonen, Z. Shipony, Z. Mukamel, T. Hagai, S. Gilad, D. Amann-Zalcenstein, A. Tanay, I. Amit, N. Novershtern, J. H. Hanna, Deterministic direct reprogramming of somatic cells to pluripotency. *Nature* **502**, 65-70 (2013).

12. F. West, S. Terlouw, D. Kwon, J. Mumaw, S. Dhara, K. Hasneen, J. Dobrinsky, S. Stice, Porcine induced pluripotent stem cells produce chimeric offspring. *Stem cells and development* **19**, 1211-1220 (2010).

13. K. Takahashi, K. Tanabe, M. Ohnuki, M. Narita, T. Ichisaka, K. Tomoda, S. Yamanaka, Induction of pluripotent stem cells from adult human fibroblasts by defined factors. *Cell* **131**, 861-872 (2007).

14. J. Yu, M. Vodyanik, K. Smuga-Otto, J. Antosiewicz-Bourget, J. Frane, S. Tian, J. Nie, G. Jonsdottir, V. Ruotti, R. Stewart, I. Slukvin, J. Thomson, Induced pluripotent stem cell lines derived from human somatic cells. *Science* **318**, 1917-1920 (2007).

15. A. Smith, J. Heath, D. Donaldson, G. Wong, J. Moreau, M. Stahl, D. Rogers, Inhibition of pluripotential embryonic stem cell differentiation by purified polypeptides. *Nature* **336**, 688-690 (1988).

16. J. Thomson, J. Itskovitz-Eldor, S. Shapiro, M. Waknitz, J. Swiergiel, V. Marshall, J. Jones, Embryonic stem cell lines derived from human blastocysts. *Science* **282**, 1145-1147 (1998).

17. M. Hirabayashi, M. Kato, T. Kobayashi, M. Sanbo, T. Yagi, S. Hochi, H. Nakauchi, Establishment of rat embryonic stem cell lines that can participate in germline chimerae at high efficiency. *Molecular reproduction and development* **77**, 94 (2010).

18. Q. Zhou, J. Brown, A. Kanarek, J. Rajagopal, D. Melton, In vivo reprogramming of adult pancreatic exocrine cells to beta-cells. *Nature* **455**, 627-632 (2008).

19. T. Vierbuchen, A. Ostermeier, Z. Pang, Y. Kokubu, T. S√°dhof, M. Wernig, Direct conversion of fibroblasts to functional neurons by defined factors. *Nature* **463**, 1035-1041 (2010).

20. P. Huang, Z. He, S. Ji, H. Sun, D. Xiang, C. Liu, Y. Hu, X. Wang, L. Hui,

Induction of functional hepatocyte-like cells from mouse fibroblasts by defined factors. *Nature* **475**, 386-389 (2011).

21. M. Ieda, J.-D. Fu, P. Delgado-Olguin, V. Vedantham, Y. Hayashi, B. Bruneau, D. Srivastava, Direct reprogramming of fibroblasts into functional cardiomyocytes by defined factors. *Cell* **142**, 375-386 (2010).

22. C. Lee, J. Friedman, J. Fulmer, K. Kaestner, The initiation of liver development is dependent on Foxa transcription factors. *Nature* **435**, 944-947 (2005).

23. J. Rossi, N. Dunn, B. Hogan, K. Zaret, Distinct mesodermal signals, including BMPs from the septum transversum mesenchyme, are required in combination for hepatogenesis from the endoderm. *Genes & development* **15**, 1998-2009 (2001).

24. J. Jung, M. Zheng, M. Goldfarb, K. Zaret, Initiation of mammalian liver development from endoderm by fibroblast growth factors. *Science* **284**, 1998-2003 (1999).

25. S. Han, N. Dziedzic, P. Gadue, G. Keller, V. Gouon-Evans, An endothelial cell niche induces hepatic specification through dual repression of Wnt and Notch signaling. *Stem cells* **29**, 217-228 (2011).

26. K. Matsumoto, H. Yoshitomi, J. Rossant, K. Zaret, Liver organogenesis promoted by endothelial cells prior to vascular function. *Science* **294**, 559-563 (2001).

27. R. Bort, M. Signore, K. Tremblay, J. Martinez Barbera, K. Zaret, Hex homeobox gene controls the transition of the endoderm to a pseudostratified, cell emergent epithelium for liver bud development. *Developmental biology* **290**, 44-56 (2006).

28. J. Martinez Barbera, M. Clements, P. Thomas, T. Rodriguez, D. Meloy, D. Kioussis, R. Beddington, The homeobox gene Hex is required in definitive endodermal tissues for normal forebrain, liver and thyroid formation. *Development* **127**, 2433-2445 (2000).

29. B. Sosa-Pineda, J. Wigle, G. Oliver, Hepatocyte migration during liver development requires Prox1. *Nature genetics* **25**, 254-255 (2000).

30. B. Hentsch, I. Lyons, R. Li, L. Hartley, T. Lints, J. Adams, R. Harvey, Hlx homeo box gene is essential for an inductive tissue interaction that drives expansion of embryonic liver and gut. *Genes & development* **10**, 70-79 (1996).

31. A. Kamiya, T. Kinoshita, Y. Ito, T. Matsui, Y. Morikawa, E. Senba, K.

Nakashima, T. Taga, K. Yoshida, T. Kishimoto, A. Miyajima, Fetal liver development requires a paracrine action of oncostatin M through the gp130 signal transducer. *The EMBO journal* **18**, 2127-2136 (1999).

32. I. Onitsuka, M. Tanaka, A. Miyajima, Characterization and functional analyses of hepatic mesothelial cells in mouse liver development. *Gastroenterology* **138**, 1525 (2010).

33. K. Asahina, H. Sato, C. Yamasaki, M. Kataoka, M. Shiokawa, S. Katayama, C. Tateno, K. Yoshizato, Pleiotrophin/heparin-binding growth-associated molecule as a mitogen of rat hepatocytes and its role in regeneration and development of liver. *The American journal of pathology* **160**, 2191-2205 (2002).

34. B. McCright, J. Lozier, T. Gridley, A mouse model of Alagille syndrome: Notch2 as a genetic modifier of Jag1 haploinsufficiency. *Development* **129**, 1075-1082 (2002).

35. L. Li, I. Krantz, Y. Deng, A. Genin, A. Banta, C. Collins, M. Qi, B. Trask, W. Kuo, J. Cochran, T. Costa, M. Pierpont, E. Rand, D. Piccoli, L. Hood, N. Spinner, Alagille syndrome is caused by mutations in human Jagged1, which

encodes a ligand for Notch1. *Nature genetics* **16**, 243-251 (1997).

36. T. Oda, A. Elkahloun, B. Pike, K. Okajima, I. Krantz, A. Genin, D. Piccoli, P. Meltzer, N. Spinner, F. Collins, S. Chandrasekharappa, Mutations in the human Jagged1 gene are responsible for Alagille syndrome. *Nature genetics* **16**, 235-242 (1997).

37. Z.-R. Yuan, N. Kobayashi, T. Kohsaka, Human Jagged 1 mutants cause liver defect in Alagille syndrome by overexpression of hepatocyte growth factor. *Journal of molecular biology* **356**, 559-568 (2006).

38. N. Tanimizu, M. Nishikawa, H. Saito, T. Tsujimura, A. Miyajima, Isolation of hepatoblasts based on the expression of Dlk/Pref-1. *Journal of cell science* **116**, 1775-1786 (2003).

39. T. Watanabe, K. Nakagawa, S. Ohata, D. Kitagawa, G. Nishitai, J. Seo, S. Tanemura, N. Shimizu, H. Kishimoto, T. Wada, J. Aoki, H. Arai, T. Iwatsubo, M. Mochita, T. Watanabe, M. Satake, Y. Ito, T. Matsuyama, T. Mak, J. Penninger, H. Nishina, T. Katada, SEK1/MKK4-mediated SAPK/JNK signaling participates in embryonic hepatoblast proliferation via a pathway different from NF-kappaB-induced anti-apoptosis. *Developmental biology* **250**,

332-347 (2002).

40. S. Kakinuma, H. Ohta, A. Kamiya, Y. Yamazaki, T. Oikawa, K. Okada, H. Nakauchi, Analyses of cell surface molecules on hepatic stem/progenitor cells in mouse fetal liver. *Journal of hepatology* **51**, 127-138 (2009).

41. K. Okada, A. Kamiya, K. Ito, A. Yanagida, H. Ito, H. Kondou, H. Nishina, H. Nakauchi, Prospective isolation and characterization of bipotent progenitor cells in early mouse liver development. *Stem cells and development* **21**, 1124-1133 (2012).

42. A. Kamiya, S. Kakinuma, M. Onodera, A. Miyajima, H. Nakauchi, Prospero-related homeobox 1 and liver receptor homolog 1 coordinately regulate long-term proliferation of murine fetal hepatoblasts. *Hepatology* **48**, 252-264 (2008).

43. T. Oikawa, A. Kamiya, S. Kakinuma, M. Zeniya, R. Nishinakamura, H. Tajiri, H. Nakauchi, Sall4 regulates cell fate decision in fetal hepatic stem/progenitor cells. *Gastroenterology* **136**, 1000-1011 (2009).

44. A. Suzuki, S. Sekiya, D. Büscher, J. Izpisúa Belmonte, H. Taniguchi, Tbx3 controls the fate of hepatic progenitor cells in liver development by suppressing

p19ARF expression. *Development* **135**, 1589-1595 (2008).

45. F. Cheng, Q. Ke, F. Chen, B. Cai, Y. Gao, C. Ye, D. Wang, L. Zhang, B. Lahn, W. Li, A. Xiang, Protecting against wayward human induced pluripotent stem cells with a suicide gene. *Biomaterials* **33**, 3195-3204 (2012).

46. D. Zhao, S. Chen, J. Cai, Y. Guo, Z. Song, J. Che, C. Liu, C. Wu, M. Ding, H. Deng, Derivation and characterization of hepatic progenitor cells from human embryonic stem cells. *PLoS One* **4**, e6468 (2009).

47. N. Takayama, S. Nishimura, S. Nakamura, T. Shimizu, R. Ohnishi, H. Endo, T. Yamaguchi, M. Otsu, K. Nishimura, M. Nakanishi, A. Sawaguchi, R. Nagai, K. Takahashi, S. Yamanaka, H. Nakauchi, K. Eto, Transient activation of c-MYC expression is critical for efficient platelet generation from human induced pluripotent stem cells. *The Journal of experimental medicine* **207**, 2817-2830 (2010).

48. H. Suemori, K. Yasuchika, K. Hasegawa, T. Fujioka, N. Tsuneyoshi, N. Nakatsuji, Efficient establishment of human embryonic stem cell lines and long-term maintenance with stable karyotype by enzymatic bulk passage. *Biochem Biophys Res Commun* **345**, 926-932 (2006).

49. N. Tanimizu, A. Miyajima, K. E. Mostov, Liver progenitor cells develop cholangiocyte-type epithelial polarity in three-dimensional culture. *Molecular biology of the cell* **18**, 1472-1479 (2007).

50. D. C. Hay, J. Fletcher, C. Payne, J. D. Terrace, R. C. Gallagher, J. Snoeys, J. R. Black, D. Wojtacha, K. Samuel, Z. Hannoun, A. Pryde, C. Filippi, I. S. Currie, S. J. Forbes, J. A. Ross, P. N. Newsome, J. P. Iredale, Highly efficient differentiation of hESCs to functional hepatic endoderm requires ActivinA and Wnt3a signaling. *Proc Natl Acad Sci U S A* **105**, 12301-12306 (2008).

51. H. Basma, A. Soto-Gutierrez, G. R. Yannam, L. Liu, R. Ito, T. Yamamoto, E. Ellis, S. D. Carson, S. Sato, Y. Chen, D. Muirhead, N. Navarro-Alvarez, R. J. Wong, J. Roy-Chowdhury, J. L. Platt, D. F. Mercer, J. D. Miller, S. C. Strom, N. Kobayashi, I. J. Fox, Differentiation and transplantation of human embryonic stem cell-derived hepatocytes. *Gastroenterology* **136**, 990-999 (2009).

52. A. Suzuki, Y. Zheng, R. Kondo, M. Kusakabe, Y. Takada, K. Fukao, H. Nakauchi, H. Taniguchi, Flow-cytometric separation and enrichment of hepatic progenitor cells in the developing mouse liver. *Hepatology* **32**, 1230-1239

(2000).

53. S. Minguet, I. Cortegano, P. Gonzalo, J. A. Martinez-Marin, B. de Andres, C. Salas, D. Melero, M. L. Gaspar, M. A. Marcos, A population of c-Kit(low)(CD45/TER119)- hepatic cell progenitors of 11-day postcoitus mouse embryo liver reconstitutes cell-depleted liver organoids. *The Journal of clinical investigation* **112**, 1152-1163 (2003).

54. E. Schmelzer, L. Zhang, A. Bruce, E. Wauthier, J. Ludlow, H. L. Yao, N. Moss, A. Melhem, R. McClelland, W. Turner, M. Kulik, S. Sherwood, T. Tallheden, N. Cheng, M. E. Furth, L. M. Reid, Human hepatic stem cells from fetal and postnatal donors. *The Journal of experimental medicine* **204**, 1973-1987 (2007).

55. S. Nava, M. Westgren, M. Jaksch, A. Tibell, U. Broome, B. G. Ericzon, S. Sumitran-Holgersson, Characterization of cells in the developing human liver. *Differentiation; research in biological diversity* **73**, 249-260 (2005).

56. H. C. Fiegel, J. J. Park, M. V. Lioznov, A. Martin, S. Jaeschke-Melli, P. M. Kaufmann, B. Fehse, A. R. Zander, D. Kluth, Characterization of cell types during rat liver development. *Hepatology* **37**, 148-154 (2003).

57. K. A. D'Amour, A. D. Agulnick, S. Eliazer, O. G. Kelly, E. Kroon, E. E. Baetge, Efficient differentiation of human embryonic stem cells to definitive endoderm. *Nature biotechnology* **23**, 1534-1541 (2005).

58. A. Ijpenberg, J. M. Perez-Pomares, J. A. Guadix, R. Carmona, V. Portillo-Sanchez, D. Macias, P. Hohenstein, C. M. Miles, N. D. Hastie, R. Munoz-Chapuli, Wt1 and retinoic acid signaling are essential for stellate cell development and liver morphogenesis. *Dev Biol* **312**, 157-170 (2007).

59. L. Zhang, N. Theise, M. Chua, L. M. Reid, The stem cell niche of human livers: symmetry between development and regeneration. *Hepatology* **48**, 1598-1607 (2008).

60. N. Koide, T. Shinji, T. Tanabe, K. Asano, M. Kawaguchi, K. Sakaguchi, Y. Koide, M. Mori, T. Tsuji, Continued high albumin production by multicellular spheroids of adult rat hepatocytes formed in the presence of liver-derived proteoglycans. *Biochem Biophys Res Commun* **161**, 385-391 (1989).

61. T. Takezawa, M. Yamazaki, Y. Mori, T. Yonaha, K. Yoshizato, Morphological and immuno-cytochemical characterization of a hetero-spheroid composed of fibroblasts and hepatocytes. *J Cell Sci* **101 (Pt 3)**, 495-501 (1992).

62. H. F. Lu, K. N. Chua, P. C. Zhang, W. S. Lim, S. Ramakrishna, K. W. Leong, H. Q. Mao, Three-dimensional co-culture of rat hepatocyte spheroids and NIH/3T3 fibroblasts enhances hepatocyte functional maintenance. *Acta biomaterialia* **1**, 399-410 (2005).

63. K. Si-Tayeb, F. K. Noto, M. Nagaoka, J. Li, M. A. Battle, C. Duris, P. E. North, S. Dalton, S. A. Duncan, Highly efficient generation of human hepatocyte-like cells from induced pluripotent stem cells. *Hepatology* **51**, 297-305 (2010).

64. J. Cai, Y. Zhao, Y. Liu, F. Ye, Z. Song, H. Qin, S. Meng, Y. Chen, R. Zhou, X. Song, Y. Guo, M. Ding, H. Deng, Directed differentiation of human embryonic stem cells into functional hepatic cells. *Hepatology* **45**, 1229-1239 (2007).

65. N. Kojima, T. Kinoshita, A. Kamiya, K. Nakamura, K. Nakashima, T. Taga, A. Miyajima, Cell density-dependent regulation of hepatic development by a gp130-independent pathway. *Biochem Biophys Res Commun* **277**, 152-158 (2000).

66. A. Kamiya, S. Kakinuma, Y. Yamazaki, H. Nakauchi, Enrichment and clonal culture of progenitor cells during mouse postnatal liver development in mice. *Gastroenterology* **137**, 1114 (2009).

67. N. Haraguchi, H. Ishii, K. Mimori, F. Tanaka, M. Ohkuma, H. M. Kim, H. Akita, D. Takiuchi, H. Hatano, H. Nagano, G. F. Barnard, Y. Doki, M. Mori, CD13 is a therapeutic target in human liver cancer stem cells. *The Journal of clinical investigation* **120**, 3326-3339 (2010).

68. N. Uchida, D. W. Buck, D. He, M. J. Reitsma, M. Masek, T. V. Phan, A. S. Tsukamoto, F. H. Gage, I. L. Weissman, Direct isolation of human central nervous system stem cells. *Proc Natl Acad Sci U S A* **97**, 14720-14725 (2000).

69. L. Zhu, P. Gibson, D. S. Currle, Y. Tong, R. J. Richardson, I. T. Bayazitov, H. Poppleton, S. Zakharenko, D. W. Ellison, R. J. Gilbertson, Prominin 1 marks intestinal stem cells that are susceptible to neoplastic transformation. *Nature* **457**, 603-607 (2009).

70. A. H. Yin, S. Miraglia, E. D. Zanjani, G. Almeida-Porada, M. Ogawa, A. G. Leary, J. Olweus, J. Kearney, D. W. Buck, AC133, a novel marker for human hematopoietic stem and progenitor cells. *Blood* **90**, 5002-5012 (1997).

71. S. Miraglia, W. Godfrey, A. H. Yin, K. Atkins, R. Warnke, J. T. Holden, R. A. Bray, E. K. Waller, D. W. Buck, A novel five-transmembrane hematopoietic stem cell antigen: isolation, characterization, and molecular cloning. *Blood* **90**,

5013-5021 (1997).

72. M. Ohgushi, Y. Sasai, Lonely death dance of human pluripotent stem cells: ROCKing between metastable cell states. *Trends in cell biology* **21**, 274-282 (2011).

73. H. Ito, A. Kamiya, K. Ito, A. Yanagida, K. Okada, H. Nakauchi, In vitro expansion and functional recovery of mature hepatocytes from mouse adult liver. *Liver international : official journal of the International Association for the Study of the Liver* **32**, 592-601 (2012).

74. N. M. Meindl-Beinker, K. Matsuzaki, S. Dooley, TGF-beta signaling in onset and progression of hepatocellular carcinoma. *Digestive diseases* **30**, 514-523 (2012).

75. K. Okita, T. Ichisaka, S. Yamanaka, Generation of germline-competent induced pluripotent stem cells. *Nature* **448**, 313-317 (2007).

76. M. Mikula, E. Fuchs, H. Huber, H. Beug, R. Schulte-Hermann, W. Mikulits, Immortalized p19ARF null hepatocytes restore liver injury and generate hepatic progenitors after transplantation. *Hepatology* **39**, 628-634 (2004).

77. E. Wandzioch, A. Kolterud, M. Jacobsson, S. Friedman, L. Carlsson, Lhx2-/-

mice develop liver fibrosis. *Proceedings of the National Academy of Sciences of the United States of America* **101**, 16549-16554 (2004).

78. F. Porter, J. Drago, Y. Xu, S. Cheema, C. Wassif, S. Huang, E. Lee, A. Grinberg, J. Massalas, D. Bodine, F. Alt, H. Westphal, Lhx2, a LIM homeobox gene, is required for eye, forebrain, and definitive erythrocyte development. *Development* **124**, 2935-2944 (1997).

79. A. Kamiya, T. Kinoshita, A. Miyajima, Oncostatin M and hepatocyte growth factor induce hepatic maturation via distinct signaling pathways. *FEBS letters* **492**, 90-94 (2001).

80. C. J. Sherr, J. M. Roberts, CDK inhibitors: positive and negative regulators of G1-phase progression. *Genes Dev* **13**, 1501-1512 (1999).

81. J. LaBaer, M. D. Garrett, L. F. Stevenson, J. M. Slingerland, C. Sandhu, H. S. Chou, A. Fattaey, E. Harlow, New functional activities for the p21 family of CDK inhibitors. *Genes Dev* **11**, 847-862 (1997).

82. M. Lee, I. Reynisdóttir, J. Massagué, Cloning of p57KIP2, a cyclin-dependent kinase inhibitor with unique domain structure and tissue distribution. *Genes & development* **9**, 639-649 (1995).

83. S. Matsuoka, M. Edwards, C. Bai, S. Parker, P. Zhang, A. Baldini, J. Harper, S. Elledge, p57KIP2, a structurally distinct member of the p21CIP1 Cdk inhibitor family, is a candidate tumor suppressor gene. *Genes & development* **9**, 650-662 (1995).

84. K. Nakayama, N. Ishida, M. Shirane, A. Inomata, T. Inoue, N. Shishido, I. Horii, D. Loh, Mice lacking p27(Kip1) display increased body size, multiple organ hyperplasia, retinal dysplasia, and pituitary tumors. *Cell* **85**, 707-720 (1996).

85. S. Parker, G. Eichele, P. Zhang, A. Rawls, A. Sands, A. Bradley, E. Olson, J. Harper, S. Elledge, p53-independent expression of p21Cip1 in muscle and other terminally differentiating cells. *Science (New York, N.Y.)* **267**, 1024-1027 (1995).

86. P. Zhang, C. Wong, R. DePinho, J. Harper, S. Elledge, Cooperation between the Cdk inhibitors p27(KIP1) and p57(KIP2) in the control of tissue growth and development. *Genes & development* **12**, 3162-3167 (1998).

87. P. Zhang, C. Wong, D. Liu, M. Finegold, J. Harper, S. Elledge, p21(CIP1) and p57(KIP2) control muscle differentiation at the myogenin step. *Genes &*

development **13**, 213-224 (1999).

88. G. Ilyin, D. Glaise, D. Gilot, G. Baffet, C. Guguen-Guillouzo, Regulation and role of p21 and p27 cyclin-dependent kinase inhibitors during hepatocyte differentiation and growth. *American journal of physiology. Gastrointestinal and liver physiology* **285**, 27 (2003).

89. M. Awad, J. Sanders, P. Gruppuso, A potential role for p15(Ink4b) and p57(Kip2) in liver development. *FEBS letters* **483**, 160-164 (2000).

90. P. O. Seglen, Hepatocyte Suspensions and Cultures as Tools in Experimental Carcinogenesis. *J Toxicol Env Health* **5**, 551-560 (1979).

91. T. Yamaguchi, S. Hamanaka, A. Kamiya, M. Okabe, M. Kawarai, Y. Wakiyama, A. Umino, T. Hayama, H. Sato, Y.-S. Lee, M. Kato-Itoh, H. Masaki, T. Kobayashi, S. Yamazaki, H. Nakauchi, Development of an all-in-one inducible lentiviral vector for gene specific analysis of reprogramming. *PloS one* **7**, (2012).

92. S. Yamazaki, A. Iwama, Y. Morita, K. Eto, H. Ema, H. Nakauchi, Cytokine signaling, lipid raft clustering, and HSC hibernation. *Annals of the New York Academy of Sciences* **1106**, 54-63 (2007).

93. I. Hatada, T. Mukai, Genomic imprinting of p57KIP2, a cyclin-dependent kinase inhibitor, in mouse. *Nature genetics* **11**, 204-206 (1995).

94. K. Ito, A. Yanagida, K. Okada, Y. Yamazaki, H. Nakauchi, A. Kamiya, Mesenchymal progenitor cells in mouse foetal liver regulate differentiation and proliferation of hepatoblasts. *Liver international : official journal of the International Association for the Study of the Liver*, (2013).

95. E. Schmelzer, L. Zhang, A. Bruce, E. Wauthier, J. Ludlow, H.-l. Yao, N. Moss, A. Melhem, R. McClelland, W. Turner, M. Kulik, S. Sherwood, T. Tallheden, N. Cheng, M. Furth, L. Reid, Human hepatic stem cells from fetal and postnatal donors. *The Journal of experimental medicine* **204**, 1973-1987 (2007).

96. M. Okabe, Y. Tsukahara, M. Tanaka, K. Suzuki, S. Saito, Y. Kamiya, T. Tsujimura, K. Nakamura, A. Miyajima, Potential hepatic stem cells reside in EpCAM+ cells of normal and injured mouse liver. *Development* **136**, 1951-1960 (2009).

97. E. Susaki, K. Nakayama, L. Yamasaki, K. I. Nakayama, Common and specific roles of the related CDK inhibitors p27 and p57 revealed by a knock-in mouse model. *Proceedings of the National Academy of Sciences of the United States*

of America **106**, 5192-5197 (2009).

98. A. Matsumoto, S. Takeishi, T. Kanie, E. Susaki, I. Onoyama, Y. Tateishi, K. Nakayama, K. Nakayama, p57 is required for quiescence and maintenance of adult hematopoietic stem cells. *Cell stem cell* **9**, 262-271 (2011).

99. P. Zou, H. Yoshihara, K. Hosokawa, I. Tai, K. Shinmyozu, F. Tsukahara, Y. Maru, K. Nakayama, K. Nakayama, T. Suda, p57(Kip2) and p27(Kip1) cooperate to maintain hematopoietic stem cell quiescence through interactions with Hsc70. *Cell stem cell* **9**, 247-261 (2011).

100. R. Pop, J. Shearstone, Q. Shen, Y. Liu, K. Hallstrom, M. Koulnis, J. Gribnau, M. Socolovsky, A key commitment step in erythropoiesis is synchronized with the cell cycle clock through mutual inhibition between PU.1 and S-phase progression. *PLoS biology* **8**, (2010).

101. K. Asahina, B. Zhou, W. Pu, H. Tsukamoto, Septum transversum-derived mesothelium gives rise to hepatic stellate cells and perivascular mesenchymal cells in developing mouse liver. *Hepatology (Baltimore, Md.)* **53**, 983-995 (2011).

102. I. Hatada, H. Ohashi, Y. Fukushima, Y. Kaneko, M. Inoue, Y. Komoto, A.

Okada, S. Ohishi, A. Nabetani, H. Morisaki, M. Nakayama, N. Niikawa, T. Mukai, An imprinted gene p57KIP2 is mutated in Beckwith-Wiedemann syndrome. *Nat Genet* **14**, 171-173 (1996).

103. P. Zhang, N. J. Liegeois, C. Wong, M. Finegold, H. Hou, J. C. Thompson, A. Silverman, J. W. Harper, R. A. DePinho, S. J. Elledge, Altered cell differentiation and proliferation in mice lacking p57KIP2 indicates a role in Beckwith-Wiedemann syndrome. *Nature* **387**, 151-158 (1997).

104. Y. Yan, J. Frisen, M. H. Lee, J. Massague, M. Barbacid, Ablation of the CDK inhibitor p57Kip2 results in increased apoptosis and delayed differentiation during mouse development. *Genes Dev* **11**, 973-983 (1997).

7 Acknowledgments

Some of the analyses were assisted by the Education and Research Support Center of Tokai University. We thank Mr. Yamazaki (Japan Science and Technology Agency, NAKAUCHI Stem Cell and Organ Regeneration Project) for operation of the flow cytometric technology, Dr. Kasai and Mr. Huan-Ting Lin (The Institute of Medical Science, The University of Tokyo) for critical reading, Dr. Miyajima (Institute of Molecular and Cellular Biosciences, The University of Tokyo) for kindly gifted CK19 antibody, and Dr. Nakayama (Medical Institute of Bioregulation, Kyushu University) for kindly gifted $p57^{Kip2}$ deficient mice.